EFFECTS OF INCLINATION, LENGTH PATTERN AND BENDING STIFFNESS OF SOIL NAILS ON BEHAVIOUR OF NAILED STRUCTURES

GEO REPORT No. 197

Y.K. Shiu & G.W.K Chang

GEOTECHNICAL ENGINEERING OFFICE
CIVIL ENGINEERING AND DEVELOPMENT DEPARTMENT
THE GOVERNMENT OF THE HONG KONG
SPECIAL ADMINISTRATIVE REGION

EFFECTS OF INCLINATION, LENGTH PATTERN AND BENDING STIFFNESS OF SOIL NAILS ON BEHAVIOUR OF NAILED STRUCTURES

GEO REPORT No. 197

Y.K. Shiu & G.W.K Chang

This report was originally produced in December 2005 as GEO Special Project Report No. SPR 6/2005

First published, December 2006

Prepared by:

Geotechnical Engineering Office,
Civil Engineering and Development Department,
Civil Engineering and Development Building,
101 Princess Margaret Road,
Homantin, Kowloon,
Hong Kong.

Table of Contents

Table of Contents

Table of Contents

Table of Contents

PREFACE

In keeping with our policy of releasing information which may be of general interest to the geotechnical profession and the public, we make available selected internal reports in a series of publications termed the GEO Report series. The GEO Reports can be downloaded from the website of the Civil Engineering and Development Department (http://www.cedd.gov.hk) on the Internet. Printed copies are also available for some GEO Reports. For printed copies, a charge is made to cover the cost of printing.

The Geotechnical Engineering Office also produces documents specifically for publication. These include guidance documents and results of comprehensive reviews. These publications and the printed GEO Reports may be obtained from the Government's Information Services Department. Information on how to purchase these documents is given on the second last page of this report.

R.K.S. Chan
Head, Geotechnical Engineering Office
December 2006

Table of Contents

Table of Contents

Table of Contents

FOREWORD

This Report presents the results of a study for the effects of inclination, length pattern and bending stiffness of soil nails on behaviour of nailed structures.

Numerical simulations have been carried out to examine the inclination effects of soil nails on nailed slopes and excavations. A review on the stabilization effect of bending stiffness of soil nails has also been undertaken.

From the study, guidance on some design aspects of soil nails are provided.

The study was carried out by Mr Y.K. Shiu and Dr G.W.K. Chang of the Standards and Testing Division.

W.K. Pun
Chief Geotechnical Engineer/Standards and Testing

ABSTRACT

The soil nailing concept involves providing a stable block of composite material by reinforcing the in situ ground with soil nails. The reinforcing action is achieved through two fundamental mechanisms of soil-nail interaction. They are the soil-nail friction that leads to axial tension or compression; and the bearing failure of soil nails that leads to development of shear forces and bending moments in nails.

A study has been carried out to review these mechanisms and examine the mechanical behaviour of soil nailed structures in respect of the following aspects:

(a) the effect of nail inclination on development of nail axial force distribution and stability improvement of slopes and excavations;

(b) the influence of nail length patterns on facing deformation in a staged-excavation;

(c) the contribution from bending stiffness of soil nails to stability improvements of slopes and excavations.

In the study, numerical simulations have been conducted to investigate the effects of nail inclination using finite difference and finite element methods with strength reduction technique. The results are compared with outcomes from limit equilibrium methods.

From the results of the study, inclinations of soil nails can affect the reinforcing action of the nails. Increase in soil nail inclination would decrease the reinforcing forces in the nails and in turn reduce the stabilizing effect. For steeply inclined soil nails, axial compressive forces may be mobilized in the nails. The compressive forces would reduce the stability of the nailed structure.

Nail length patterns influence the displacement characteristics of nailed excavations. Soil nails placed in the upper part of a nailed structure in a staged-excavation contributes more towards reducing the horizontal displacement. Those installed in the lower part are more effective in improving stability of the structure.

Under working conditions, shear and bending resistance of soil nails have little contributions to the system of forces maintaining stability within the soil nailed structure. Even when failure conditions are approached, the contribution of shear and bending action may be more significant but is still small. Soil nail used in axial tension is much more efficient than that used in shear and bending.

This report presents the details and results of the study. It also provides guidance on some design aspects of soil nails.

CONTENTS

1. INTRODUCTION

The soil nailing concept involves providing a stable block of composite material by reinforcing the in situ ground with soil nails. Without considering the effect of soil nail heads, the reinforcing action is achieved through two fundamental mechanisms of soil-nail interaction. They are the soil-nail friction that leads to axial tension or compression; and the nail bearing failure that leads to development of shear forces and bending moments in nails. In these two mechanisms, the interactions between soil and nails are complex and the forces developed in the nails are influenced by many factors such as the bearing capacity of the soil to resist stresses from the nail, relative stiffness of the nail and soil, and the tensile strength, orientation, shearing strength and bending capacity of the nail.

This study examines the mechanical behaviour of soil nailed structures in respect of the following aspects:

(a) the effect of nail inclination on development of nail axial force distribution and stability improvement of slopes and excavations;

(b) the influence of nail length patterns on facing deformation in a staged-excavation;

(c) the contribution from bending stiffness of soil nails to stability improvements of slopes and excavations.

2. EFFECT OF NAIL INCLINATION

2.1 General

Unlike the reinforcement in reinforced fill structures, which are placed in horizontal direction, soil nails can be installed in the ground at various inclinations. In cramped sites, soil nails are sometimes installed at large inclinations with little attention being paid to the effect of the nail orientation on the strength of the soil mass. Different nail inclinations may produce different effects on the behaviour of nailed structures.

In this report, nail inclination, α, is the angle of a soil nail made with the horizontal; and nail orientation, θ, is the angle between soil nail and the normal to the shearing surface of soil. The typical relationship between α and θ is presented in Figure 1.

2.2 Previous Laboratory Studies

Many researchers have carried out different laboratory tests to study the effect of soil nail inclination on strengthening of soil. A review of the previous studies by Jewell (1980), Jewell & Wroth (1987), Marchal (1986), Hayashi et al (1988), Palmeira and Milligan (1989) and Johnson et al (2002) has been conducted and the results are presented in Appendix A. A significant finding of these studies is that the overall shearing strength of a reinforced soil is dependent on the orientations of reinforcement.

By varying the orientation of the reinforcement, the reinforcement can either increase or decrease the shear strength of the soil. When the reinforcement is placed in the direction of tensile strain of soil, tensile forces are developed in the reinforcement. Consequently, there is an increase in shear strength of the reinforced soil. When the reinforcement is oriented in the direction of compressive strain of the soil, compressive forces are induced in the reinforcement. This leads to a decrease in the shear strength of the reinforced soil. Results of the previous studies are given in Appendix A.

3. NUMERICAL ANALYSES - EFFECTS OF NAIL INCLINATION AND NAIL LENGTH PATTERN

3.1 General

To study the effects of nail inclination and nail length pattern, numerical simulations were carried out using the two-dimensional finite difference code, Fast Lagrangian Analysis of Continua (FLAC), which was developed by Itasca (1996). The simulations were divided into three principal parts:

(a) investigation of the effect of soil nail inclination on stability of a slope,

(b) investigation of the effect of soil nail inclination on deformations of nailed excavations, and

(c) investigation of the effect of nail length patterns and shotcrete facing thickness on deformation and stability of nailed excavations.

The soil nail was modelled as a cable element which does not take any shear and bending moment. Soil-nail interaction was represented by a spring-slider system having shear springs located at the nodal points along the cable elements.

3.2 Effect of Soil Nail Inclination on Stability of Slopes

3.2.1 Slope and Material Parameters

A simulated slope of 20 m in height, standing at an angle of 55°, and with an up-slope of 10° in gradient was adopted for the analysis. The initial shear strength parameters of the soil were assumed to be c' = 10 kPa, and ϕ' = 43°. For the slope without soil nails, FLAC analysis gave a Factor of Safety (FoS) of 1.0, which compared well with a value of 1.1 using the Morgenstern & Price (M&P) limit equilibrium method. Figure 2 shows the geometry of the slope and the material parameters used in the numerical analysis. Seven rows of nails were provided and this corresponds to a vertical nail spacing (S_v) of 2.5 m. The horizontal spacing of the nails (S_h) was taken to be 1.5 m. Each soil nail was 20 m long with a 40 mm diameter steel bar in a 100 mm grouted hole. The nail heads were modelled as infinitely long concrete beams of 400 mm in width and 250 mm in thickness for a plane strain analysis in FLAC.

A Mohr Coulomb model was used for the soil. The nail heads were modelled as elastic elements. A cable element was used to represent the soil nail as the bending stiffness of the soil nail was not considered. Developments of the tensile forces in the nails were governed either by the tensile strength of the nail or the peak shear strength at the soil-grout interface.

3.2.2 Analytical Approach

Slope stability analysis was first carried out on the unreinforced slope. From the results of the analysis, the unreinforced slope has a minimum factor of safety (FoS) close to 1.0 for the initial soil strength parameters of $c_i' = 10$ kPa, and $\phi_i' = 43^o$.

In slope engineering, the FoS is conventionally defined as the ratio of the actual soil shear strength to the minimum shear strength required for equilibrium. As pointed out by Duncan (1996), FoS can also be defined as "the factor by which the shear strength of the soil would have to be divided to bring the slope into a state of barely equilibrium". FoS can therefore be determined simply by reducing the soil shear strength until failure occurs. This strength reduction approach is often used to compute FoS using finite element or finite difference programs (Dawson et al (1999), Krahn (2003)). In this study, the approach was adopted to determine the FoS of the slope with different nail inclinations.

The nail inclination was varied between 0° and 65°. For each nail inclination, the factor of safety (FoS) was determined by progressively reducing the shear strength of the soil in the model until numerical non-convergence of unbalanced forces and displacements at chosen monitoring points occurred. This analysis was done by trial and error using parameters c_m' and ϕ_m', where

$$c_m' = c_i' / FoS = 10 / FoS \quad (kPa) \quad \text{..... (1)}$$

$$\phi_m' = \tan^{-1} (\tan \phi_i' / FoS) = \tan^{-1} (\tan 43^o / FoS) \quad \text{..... (2)}$$

Knowing that the FoS before provision of soil nails was 1, increase in FoS due to the soil nails with that inclination angle could then be determined.

3.2.3 Results of Numerical Simulations

Outputs of axial nail forces and shear strain distribution of soil obtained from the FLAC analyses are given in Appendix B (Figures B1 to B8).

In the simulation, increases in FoS (ΔFoS) due to the soil nails were calculated for different nail inclinations α. Figure 3 shows the relationship between the calculated ΔFoS and α for the model slope. The ΔFoS is close to 1.0 with little variations for the range of α between 0° and 20°. The ΔFoS decreases substantially as α increases beyond 20°, reflecting that the reinforcing action of the nails reduces rapidly with increasing nail inclinations. When α equals 65°, the ΔFoS is close to 0. This indicates that soil nails (modelled as cable elements) at such large inclinations do not provide any appreciable stabilizing effect.

Figure 4 compares the distribution of axial nail forces at limit equilibrium between two nail inclinations of 20° and 55° at limit equilibrium condition. For $\alpha = 20°$, tensile forces are mobilized in all the soil nails and the nail orientations θ are all positive. For $\alpha = 55°$, compression forces are induced in the upper four rows of the nails whereas tension forces are developed in the lower three rows. The nail orientations are negative for the nails with compression forces and positive for nails with tensile forces.

The forces in the upper nails change from tension to compression when the nail orientation changes from positive to certain negative values (Figure 5) where the orientations of the nails are close to the directions of the compressive strain of the soil. This is consistent with the experimental test results reported by Jewell (1980) and Jewell & Wroth (1987).

The maximum axial force in a nail is T_{max} which is taken to be positive if in tension and negative if in compression. Figure 6 shows the variations of the maximum nail forces with depths for $\alpha = 0°$ to 55°.

The total of the maximum tensile forces mobilised in all the soil nails (ΣT_{max}) at limit equilibrium condition of the model are given below:

Inclination of Soil Nails, α	Total of Maximum Nail Tensile Forces, ΣT_{max}
0°	949 kN/m
5°	933 kN/m
10°	981 kN/m
20°	974 kN/m
30°	850 kN/m
45°	725 kN/m
50°	342 kN/m
55°	60 kN/m
65°	0 kN/m

The above values are plotted in Figure 7 which shows that ΣT_{max} decreases with increasing α. ΔFoS tends to be zero when ΣT_{max} is close to zero. The similarity between Figure 3 and Figure 7 indicates that ΔFoS is related to ΣT_{max}. To study the relationship between ΣT_{max} and the ΔFoS, the ΔFoS of the slope at different α are re-calculated using the Morgenstern & Price (M&P) method. Nail forces derived from the FLAC analyses are used in this analysis. The following two cases have been considered:

(a) maximum axial forces (T_{max}) at individual nail locations; and

(b) the total of the maximum axial forces of the nails is represented by the single force ΣT_{max} which is applied at the surface at the mid-height of the slope, i.e. at the same location of nail SN4.

A typical arrangement of applied forces for the above two cases at $\alpha = 55°$ is shown in Figure 8. The relation between ΔFoS and α for the two cases is presented in Figure 9. The

results obtained from the FLAC analysis are also included in the Figure for comparison. It can be observed from the Figure that the trend of increase in ΔFoS is similar for all the three cases and the maximum difference in ΔFoS is only about 0.2 at $\alpha = 10°$. This indicates that the FoS of a nailed slope is related to ΣT_{max} . The finding agrees with the results of numerical simulations reported by Shiu & Chang (2004).

Shear and bending resistances can also be developed in soil nails. As will be discussed in Section 4 below, the beneficial effect of shear and bending capacity of nails is small, and the reinforcing action of the nails is predominantly derived from axial tensile forces.

3.2.4 Discussion of Results

Conventional limit equilibrium approach using the method of slices is commonly adopted for soil nail design. In these methods, required nail forces are computed for different potential failure surfaces. The lengths of the nails extending beyond the potential failure surfaces are considered to contribute to the stabilising forces. These forces are assumed to be acting in tension. This assumption is valid only if the nails are placed at small inclinations, i.e. close to the direction of principal tensile strain increment in soil. It may not be valid for steeply inclined soil nails. As demonstrated in the numerical simulations above, compressive forces rather than tensile forces can be induced in steep nails. In such a case, the limit equilibrium approach would over-estimate the reinforcing effect of the nails and the overall factor of safety of the slope. An example is presented below to illustrate this.

3.3 Illustrative Example - Effect of Soil Nail Inclination on Slope Stability

Cut slope no. 11W-B/C41 is a slope feature with mixed maintenance responsibility. It is located at Tai Po Road, Sham Shui Po. The upper portion of the slope lies within unallocated Government land and the lower portion within a private lot. A Stage 3 Study was carried out in 2000 on the Government portion of the slope (GEO, 2000). The study showed that the slope portion under consideration had a minimum factor of safety of 0.72 which is below the required value of 1.2. Soil nailing was recommended to improve the stability of the slope. The soil nailing scheme called for 4 rows of 9 m long soil nails with vertical and horizontal spacings of 1.5 m and 2 m respectively. The design was based on the conventional limit equilibrium approach using the Morgenstern and Price method. The required stabilizing force was calculated to be 60 kN/m and it was assumed that this force was distributed evenly between the nails. The inclination of the soil nails was 10^o and the size of nail head was 400 mm x 400 mm x 250 mm thick. Typical details of the soil nailing works are shown in Figure 10.

FLAC analyses were undertaken to determine the factors of safety of the slope for two cases: (i) slope without soil nails; and (ii) slope with the recommended soil nails as shown in Figure 11. Again the analyses adopted the strength reduction approach. The FoS for the cut slope without the soil nails was calculated to be 0.72, the same as that determined from the M&P method. For the slope with the soil nails, the FLAC analysis gave a factor of safety of 1.6 which is higher than the designed FoS of 1.2. This is considered reasonable because the total nail length provided is actually longer than that required for the purpose of

maintaining constant nail length in different rows. Figure 12 shows the distributions of axial forces along the soil nails at limit equilibrium condition. Tension forces are developed in all the soil nails.

In order to examine the effect of nail inclination, the inclination angle α was increased from 10^o to 55^o while the number and spacing of the nails were kept unchanged. This is a hypothetical case. The length of the soil nails was determined using the conventional limit equilibrium design approach. Tension forces were assumed to be developed in all soil nails. For a minimum FoS of 1.2, the total nail force required for α of 55^o was 156 kN/m. Using this total nail force, the required nail length was calculated to be 10 m, i.e. 1 m longer than that required when $\alpha = 10^o$. Figure 13 shows the details of the soil nail pattern derived from the limit equilibrium method.

FLAC analysis was carried out using the same nail pattern as that shown in Figure 14. The calculated factor of safety was 0.85 which is well below 1.2. Figure 15 shows the distributions of the axial forces developed in the nails. Compression force was developed in the top row of nails whereas tension forces were mobilized in the lower three rows of nails. The variations of the maximum nail forces ($\alpha = 10^o$ and $\alpha = 55^o$) with relative to depth are plotted in Figure 16. The total of all the maximum nail forces (ΣT_{max}) is about 170 kN/m for $\alpha = 10^o$ and 27 kN/m for $\alpha = 55^o$. The results show that increased nail inclination results in substantial decrease of nail tension forces, leading to a significant decrease of the reinforcing effect of the nails. This agrees well with the analytical results of the simulated slope presented in Section 3.2.3 above. In the limit equilibrium analysis presented above, the assumption that tensile forces are developed in all the nails is not valid.

3.4 Effect of Soil Nail Inclination on Deformation and Stability of Nailed Excavations

3.4.1 The Model

To acquire a better understanding of the influence of nail inclination, numerical simulation was also conducted on nailed excavations. The vertical excavation was taken to be 6 m in height (see Figure 17). Four rows of 10 m long nails, each with a 40 mm diameter bar in a 100 mm diameter grouted hole, were assumed. Both the vertical and horizontal spacings were taken as 1.5 m. The soil parameters were $c' = 10$ kPa and $\phi' = 40^o$, unit weight = 19 kN/m^3 and an elastic modulus = 20 MPa. The shotcrete facing used was 100 mm in thickness and it was assumed to be connected to the soil nails.

The construction sequence of the nailed excavation was modelled in the analysis, see Figure 18. Construction progressed incrementally in a top down manner by repeating two steps of construction. The first step began with soil being excavated to a depth of 0.5 m below the level of soil nail. Step 2 consisted of installing the soil nail and concrete facing. Steps 1 and 2 were repeated until the full excavation depth (6 m) was attained. Figure 18 shows the excavation sequence considered in the analysis. The effects of nail inclinations were studied by changing the nail inclinations between 0^o and 35^o.

For $\alpha = 35^o$, the excavation collapsed when the excavation reached a depth of 5.5 m, before installation of the bottom nail. For α less than 35^o, the excavations were stable throughout the whole construction process.

3.4.2 Axial Forces Mobilised in the Soil Nails

Figure 19 shows the variations in maximum axial nail forces (T_{max}) with excavation depth for different α values. The maximum forces mobilized in the nails are not constant and they vary with depth. Relatively large forces are mobilised in the first nail. This may probably be due to the cantilever effect before the second row of nails is placed. The forces increase from row 2 to row 3 of the nail, below which they start to decrease with depth. This variation in maximum nail forces is consistent with the field monitoring results observed by Shiu et al (1997), see Figure 20. Except for row 1, the maximum tensile forces mobilised in individual nails generally decrease with increasing nail inclinations, indicating that the reinforcing action of the nails reduces when nail inclination increases. As mentioned above, for $\alpha = 35^o$, the excavation collapsed before the installation of the bottom nails.

Plots of the results of the FLAC analyses showing the distribution of axial forces along individual nails and shear strain and displacements of the nailed soil mass for $\alpha = 0^o$ to 35^o are given in Appendix C (Figures C1 to C6).

3.4.3 Horizontal Deformation of the Excavation Face

The development of nail forces is a function of the displacements in the nailed soil mass. As reported above, the distribution and magnitude of the axial forces are affected by the nail inclinations, and hence the deformation. Figure 21 shows the profiles of horizontal deformation of the excavation face as a function of nail inclinations at the final stage of excavation. The horizontal deformation increases with increasing nail inclinations, and there is a sharp increase in deformations when α increases from 25^o to 30^o. The analytical results show that the magnitude of the horizontal displacement is influenced by nail inclination.

3.5 Effect of Nail Length Pattern on Deformation

For limit equilibrium design methods, it is possible to define a wide variety of nail length patterns that satisfy stability requirements but that may not be satisfactory in terms of serviceability. It is specially the case for soil nailed excavations using the top-down method of construction.

FLAC analyses have been carried out to review the effect of different nail length patterns on deformation of excavations. The excavation was taken to be 6 m deep with four rows of soil nails. The following three nail length patterns were considered in the analysis (Figure 22):

- Pattern (1) - nail length increasing with depth;
- Pattern (2) - constant nail length;
- Pattern (3) - nail length decreasing with depth.

In each of the three patterns, the total length of soil nails was 32 m. The reinforcement was 40 mm diameter steel bar grouted in a 100 mm hole. The nail inclination was 10^o. Both the vertical and horizontal spacings were taken as 1.5 m. The soil strength parameters used were $c' = 5$ kPa and $\phi' = 39^o$, with a unit weight of 19 kN/m^3 and an elastic

modulus of 10 MPa. The shotcrete facing used was 100 mm in thickness and it was connected to the soil nails. The excavation sequence for the three cases is the same as that shown in Figure 18.

From the FLAC analysis, the FoS corresponding to patterns (1), (2) and (3) after completion of construction are 1.8, 1.7 and 1.5 respectively. The profiles of horizontal deformations of the excavation faces obtained from the FLAC analysis for the three nail length patterns are plotted in Figure 23. Although nail length pattern (1) has the highest FoS, its horizontal deformation is the largest and this is followed by pattern (2). Nail length pattern (3), despite its lowest FoS, has the smallest deformation. This illustrates that in a nailed excavation, installing longer nails at the top of the excavation will help limit the amount of horizontal ground movement.

The result shows that soil nails placed in the upper part of a nailed structure in a staged-excavation contributes more toward reducing the horizontal displacement. Those nails installed in the lower part are more effective in improving stability of the structure. It is due to their larger anchorage lengths beyond the potential failure surfaces.

3.6 Effect of Shotcrete Facing Thickness on Deformation of Nailed Excavation

The effect of shotcrete facing thickness on nailed excavation was also studied using the FLAC model as shown in Pattern (2) of Figure 22. Different facing thicknesses (t) of 25 mm, 75 mm, 100 mm and 200 mm were used in this parametric study. The maximum nail force (T_{max}) for each nail, the total of the maximum nail forces for all nails (ΣT_{max}) and the horizontal deformation ΔH at the crest are tabulated in Table 1.

It can be seen from Table 1 that the nail forces are quite similar for all thicknesses (t), indicating that the FoS after the nailed excavation are about the same for all cases. However, the horizontal deformation at crest is 12 mm when t = 25 mm. The deformation decreases by about 21% to 9 mm when t is increased to 75 mm. When t is increased beyond 75 mm, the horizontal deformation is not sensitive to facing thickness. Similar results were reported by Babu (2002), which showed that for facings of 75, 100 and 150 mm thick, there was no significant difference in respect of horizontal displacement.

3.7 Overseas Practices for Soil Nail Inclination

Most of the overseas design approaches recognize the importance of soil nail inclinations in respect of nailed structures. For the practice in USA (FHWA, 1998), France (French National Research Project, 1991) and Japan (JHPC, 1988), nail inclinations are to be kept to be as small as practicable. For installation reasons, they are normally placed at angles of inclination of 5^o to 15^o. According to French National Research Project (1991), if soil nails are placed in such an inclination that compressive forces are developed in the nails, the effect of compressive forces should be taken into account in design.

3.8 Discussion

Behaviour of nailed structures is a strain compatibility problem. A nail force develops through the interaction among the deforming soil, the nail and nail head. An important point here is that depending on the nail orientation, compressive forces rather than tension forces can be mobilized in soil nails. This contradicts the common design assumption used in limit equilibrium methods that only tensile forces are developed in nails. The limit equilibrium methods do not consider strains and displacements, and as a result, they would give rise to invalid results in calculating nail forces and factors of safety of nailed slopes with steeply inclined nails. Care is therefore required when using these methods for the design of steeply inclined soil nails. The development of compressive force in soil nails should be considered in such cases.

4. EFFECT OF BENDING STIFFNESS OF SOIL NAILS

4.1 General

Steel nails can also sustain shear forces and bending moments and this ability may also enhance the shear strength of soil. The development of shear force in nails involves a mechanism which is dependent on the relative stiffness of the nail and the ground mass, the soil bearing strength, orientation and shear deformation of reinforcement and the thickness of shear zone.

The ability of soil nails to increase the shear strength of soil by acting under combined loading of shear and tension is one of the more controversial aspects of design. The presence of axial tensile/compressive force in a bar reduces the maximum bending moments that can be supported. In turn, the maximum shear force that can be developed in a bar depends on the maximum bending moment. There is therefore a connection between the maximum axial force and the maximum shear force that a soil nail can support.

4.2 Multicriteria Method

Schlosser (1982) developed a multicriteria method to determine the combination of limiting forces causing failure. The method takes into account the contribution of reinforcement shear and bending moments. Other methods, such as those proposed by Juran et al (1990) and Bridle (1989), either fully or partly employ the multicriteria method. The multicriteria method is based on four failure criteria:

(i) the friction between nail and soil (pull-out failure);

(ii) the bearing capacity of soil for resisting loads imposed by the nail;

(iii) the capacity of the nail to resist shear while being subjected to axial force at the same time (strength criterion for soil nail); and

(iv) the capacity of the nail to resist shear once it has started deforming plastically by bending (plastic hinge).

The multicriteria method is a combination of elastic and plastic analyses. Figure 24 shows the graphical presentation of these criteria in terms of axial and shear force. In considering the deformation of the nail caused by lateral earth pressure, the nail is assumed to behave like a laterally loaded pile, see Figure 25. According to Schlosser (1982), the strength criterion is given by:

$$\left(\frac{2P_s}{T_p}\right)^2 + \left(\frac{T}{T_p}\right)^2 = 1 \quad \text{..... (3)}$$

where T and P_s are the nail axial force and nail shear force respectively, and T_p is the axial capacity of the nail. This criterion is applicable to the location where the bending moment in the nail is zero, i.e. where the nail intersects the shear plane.

There has been much debate on the Schlossor's multicritera method. The main issues are related to the validity of the failure criteria of the nail under the combined loading e.g. the link between shear stress and bending moment in a nail is not defined, use of Mohr's Circle to define the strength of nail is not valid, etc. Details of the discussion are given in Schlosser (1982, 1991), Juran et al (1990), Jewell & Pedley (1990 and 1992) and Pedley et al (1990a and 1990b). Subsequently, the multicriteria method has been refined to incorporate these issues. Details of the refined method can be found in Recommendations Clouterre (French National Research Project (1991)).

Although there have been debate amongst researchers as to the behaviour of soil reinforcement under the combined loadings, there appears to be a common understanding that the reinforcing action of soil nails is predominantly derived from the axial tensile forces in nails and the beneficial effect of shear and bending capacity of nail is of secondary influence only. Furthermore, it is also a common view that the shear and bending forces are mobilised in nails only when a nailed structure is close to failure. Schlosser (1991), who has developed the multicriteria method, stated that

> "at failure, the bending and shear resistances of grouted nails are mobilised and therefore have to be taken into account…However, one should note that the principal resistance remains the tensile force exerted in the nails and that bending and shear resistances have always a limited effect on the global safety factor (less than 15%)".

4.3 Previous Studies Relating to Bending Stiffness

Apart from the work by Schlosser (1982), the effect of the bending stiffness of the nail on nail forces and displacements has also been investigated by many other researchers. A review of the previous studies relating to bending stiffness (Marchal (1986), Gigan & Delmas (1987), Pluemelle et al (1990), Pedley (1990), Jewell and Pedley (1990 & 1992), Davies et al (1993), Bridle & Davies (1997), Davies & Le Masurier (1997),

Smith and Su (1997) and Tan et al (2000)) has been undertaken and the findings are summarised in Appendix D. The most notable and comprehensive investigation is the laboratory and theoretical study reported by Pedley (1990) and Jewell and Pedley (1990 & 1992). In that study, both the laboratory and theoretical results show that reinforcement bending stiffness allows only a small additional shear force to be mobilised in the soil nail, and that soil nail used in shear and bending is much less efficient than that used in axial tension. Details of the study are also given in Appendix D.

5 NUMERICAL ANALYSIS - EFFECT OF BENDING STIFFNESS

5.1 Slope and Material Parameters

Numerical simulations using the two-dimensional plane strain finite element programme PLAXIS were undertaken to examine the effect of bending stiffness of soil nails. The model slope shown in Figure 2 was again adopted in the simulations. The nail was modelled as a beam element which can take axial force, shear force and bending moment. For grouted nails, the grout tends to crack under tension. As such only the bending stiffness of the steel bar was considered.

The plastic axial capacity of the steel bar (T_p) is given by:

$$T_p = (A_s)(\sigma_y) \quad \text{..... (4)}$$

where A_s is the cross-sectional area of the steel bar and σ_y is the steel yield strength. The plastic bending moment capacity of the steel bar (M_p) is given by:

$$M_p = \frac{D^3\sigma_y}{6} \quad \text{..... (5)}$$

where D is the diameter of the steel bar.

When the combination of a bending moment (M) and an axial force (T) occur in a bar, the actual bending moment or axial force at which plasticity occurs is lower than M_p or T_p respectively. According to Calladine (2000), the relationship between M_p and T_p is shown in Figure 26. The limiting plastic envelope, which is safe for a bar of any cross-section, is given by:

$$\frac{M}{M_p} + \frac{T}{T_P} = 1 \quad \text{..... (6)}$$

In the simulations, the FoS of the slope with the soil nails at a given inclination was determined by the strength reduction approach. The nail inclination was varied between 0^o and 65^o. The increases in FoS (ΔFoS) due to the soil nails were then determined on the basis that the slope had a FoS of 1 before provision of the soil nails.

5.2 Results of Numerical Simulations

Outputs of the PLAXIS analysis for the two cases of $\alpha = 20°$ and $\alpha = 55°$ are given in Appendix E (Figures E1 to E10). They include the axial forces, shear forces and bending moments mobilised in the nails, the deformed shapes of the nails and the shear strains developed in the slope. Tensile forces are mobilized in all the soil nails for $\alpha = 20°$ whereas for $\alpha = 55°$, compressive axial forces are mobilised in the upper nails and tensile forces in the lower nails. This modelling result is similar to that of the FLAC analysis described in Section 3.2 above.

Figure 27 shows the total of the maximum tensile forces mobilised in all the soil nails (ΣT_{max}) at limit equilibrium condition of the slope model. The maximum shear force in a nail at the location where the shear plane intersects the nail is Ps_{max}. The total of the maximum shear forces (ΣPs_{max}) mobilised in the soil nails at limit equilibrium condition of the model are plotted in Figure 27. The value of ΣPs_{max} rises steadily with increasing nail inclination. The rise is small, from 31.4 kN/m at $\alpha = 10°$ to 76 kN/m at $\alpha = 55°$. In contrast, the value of ΣT_{max} decreases rapidly with increasing nail inclination, very similar to the result of the previous FLAC analysis (Figure 7). For small nail inclinations, ΣT_{max} is much larger than ΣPs_{max}.

Figure 28 shows the relationship between the increase in FoS (ΔFoS) and nail inclination (α) determined from the PLAXIS analysis. The results obtained from the earlier FLAC analysis are also included in the Figure for comparison. Despite the fact that the PLAXIS analysis has considered the bending stiffness of the soil nails and the FLAC analysis has ignored this aspect, there is only small disparity in the values of ΔFoS calculated by these methods. The results of both the PLAXIS and FLAC analyses indicate that the ΔFoS decreases substantially as α increases beyond 20°. They also show that ΔFoS at $\alpha = 55°$ is close to zero, indicating that the nails at this inclination have no reinforcing effect.

Comparing between Figures 27 and 28, it can be noted that both ΔFoS and ΣT_{max} generally decrease with increasing nail inclinations. This similarity illustrates that ΔFoS is strongly influenced by the nail axial force. On the other hand, ΣPs_{max} shows an opposite trend to that of ΔFoS, i.e. ΣPs_{max} increases with increasing nail inclinations. This demonstrates that ΔFoS is not sensitive to the shear resistances in the nails.

The modelling result indicates that only small shear forces are mobilised in soil nails and they provide little reinforcing effect to the slope. The resisting mode of the nails relies primarily on axial tensile forces, except for the case of $\alpha = 55°$ where the total maximum shear force is comparable to the total tensile force.

5.3 Development of Axial, Shear and Bending Resistances with respect to Failure Criteria

The results of the PLAXIS analysis are compared with the different failure criteria mentioned in Section 4.2 above. These criteria include soil bearing failure, plastic hinge and nail material strength. Pullout failure is not considered as long soil nails (20 m) have been used in the analysis and the modelling results do not show any signs of pullout failure.

For the soil bearing failure, the following equation derived by Jewell and Pedley (1992) has been used to determine the soil bearing capacity, σ'_b:

$$\sigma_b' = \frac{\sigma_v'(1+K_a)}{2}\tan\left[\frac{\pi}{4}+\frac{\phi'}{2}\right]\exp\left\{\left(\frac{\pi}{2}+\phi'\right)\tan\phi'\right\} \quad \text{..... (7)}$$

where K_a is the active earth pressure coefficient and σ'_v is effective vertical stress in the soil.

For the plastic hinge failure of the soil nail (steel bar), the following equation developed by Pedley (1990) is used:

$$\frac{P_s}{T_p} = \frac{8}{3\pi\ (l_s/D)}\left\{1-\left[\frac{T}{T_p}\right]^2\right\} \quad \text{..... (8)}$$

where l_s is the distance between the points of maximum moment in the nail on either side of shear plane (see Figure 25) and D is the diameter of the bar. The derivation of the equation can be found in Appendix D.

Figure 29 shows the limiting envelopes for the three failure criteria. It can be noted that the limiting envelope for the plastic hinge failure is most critical. The shear forces and axial forces developed in the individual nails for the two cases of $\alpha = 20°$ and $\alpha = 55°$ are shown in the Figure for comparison. The shear and axial forces are taken at locations where the soil shear plane intersects the nails. The Figure indicates that all the shear and axial forces are within the limiting envelope for plastic hinge failure. The shear forces mobilised in nails of $\alpha = 55°$ are larger than those in nails of $\alpha = 20°$, but the differences are small. In contrast, nails of $\alpha = 20°$ have much larger mobilised tensile forces than nails of $\alpha = 55°$.

Figure 30 presents the stress conditions of the nails for the two cases of $\alpha = 20°$ and $\alpha = 55°$. The bending moment (M) and the axial force (T) developed in the nails at limit equilibrium condition of the model slope are normalised by the plastic moment capacity (M_p) and the full plastic axial capacity (T_p) respectively. The values of M and T are the maximum moment and maximum axial force at or near the location where the shear plane intersects the nail. It can be observed from the Figure that the bending resistances mobilised in the nails of $\alpha = 55°$ are close to the fully plastic moment ($M/M_p = 1$). Even though the moment capacity is almost fully mobilised, the shear resistances induced in the nails are still small (see Figure 29). For nails of $\alpha = 20°$, the bending resistances developed in the nails are much smaller.

5.4 Discussion

It has been demonstrated by many researchers by means of laboratory tests, theoretical analysis and monitoring of in-service and test nailed structures that the contribution of shear/bending is negligible under the service load conditions. Large soil displacements are required to mobilise shear and bending forces in the nails. As explained by Gässler (1997), in limit equilibrium design, it is assumed that "the maximal resistance of the soil and of the nails in the various rows is simultaneously mobilised at failure. For vertical or near to the

vertical slopes this hypothesis is only valid for tensile resistance (in other words: the pulling-out resistance) of the nails, but not for shear forces due to bending. In sandy or clayey soils, the latter are mobilised too late! This was measured by instrumented nails during failure of several full scale test walls".

Even when failure conditions are approached, the contribution of shear/bending action may be more significant but is still small. Under such conditions close to failure, the amount of soil displacements renders the nailed structure unserviceable. For these reasons, most soil nailing design methods of soil nailing design, such as those used in USA (FHWA, 1998), UK (Department of Transport, 1994), Japan (JHPC, 1998) and Germany (Gässler, 1997) ignore any beneficial effects from the mobilisation of shear force or bending stress in the nails. An exception to this is the French design approach (French National Research Project, 1991) in which the contributions of shear and bending of the nails are considered. It should however be noted that the French National Research Project (1991) emphases that shear forces are mobilised in nails only when the structures are near failure.

It is stated in FHWA (1997) that a design approach which considers both the axial tensile forces and shear forces has created confusion in respect of the terminology and design of soil nailing: "for many, the term nail is used to define a tensile reinforcing element (whereas shear reinforcing elements are termed dowels), whereas for others, the term nail appears to define any small diameter reinforcing element that can act in both tension and shear. Similarly, the confusion appears to extend to the designers themselves, wherein certain designers orient the reinforcing elements approximately parallel to the direction of anticipated maximum tensile strains (nailing action) and others orient the reinforcing elements approximately perpendicularly to the anticipated direction of maximum shear strain (doweling action)".

To avoid unnecessary confusion, the function and role of soil nailing are clearly defined in FHWA (1998): "in soil nailing, the reinforcement is installed horizontally or sub-horizontally (approximately parallel to the direction of major tensile straining in the soil) so that it contributes to the support of the soil partially by directly resisting the destabilizing forces and partially by increasing the normal loads (and hence the shear strength) on potential sliding surfaces".

6. CONCLUSIONS

Inclinations of soil nails can affect the reinforcing action of the nails. Increase in soil nail inclination would decrease the reinforcing forces in the nails and in turn reduce the stabilizing effect. For steeply inclined soil nails, axial compressive forces may be mobilized in the nails. The compressive forces would reduce the stability of the nailed structure.

The behaviour of a nailed slope is affected by strain compatibility of different components. The limit equilibrium method of slices does not consider strains and displacements and as a result, it may create difficulties in calculating nail forces and factors of safety of nailed slopes. Care is therefore required in using this method for the design of steeply inclined soil nails.

Nail length patterns influence the displacement characteristics of nailed excavations. Soil nails placed in the upper part of a nailed structure in a staged-excavation contributes

more towards reducing the horizontal displacement. Those installed in the lower part are more effective in improving stability of the structure. This is because of their contribution in relation to the potential failure surfaces and their larger anchorage beyond the potential failure surfaces.

Under working conditions, shear and bending resistances of soil nails have little contributions to the system of forces maintaining stability within the soil nailed structure. Even when failure conditions are approached, the contribution of shear and bending action may be more significant but is still small. Soil nail used in axial tension is much more efficient than that used in shear and bending. Soil movements required to mobilise axial force are much less than those required for shear force in the reinforcement. As a result of the mobilization of shear and bending resistances at large deformations, a nailed structure tends to exhibit relatively ductile failure rather than sudden failure.

To ensure that the predominant action of nails is in tension, soil nails should be installed at small inclinations which correspond to tensile strains of soil. Under this condition, shear force and bending moment that are mobilised in the soil nails would be small. Besides, steel soil nails can undergo large shear deformations and the deformations can induce additional axial tensile forces in the nails, which in turn help strengthen the soil. As such, there is no need to check the shear and bending capacity of the steel soil nails in normal designs. However, if the nails are steeply inclined, shear forces and bending moments induced in the nails will become more significant. The structural capacity of the nail to sustain the combined loading of tension (or compression), shear and bending should be considered.

7. RECOMMENDED DESIGN APPROACHES

It is recommended that soil nails should be installed at inclinations close to the horizontal so that the predominant action of the nails is in tension. An inclination angle of 10^o to 20^o is preferred for better reinforcing effect and facilitating grouting of drillholes under gravity or low pressure. At these inclinations, contribution from the shear and bending resistances mobilised in the nails is not significant and may be discounted.

Where it is necessary to increase nail inclination to meet physical constraints, careful consideration should be given to the effectiveness of the soil nails and the amount of slope deformation to mobilise the nail force. Designs using nails with inclinations greater than 20^o should demonstrate their effectiveness, for example, using stress-strain analysis. For steeply inclined nails, the capacity of the nails to take the combined loads of tension (or compression), shear and bending should be checked.

Where deformation of a nailed excavation may cause damage to nearby structures, services and land, a deformation analysis should be carried out to demonstrate that the anticipated ground movements are within acceptable limits. Stress-strain finite element or finite difference softwares or other suitable tools may be used for the analysis. Increasing the length of soil nails near the top of the nailed excavation beyond the potential slip surface can be an effective means to reduce its horizontal deformations.

8. REFERENCES

Babu, G.L.S., Murthy, B.R.S. and Srinivas A. (2002). Analysis of Construction Factors influencing the Behaviour of Soil-Nailed Earth Retaining Walls. Ground Improvement, 6, No. 3, pp 137-143.

Bridle, R.J. (1989). Soil nailing - analysis and design. Ground Engineering, September, pp 52-56.

Bridle, R.J. and Davies, M.C.R. (1997). Analysis of soil nailing using tension and shear: experimental observations and assessment. Geotechnical Engineering, Proceedings of the Institution of Civil Engineers, July, pp 155-167.

Calladine, C.R. (2000). Plasticity for Engineers: Theory and Applications. Horwood Publishing Limited, 318p.

Davies, M.C.R., Jacobs, C.D. and Bridle, R.J. (1993). An experimental investigation of soil nailing. Retaining Structures, Proceedings of the Conference of Retaining Structures, Thomas Telford, 20 - 23 July.

Davies, M.C.R. and Le Masurier, J.W. (1997). Soil/Nail Interaction Mechanism from Large Direct Shear Tests. Proceedings of the Third International Conference on Ground Improvement GeoSystems, London, pp 493-499.

Dawson, E.M., Roth, W.H. and Drescher, A. (1999). Slope stability analysis by strength reduction. Géotechnique, Vol. 49, No. 6, pp 835-840.

Department of Transport (1994). Design Manual for Roads and Bridges: Design Methods for the Reinforcement of Highway Slopes by Reinforced Soil and Soil Nailing Techniques, HA68/94, Department of Transport, UK.

Duncan, J.M. (1996). State of the art: limit equilibrium and finite element analysis of slopes. Journal of Geotechnical Engineering. ASCE122, No. 7, pp 557-596.

FHWA (1997). FHWA International Scanning Tour for Geotechnology, September-October 1992, Soil Nailing Summary Report. Federal Highway Administration, Washington, D.C.

FHWA (1998). Manual for Design & Construction monitoring of Soil Nail Walls. Federal Highway Publication No. SA-96-069R, U.S. Department of Transportation, Federal Highway Administration, Washington, D.C.

French National Research Project (1991). Recommendations Clouterre: Soil Nailing Recommendations for Designing, Calculating, Constructing and Inspecting Earth Support Systems Using Soil Nailing (English Translation), Presses de lecole Nationale des Ponts et Chaussees.

Table of Contents
Table of Contents
Table of Contents
Table of Contents

Gässler, G. (1997). Design of reinforced excavations and natural slopes using new European Codes. Earth reinforcement. (edited by Ochiai, N. Yasufuku & K. Omine, Balkema, Rotterdam, pp 943-961.

GEO (2000). Slope No. 11NW-B/C41 (Government Portion), 58 Tai Po Road, Shum Shui Po. Stage 3 Study Report S3R 97/2000. Geotechnical Engineering Office, Hong Kong.

Gigan, J.P. and Delams, P. (1987). Mobilisation of stresses in nailed structures. English translation, Transport and Road Research Laboratory, Contractor Report 25.

Hayashi, S. and Ochiai, H., Yoshimoto, A., Sato, K. and Kitamura, T. (1988). Functions and Effects of Reinforcing Materials in Earth Reinforcement. Proceedings of International Geotechnical Symposium on Theory and Practice of Earth Reinforcement, Fukuoka, 5-7 October, pp 99-104.

Itasca (1996). Fast Lagrangian Analysis of Continua (FLAC) Manual, Version 4.0. Itasca Consulting Group, Inc., Minnesota.

Japan Highway Public Corporation (JHPC) (1998). Design & Works Outlines on the Soil-Cutting Reinforcement Soilworks (English Translation), Japan Highway Public Corporation.

Jewell, R.A. (1980). Some effects of reinforcement on the mechanical behaviour of soils. PhD thesis, University of Cambridge.

Jewell, R.A. and Wroth, C.P. (1987). Direct shear tests on reinforced sand. Géotechnique, Vo. 37, No. 1, pp 53-68.

Jewell, R.A. and Pedley, M.J. (1990). Soil nailing design: the role of bending stiffness. Ground Engineering, March, pp 30-36.

Jewell, R.A. and Pedley, M.J. (1992). Analysis for Soil Reinforcement with Bending Stiffness. Journal of Geotechnical Engineering, ASCE, Vol. 118, No. 10, October, pp 1505-1528.

Johnson, P.E., Card, G.B. and Darley, P. (2002). Soil nailing for slopes, (TRL Report TRL537). TRL Limited, UK, 53 p.

Juran, I., Baudrand, G., Farrag, K. and Elias, V. (1990). Kinematical Limit Analysis for Design of Soil-Nailed Structures, ASCE Journal of Geotechnical Engineering, Vol. 116, No. 1, January, pp 54-72.

Krahn, J. (2003). The 2001 R.M. Hardy Lecture: The limits of limit equilibrium analyses. Canadian Geotechnical Journal, Vol. 40, pp 643-660.

Marchal, J. (1986). Soil nail - experimental laboratory study of soil nail interaction (English Translation), Transport and Road Research Laboratory, Department of Transport, Contractor Report No. 239.

Table of Contents
Table of Contents
Table of Contents
Table of Contents

Palmeira, M. and Milligan, G.W.E. (1989). Large Scale Direct Shear Tests on Reinforced Soil. Soils and Foundations, Vol. 29, No. 1, March, pp 18-30.

Pedley, M.J., Jewell, R.A. and Milligan, G.W.E. (1990a.). A large scale experimental study of soil-reinforced interaction - Part I. Ground Engineering, July/August, pp. 45-49.

Pedley, M.J., Jewell, R.A. and Milligan, G.W.E. (1990b.). A large scale experimental study of soil-reinforced interaction - Part II. Ground Engineering, September, pp. 44-50.

Pedley, M.J. (1990). The Performance of Soil reinforcement in Bending and Shear, PhD thesis, University of Oxford.

Plumelle, C., Schlosser, F., Delage, P., and Knochenmus, G. (1990). French National Research Project on Soil Nailing. Proceedings of a Conference of Design and Performance of Earth Retaining Structures, ASCE Geotechnical Special Publication No. 25, edited by Philip C. Lambe and Lawrence A. Hansen, June 18-21, pp 660-675.

Schlosser, F. (1982). Behaviour and design of soil nailing. Proceedings of Symposium on Recent Developments in Ground Improvements, Bangkok, 29 Nov. - 3 Dec., pp 399-413.

Schlosser, F. (1991). Discussion - The multicriteria theory in soil nailing. Ground Engineering, November, pp. 30 - 33.

Shiu, Y.K. and Chang, W.K.G. (2004). Soil Nail Head Review. Special Project Report SPR 8/2004. Geotechnical Engineering Office, Hong Kong, 104 p.

Shiu, Y.K., Yung, P.C.Y., and Wong, C.K. (1997). Design, Construction and Performance of Soil Nailed Excavation in Hong Kong. Proceedings of the XIVth International Conference Soil Mechanics and Foundation Engineering, 6-12 September, Hamburg, Germany, pp 1339-1342.

Smith, I.M. and Su, N. (1997). Three-dimensional FE Analysis of a Nailed Wall Curved in Plan. International Journal for Numerical and Analytical Mehtods in Geomechanics, vol. 21, pp 583-597.

Tan, S.A., Luo, S.Q. and Yong, K.Y. (2000). Simplified models for soil-nail lateral interaction. Ground Improvement, Thomas Telford, Volume 4, Number 4, October, pp 141-152.

Table of Contents
Table of Contents
Table of Contents
Table of Contents

LIST OF TABLES

Table 1 - Summary of Nail Head Forces, Maximum Tensile Forces in Nails and Horizontal Deformations at Crest for Different Thickness of Facing

Nail no.	z (m)	T_{max} (kN)			
		t = 25 mm	t = 75 mm	t = 100 mm	t = 200 mm
N1	0.5	19.04	18.83	18.86	17.48
N2	2.0	18.51	15.83	15.50	17.19
N3	3.5	23.37	25.77	25.23	25.27
N4	5.0	13.08	14.67	15.08	12.90
ΣT_{max} (kN)		74.00	75.10	74.67	72.84
ΔH at crest (mm)		11.82	9.28	8.60	7.46

Legend:

ΔH	Horizontal deformation at crest	t	Shotcrete facing thickness
T_{max}	Maximum axial soil nail force / metre run	z	Vertical distance measured from crest

LIST OF FIGURES

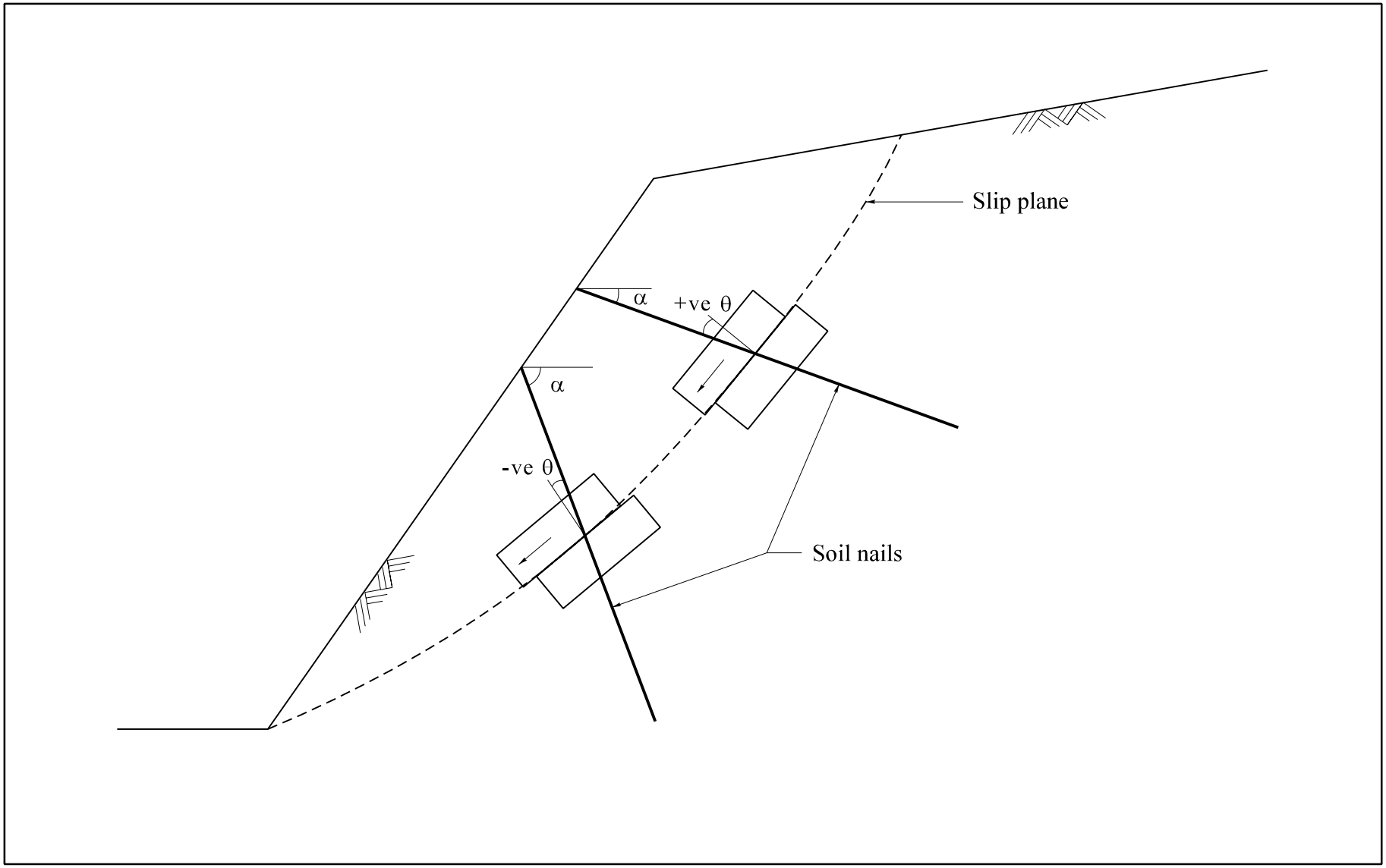

Figure 1 - Relationship between Nail Inclination α and Nail Orientation θ

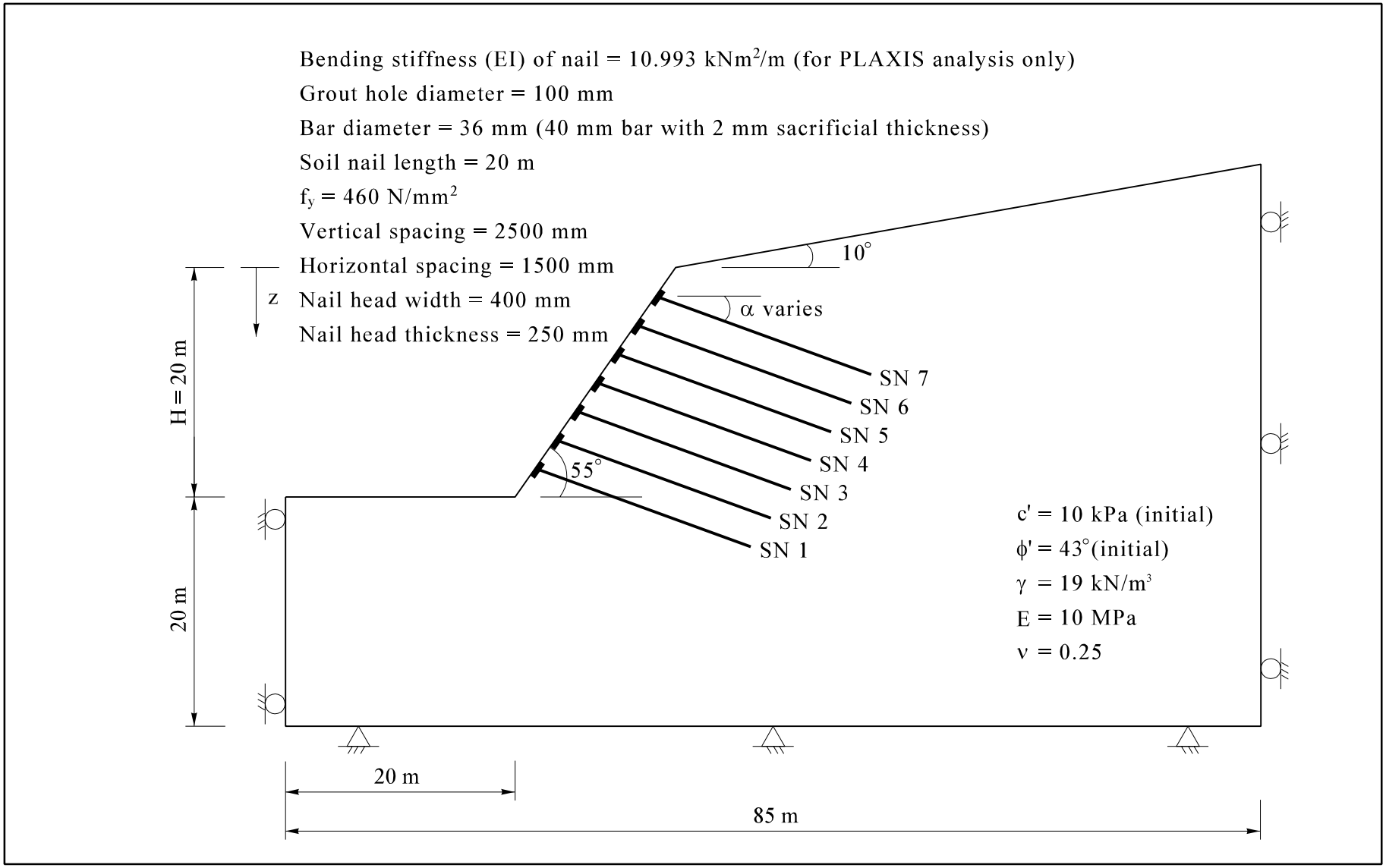

Figure 2 - Geometry and Material Parameters of Model Slope for Study of Nail Inclinations

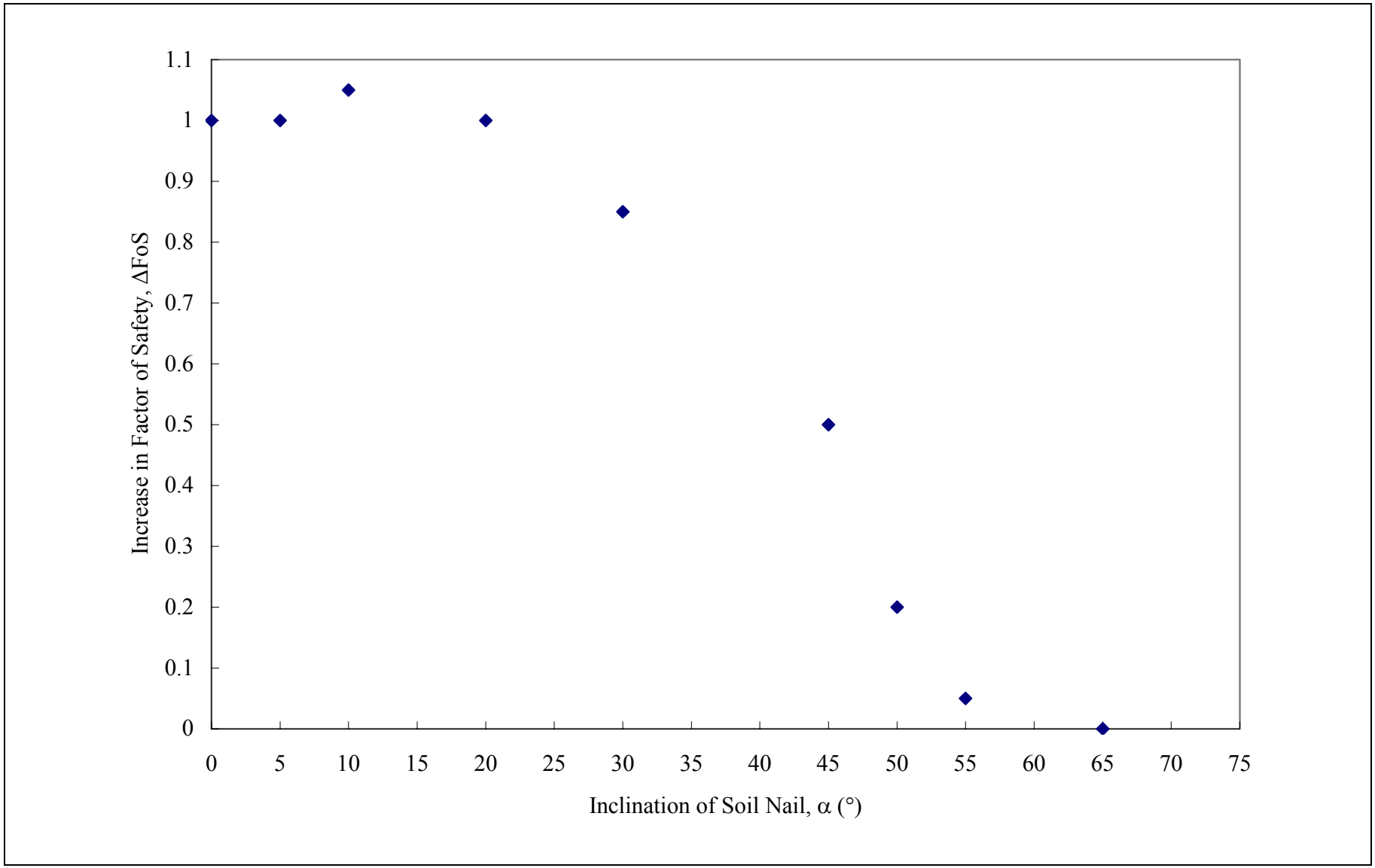

Figure 3 - Variation of ΔFoS with Nail Inclination

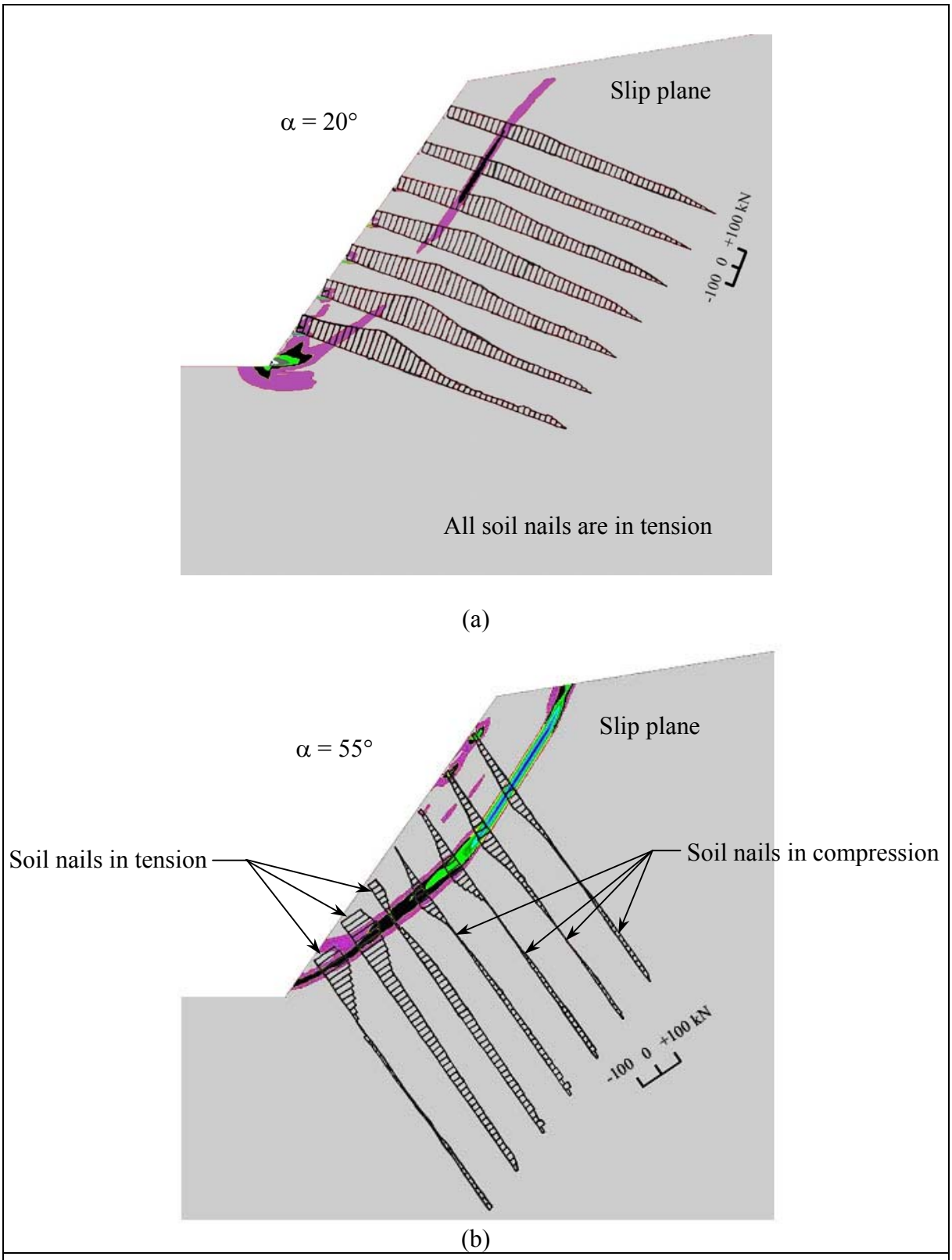

Figure 4 - Axial Force Distribution in Nails for (a) $\alpha = 20^{\circ}$ and (b) $\alpha = 55^{\circ}$

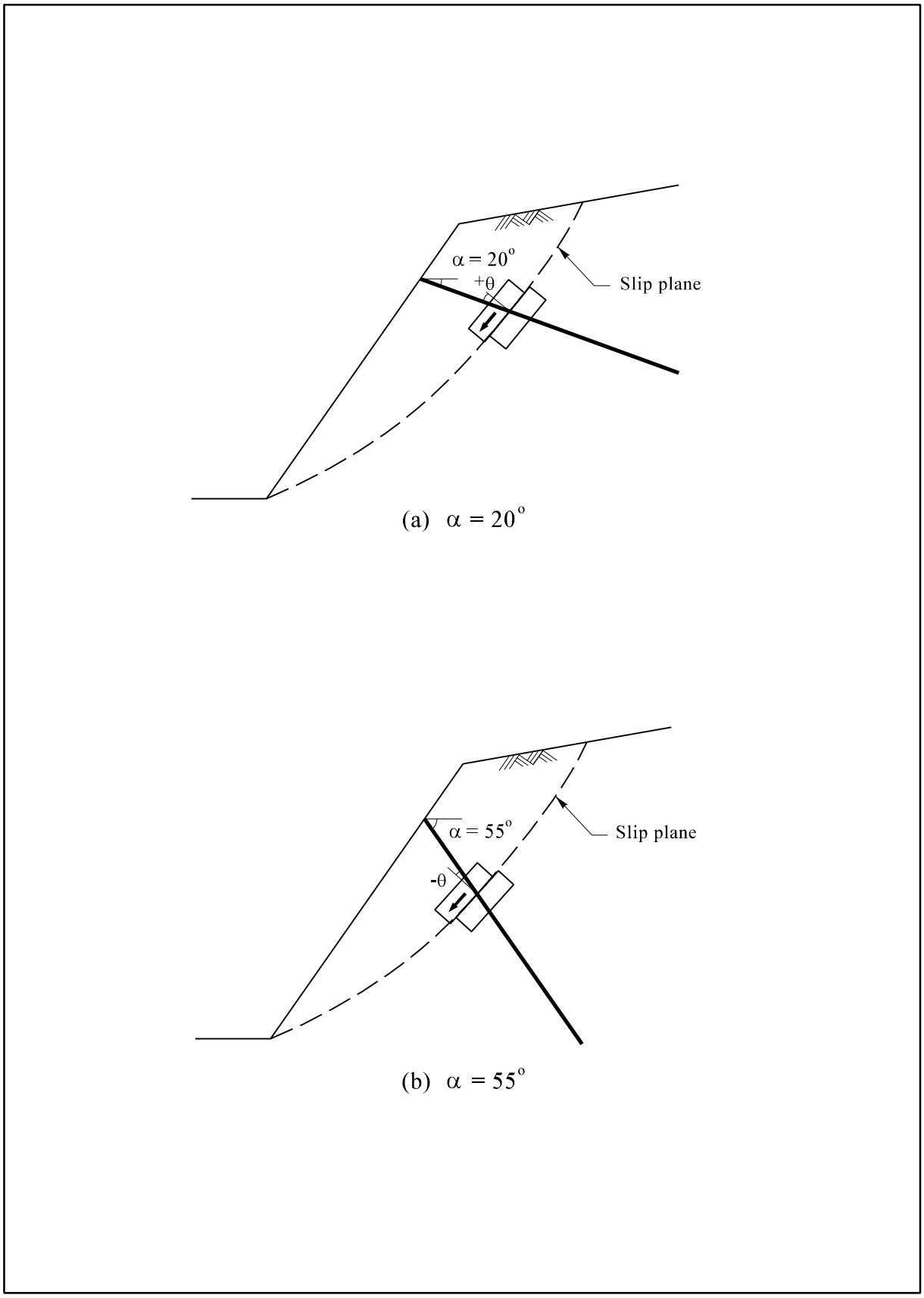

Figure 5 - Relationship between Nail Inclination α and Orientation θ for the Simulated Slope

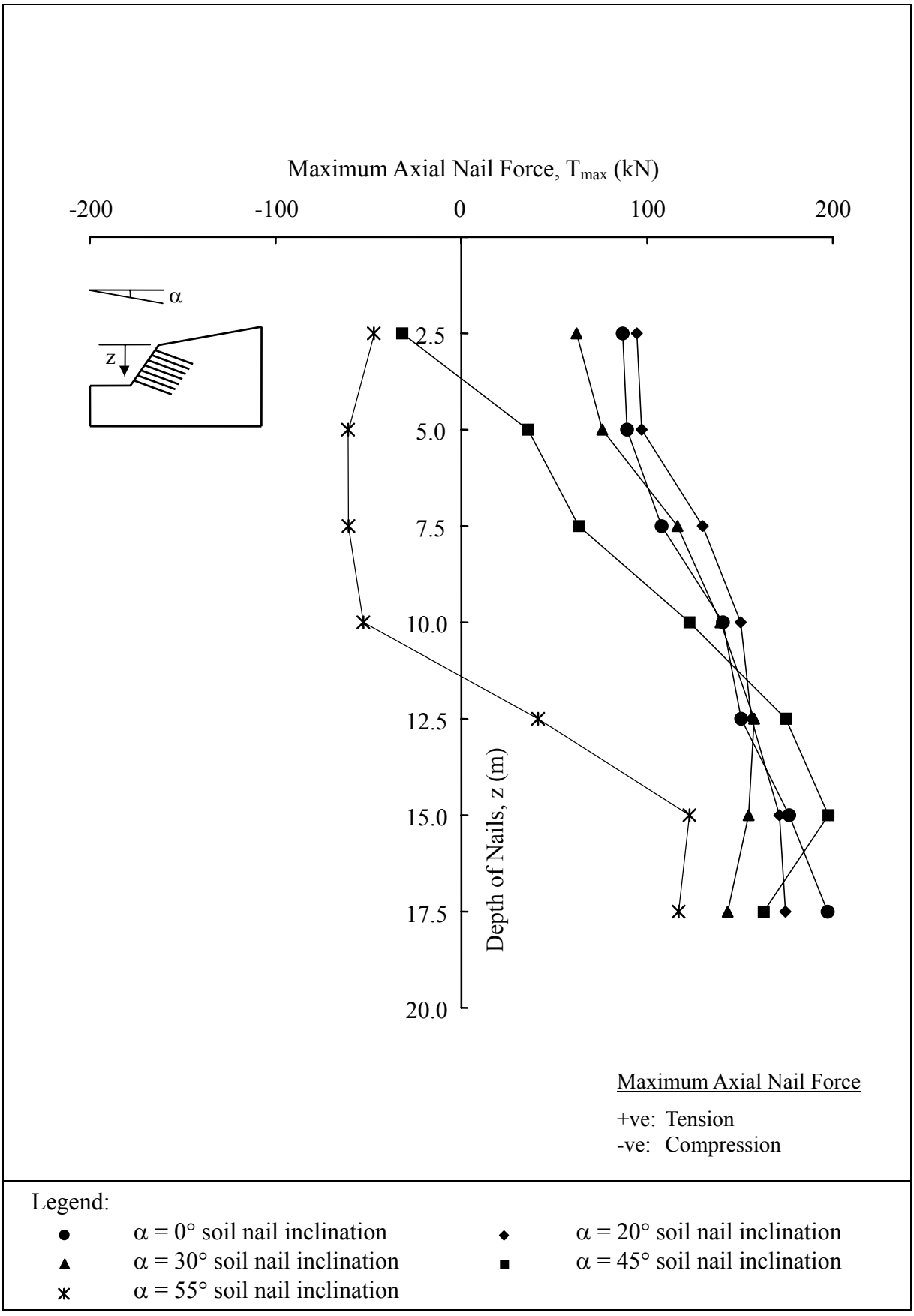

Figure 6 - Variation of Maximum Axial Nail Forces in Nails with Depth

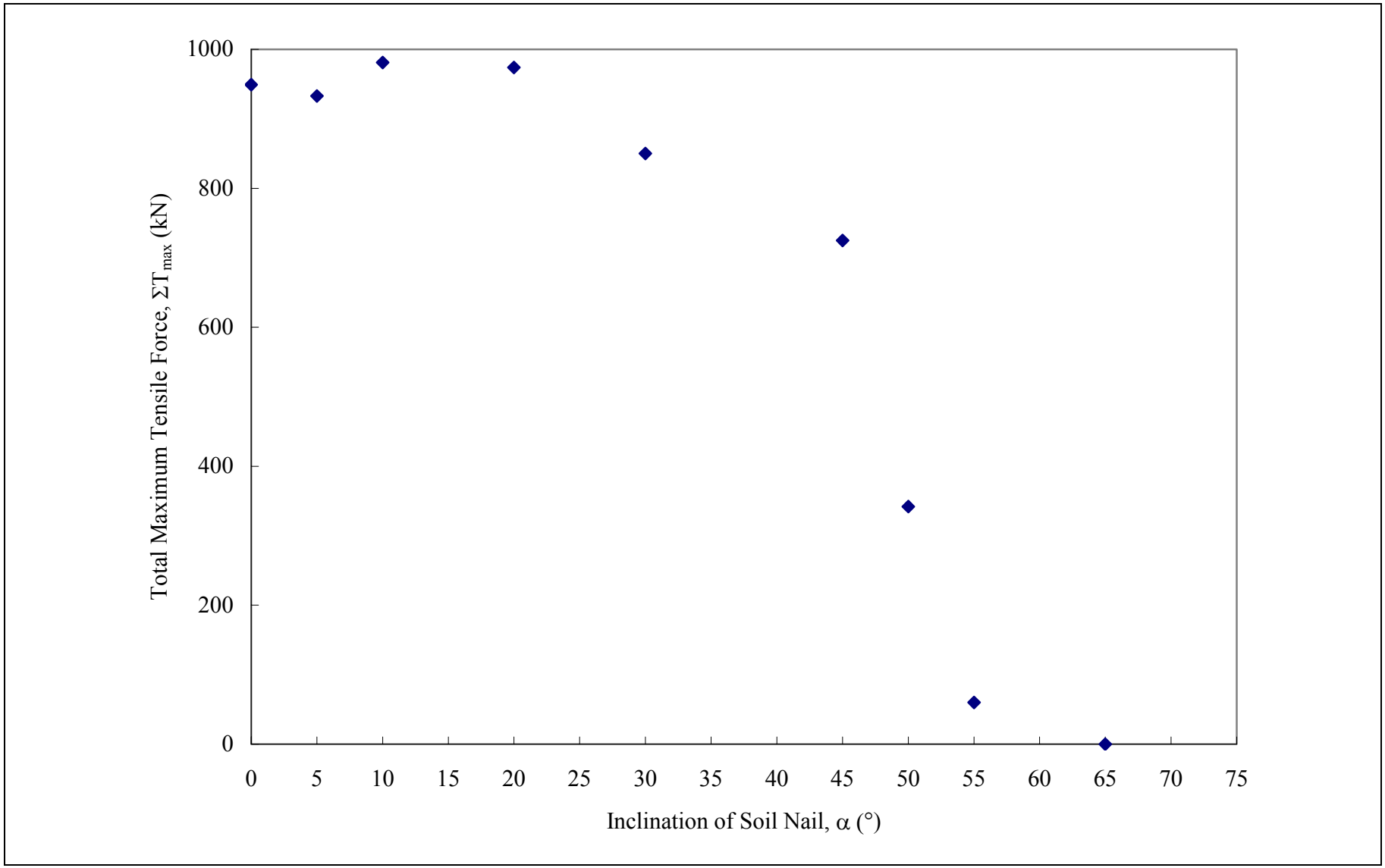

Figure 7 - Variation of Total Maximum Tensile Force (ΣT_{max}) and Nail Inclination

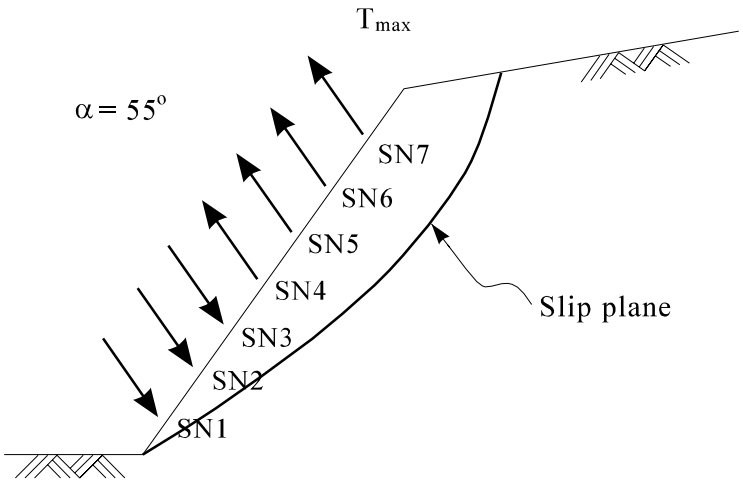

Case (a) - Maximum Axial Nail Forces (T_{max}) Applied at Individual Nail Locations

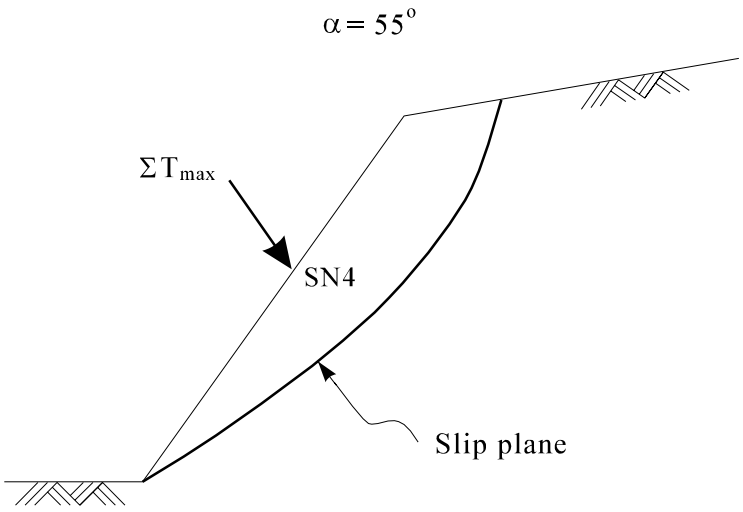

Case (b) - Single Force ΣT_{max} Applied at Mid-slope Height (SN4 Position)

Figure 8 - Simulation of Applied Forces on Slope Surface at $\alpha = 55^o$ for the Study of Nail Inclination Effect

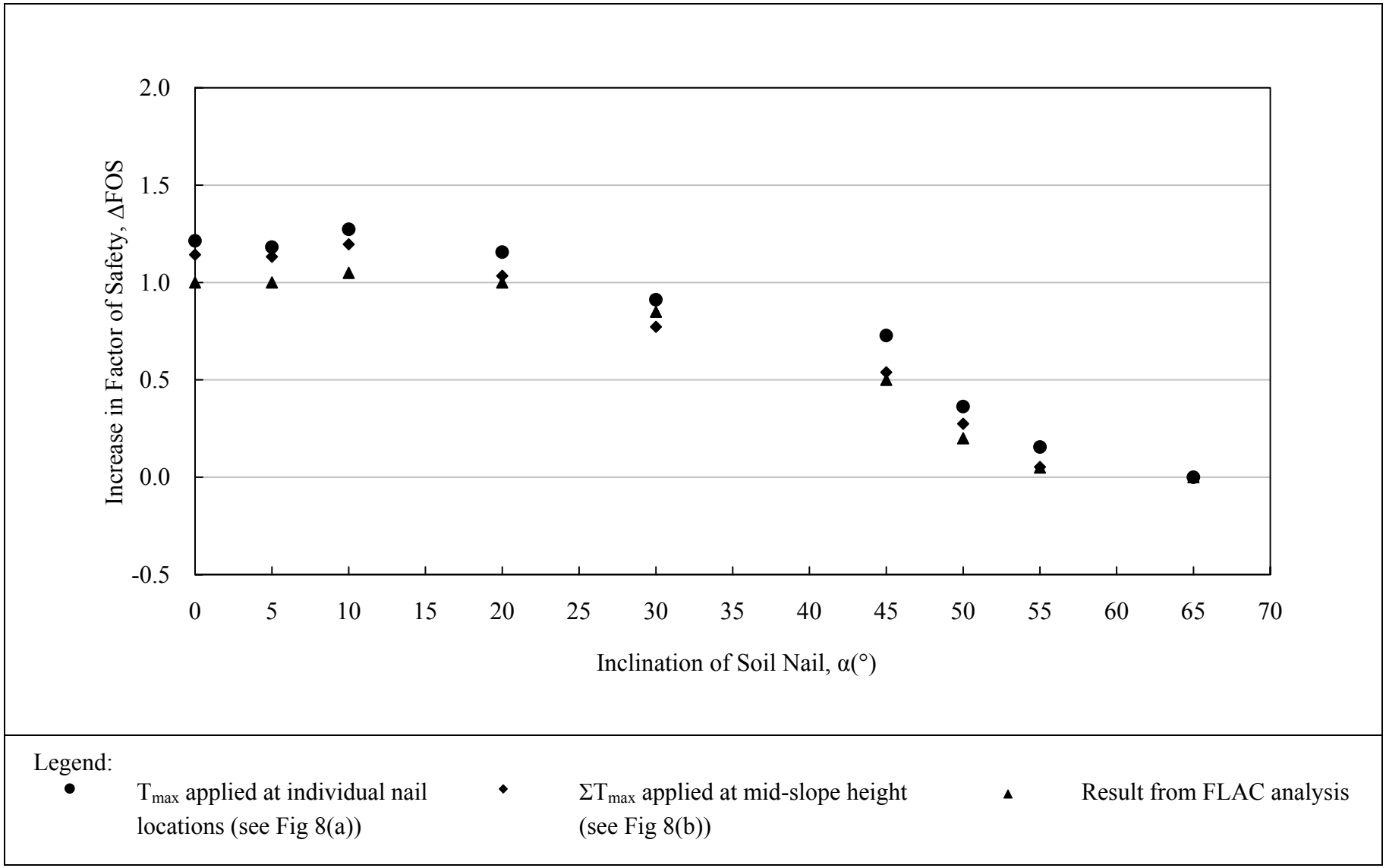

Figure 9 - Comparison of Results of Limit Equilibrium Methods and FLAC

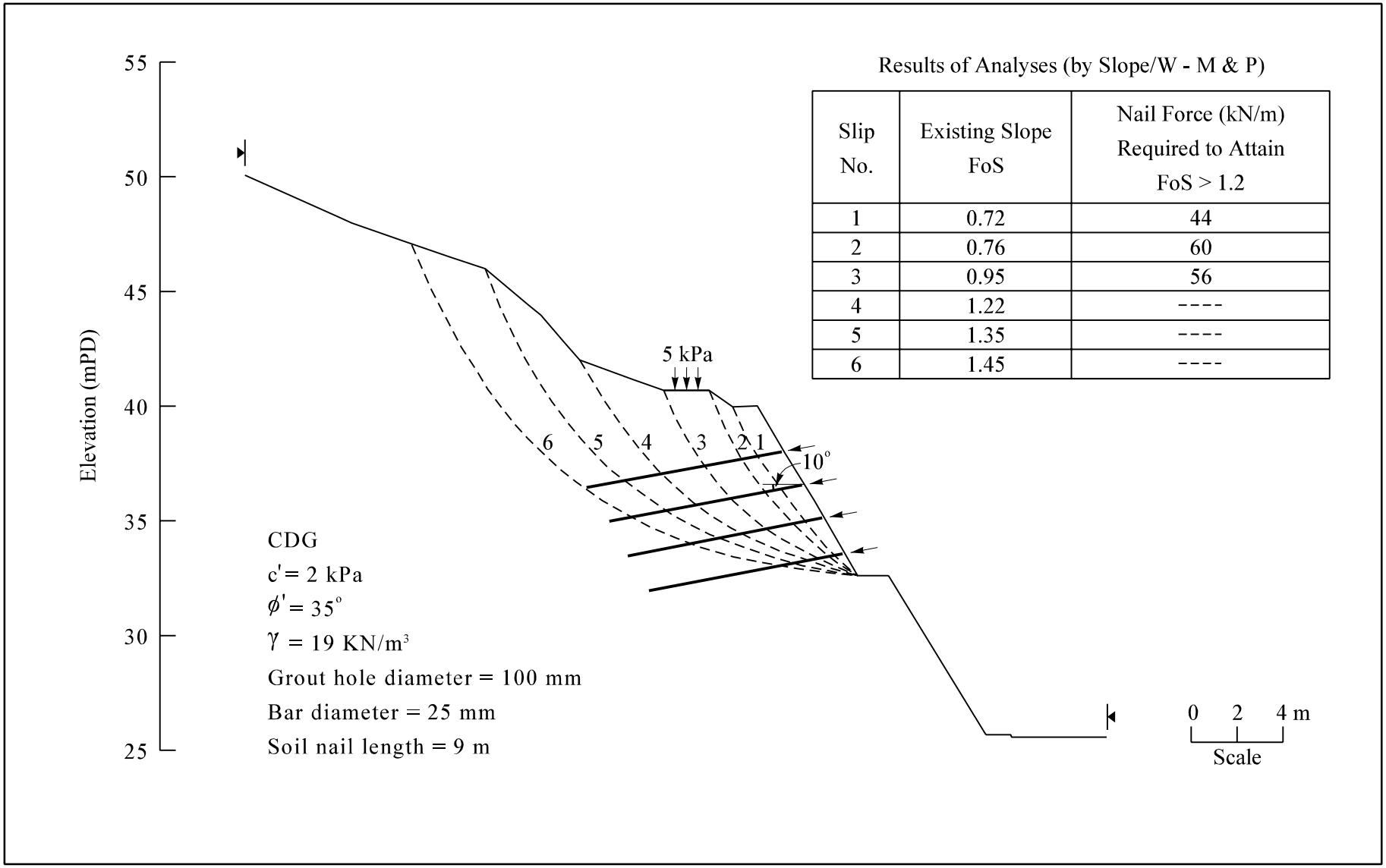

Figure 10 - LPM Design for Slope No. 11NW-B/C41 (Section 1-1) (Extracted from GEO, 2000)

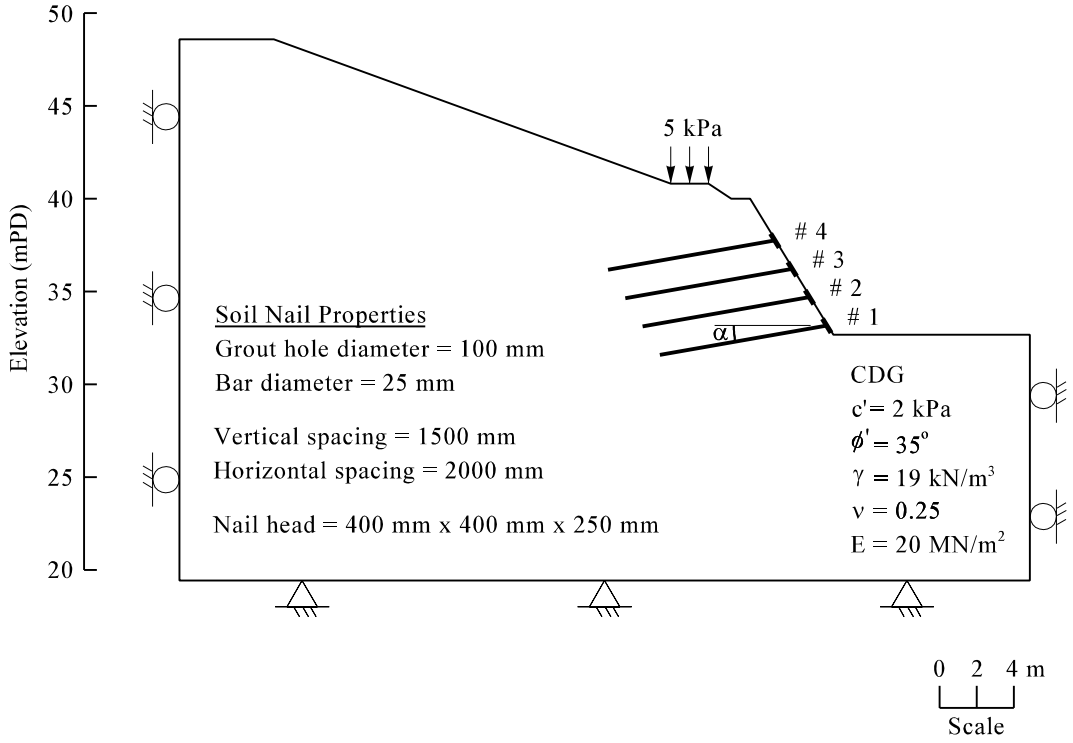

$\alpha = 10^{\circ}$, soil nail length = 9 m

Figure 11 - Geometry and Parameters Used in Numerical Simulation for Cut Slope No. 11NW-B/C41

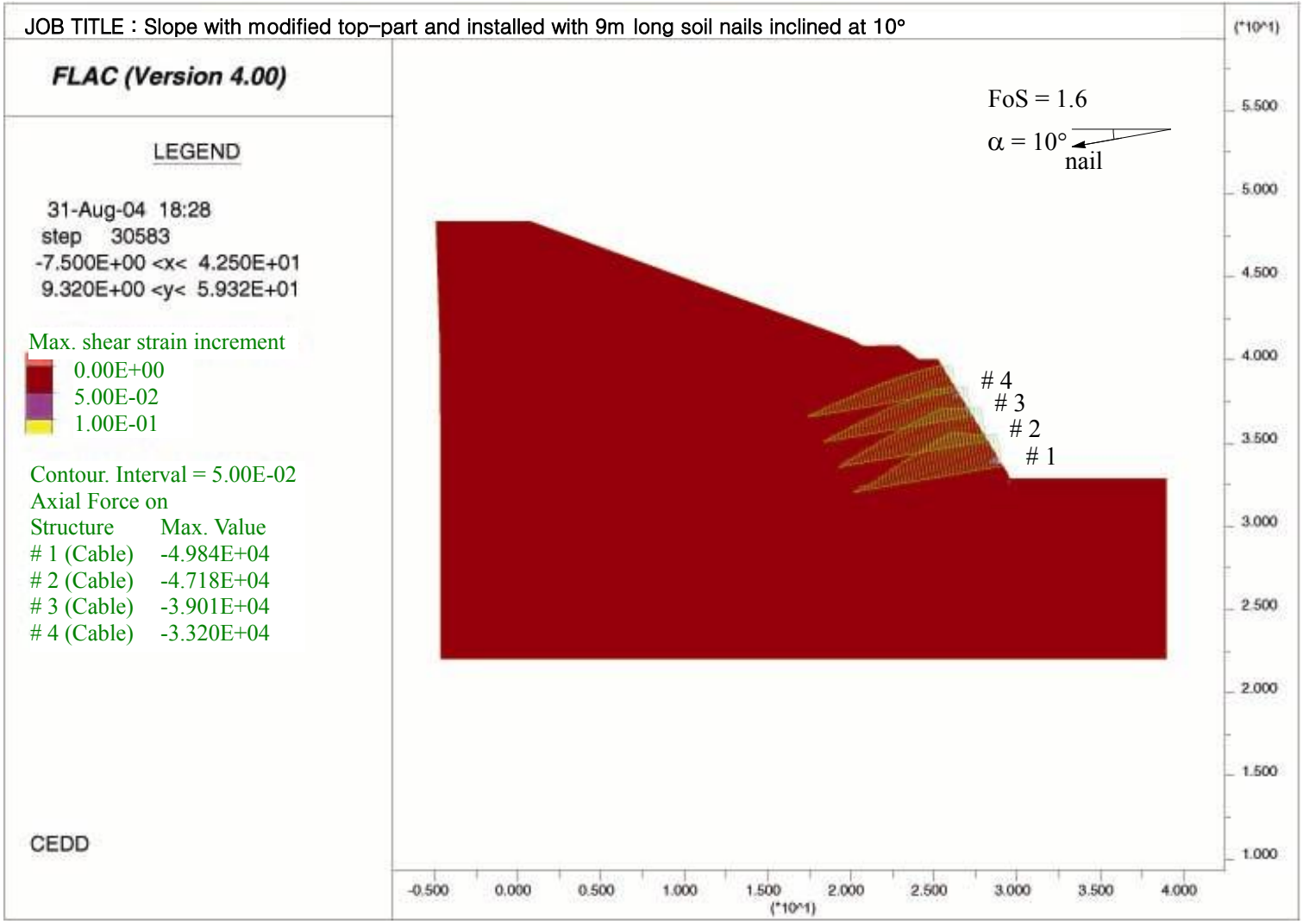

Figure 12 - Axial Nail Forces and Soil Shear Strains for Slope No. 11NW-B/C41 (Section 1-1), α = 10°

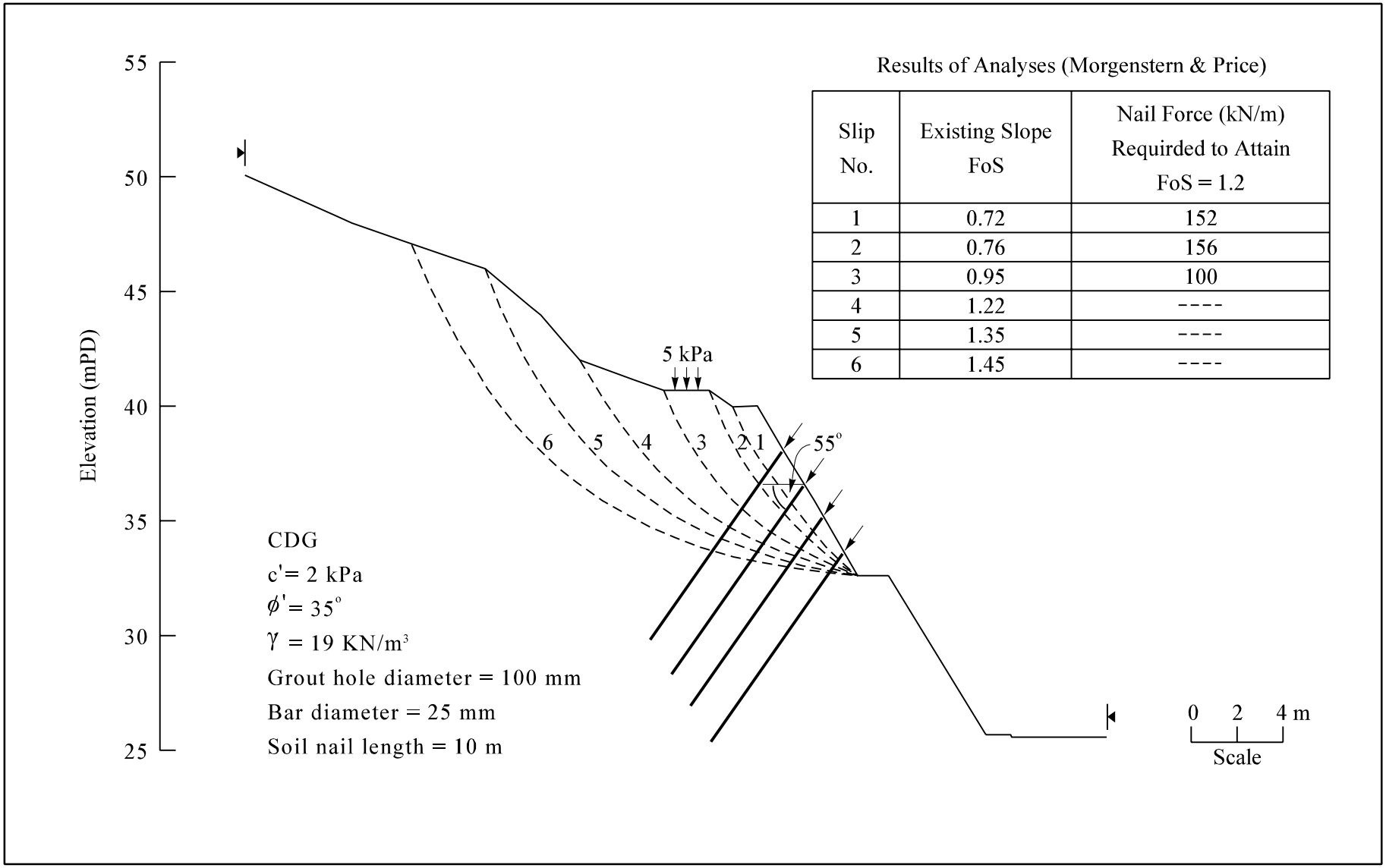

Figure 13 - Results of Limit Equilibrium Method for Nail Inclination $\alpha = 55^{\circ}$ (Slope No. 11NW-B/C41 (Section 1-1))

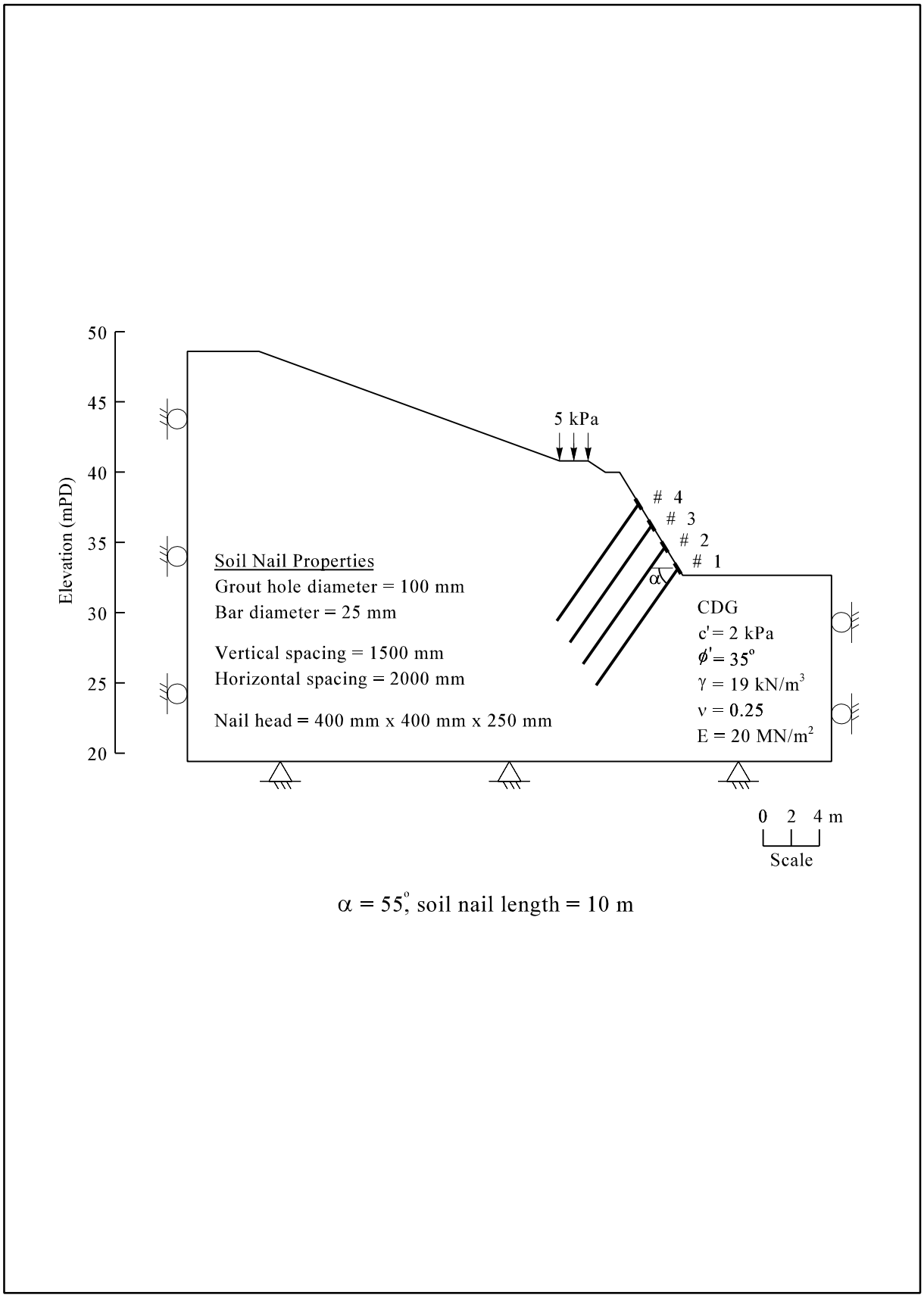

Figure 14 - Geometry and Parameters Used in Numerical Simulation for Cut Slope No. 11NW-B/C41, $\alpha = 55^{\circ}$

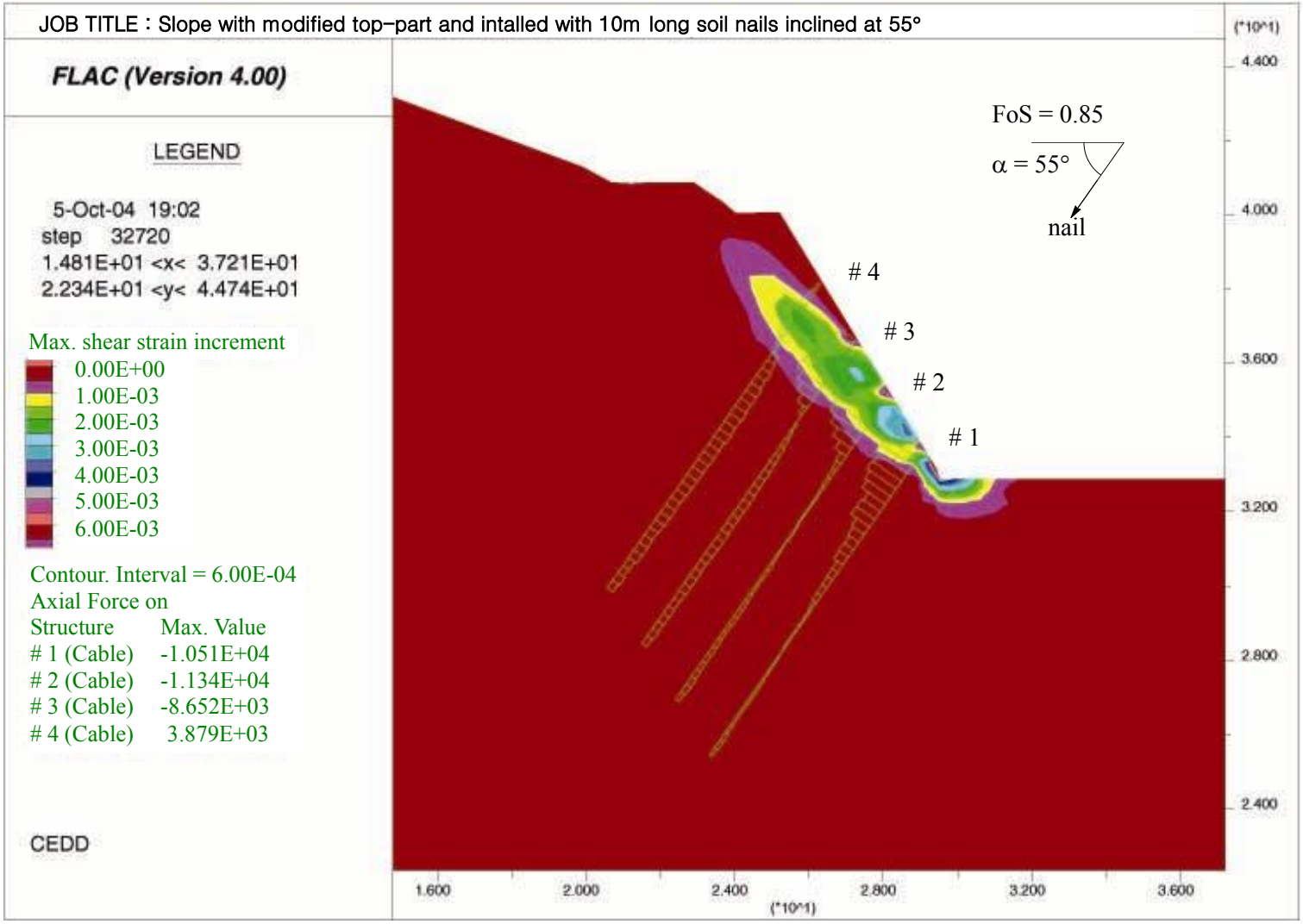

Figure 15 - Axial Nail Forces and Soil Shear Strains for Slope No. 11NW-B/C41 (Section 1-1), α = 55°

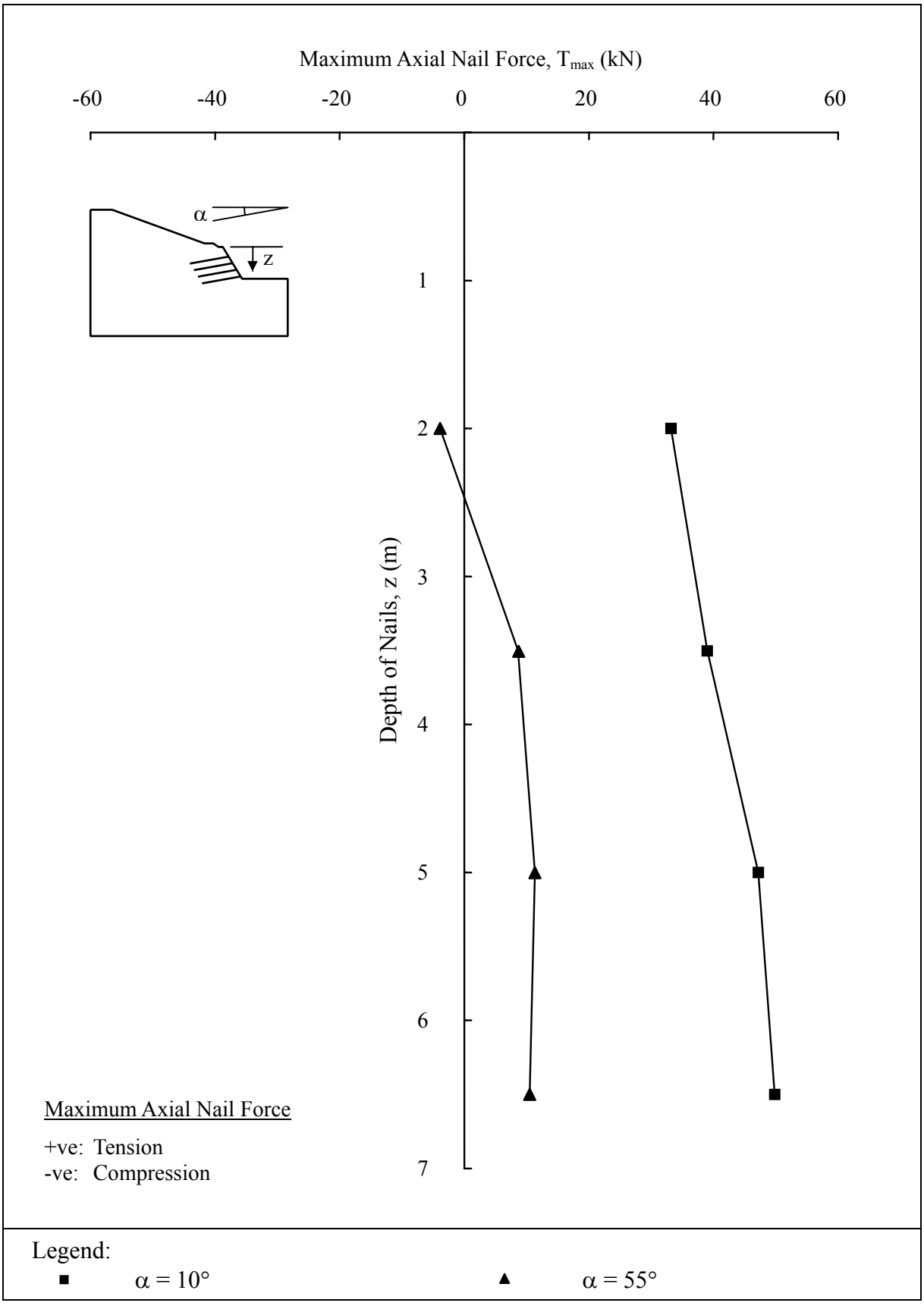

Figure 16 - Variations of Maximum Axial Nail Forces in Nails with Depth
(Slope No. 11NW-B/C41 (Section 1-1))

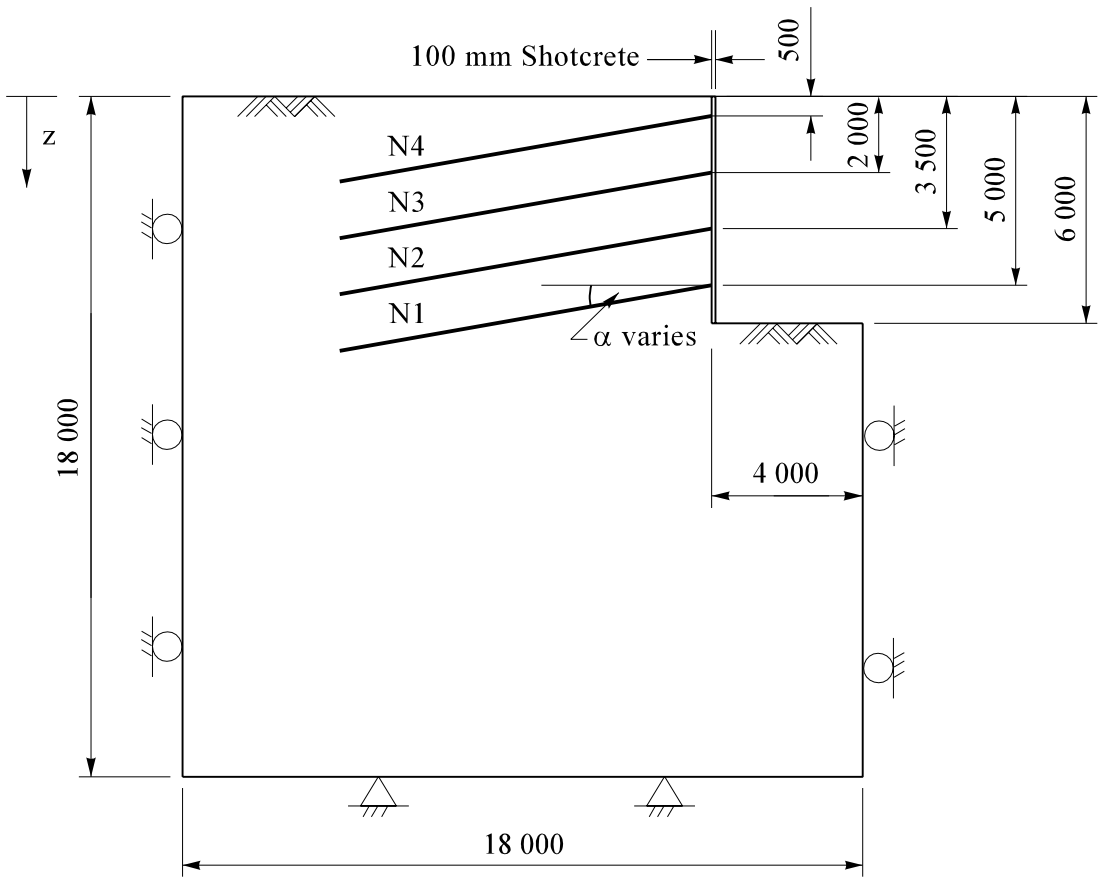

All dimensions are in mm

Soil Nails Properties:	Soil Parameters:
Grout hole diameter = 100 mm	$c' = 10$ kPa
Bar diameter = 40 mm	$\phi' = 40^{o}$
Soil Nail length = 10 m	$\gamma = 19$ kN/m^3
Vertical spacing = 1 500 mm	$E_{soil} = 20$ MPa
Horizontal spacing = 1 500 mm	$\nu_{soil} = 0.25$
fy = 460 N/mm^2	

Figure 17 - Numerical Model for the Study of the Effect of Nail Inclination (α) on Nailed Excavation

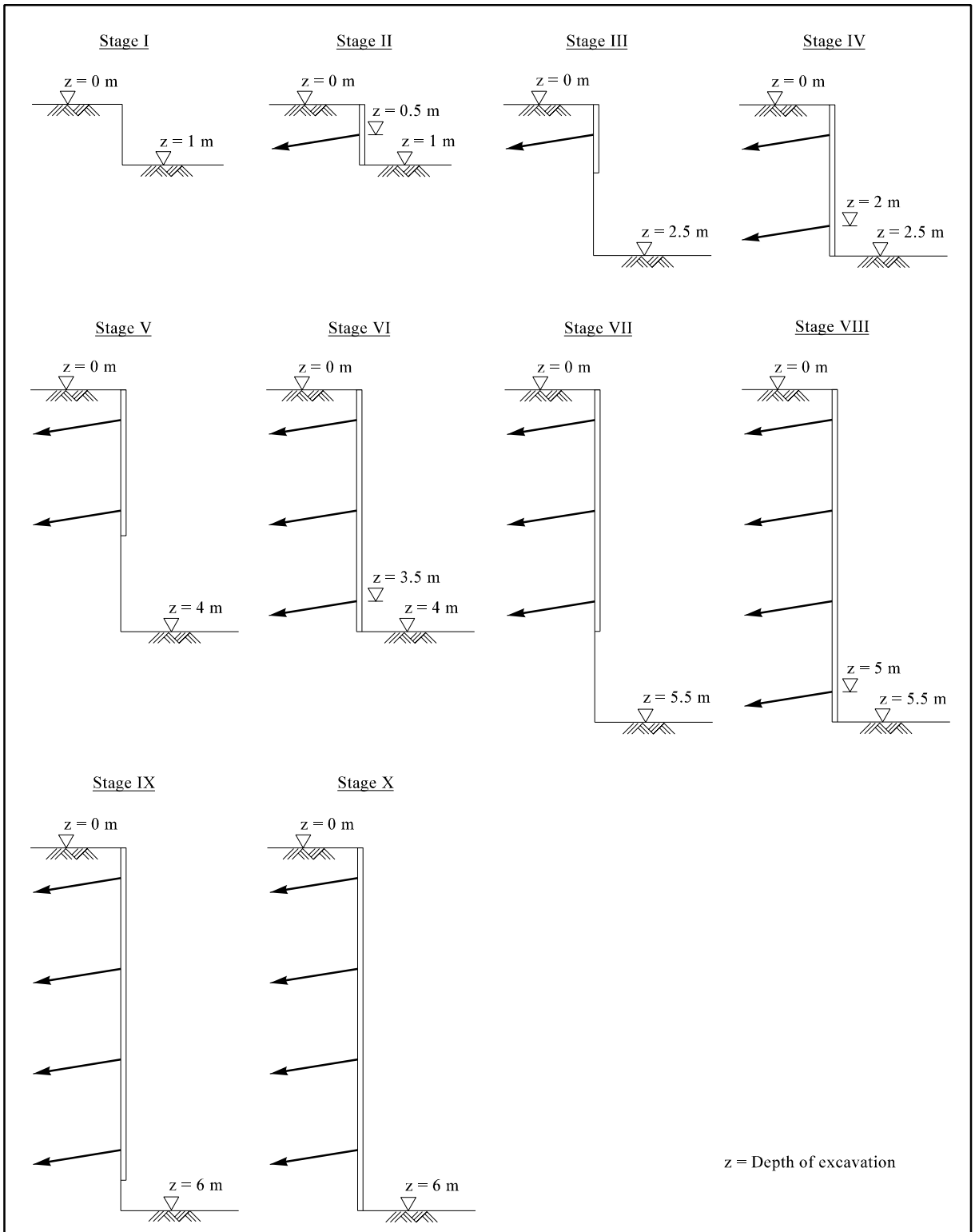

Notes:	Stage I:	Excavate to z = 1 m.	Stage II:	Install soil nail at z = 0.5 m and shotcreting.
	Stage III:	Excavate to z = 2.5 m.	Stage IV:	Install soil nail at z = 2 m and shotcreting.
	Stage V:	Excavate to z = 4 m.	Stage VI:	Install soil nail at z = 3.5 m and shotcreting.
	Stage VII:	Excavate to z = 5.5 m.	Stage VIII:	Install soil nail at z = 5 m and shotcreting.
	Stage IX:	Excavate to z = 6 m.	Stage X:	Shotcreting to full depth.

Figure 18 - Excavation Sequence Simulated in Numerical Analysis

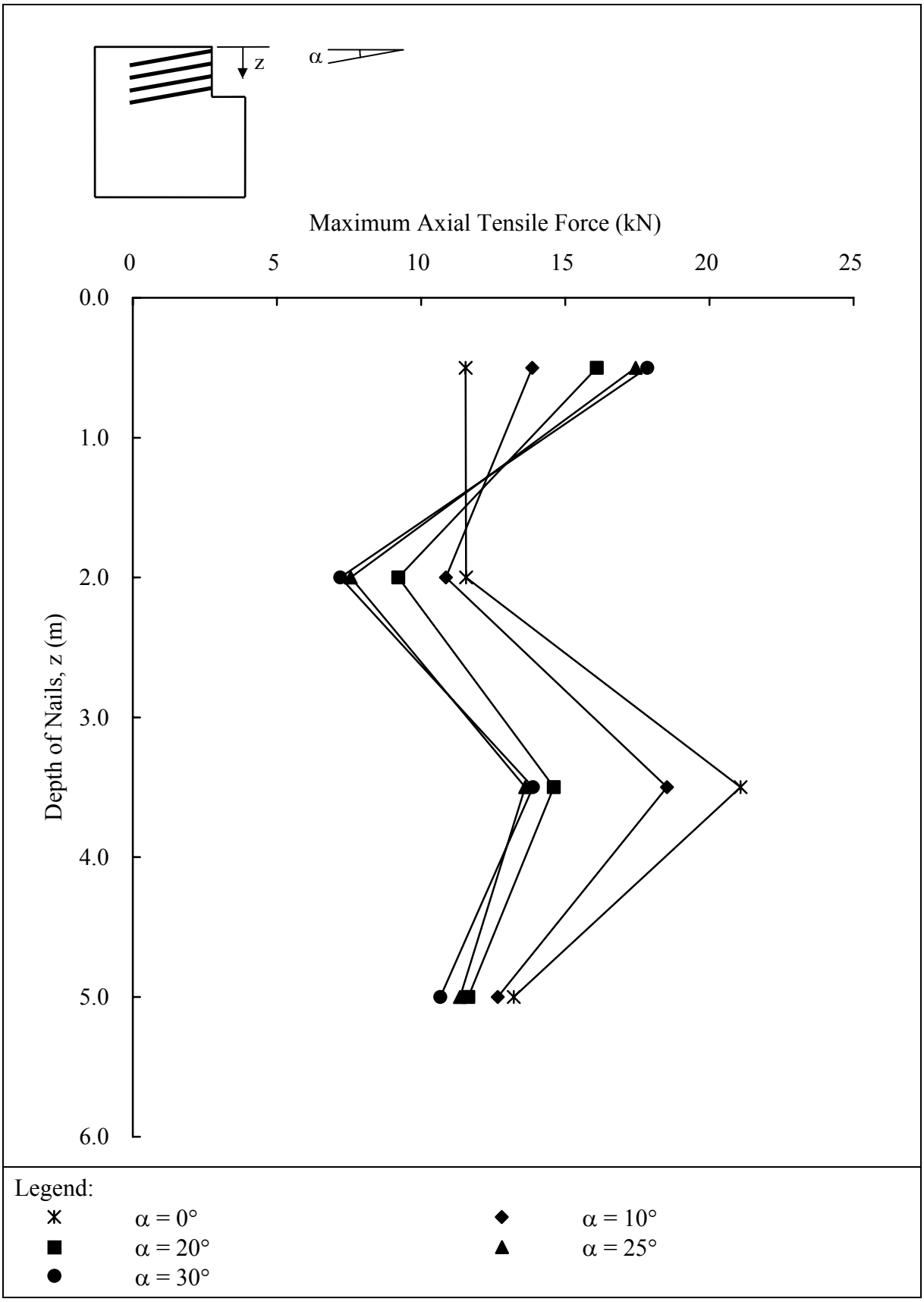

Figure 19 - Variations of Maximum Axial Nail Forces with Depth for the Excavation Models at Final Stage

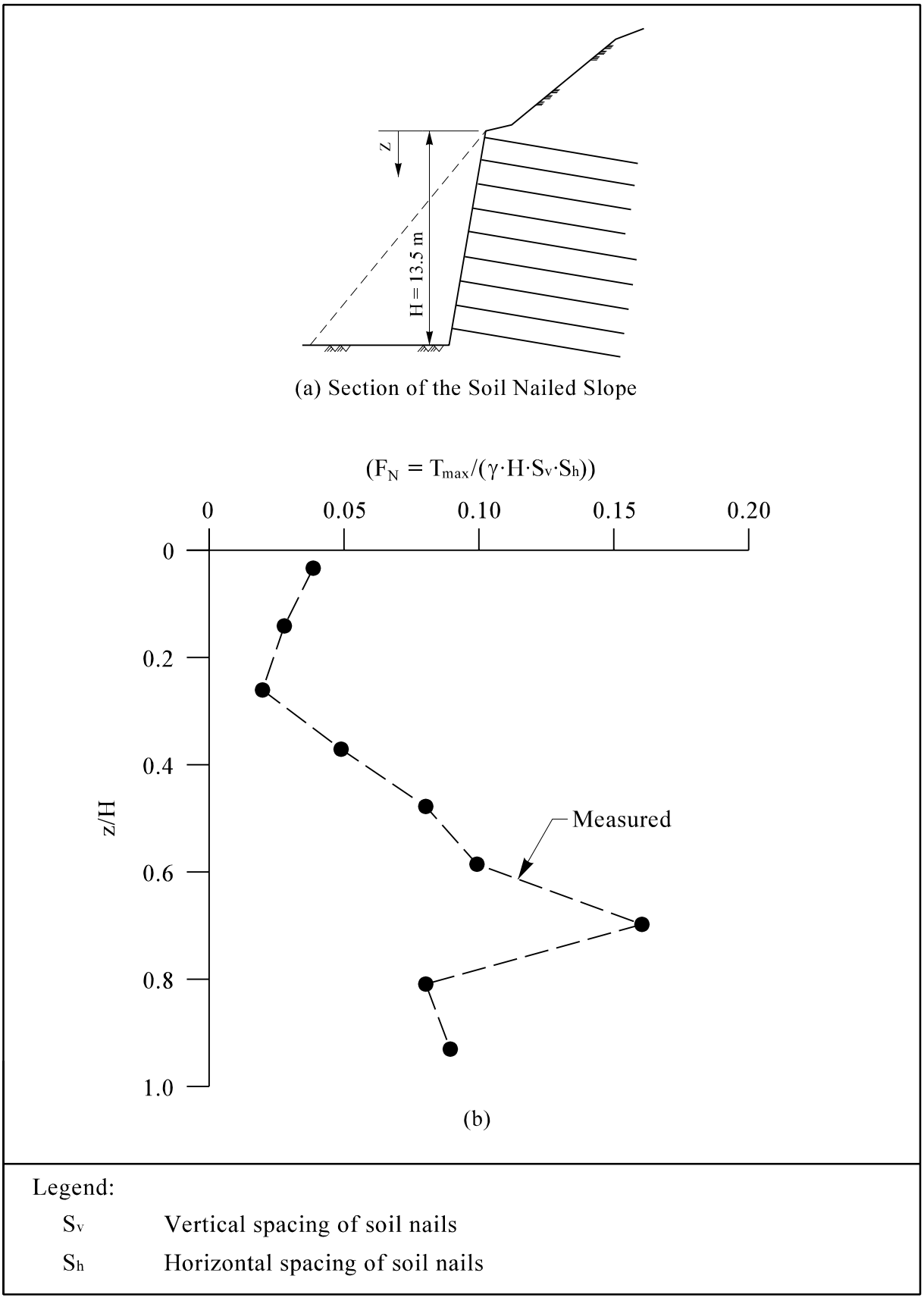

Figure 20 - Distribution of Measured Normalized Maximum Nailed Forces from Field Monitoring (after Shiu et al, 1997)

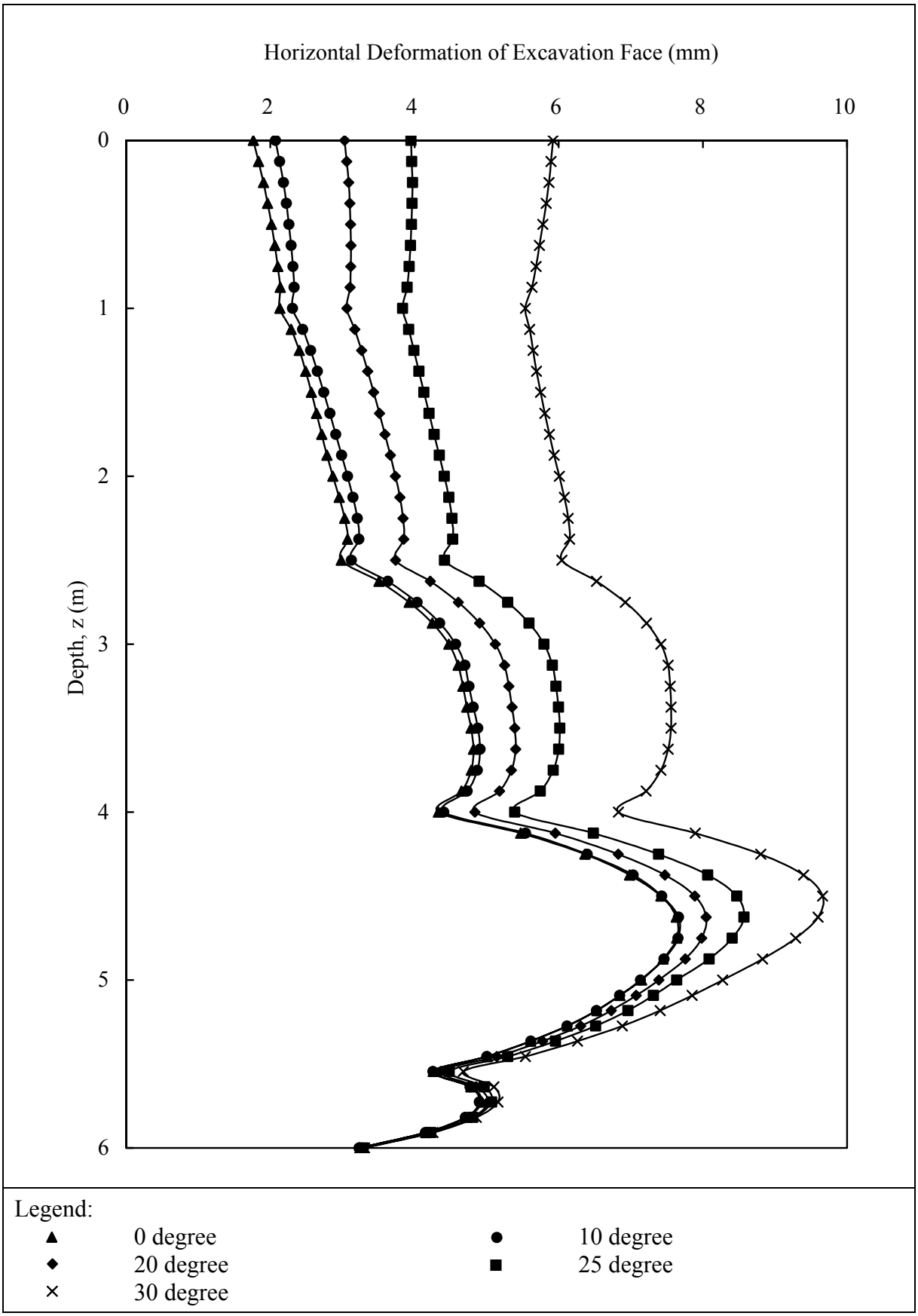

Figure 21 - Profiles of Horizontal Deformations of Excavation Face

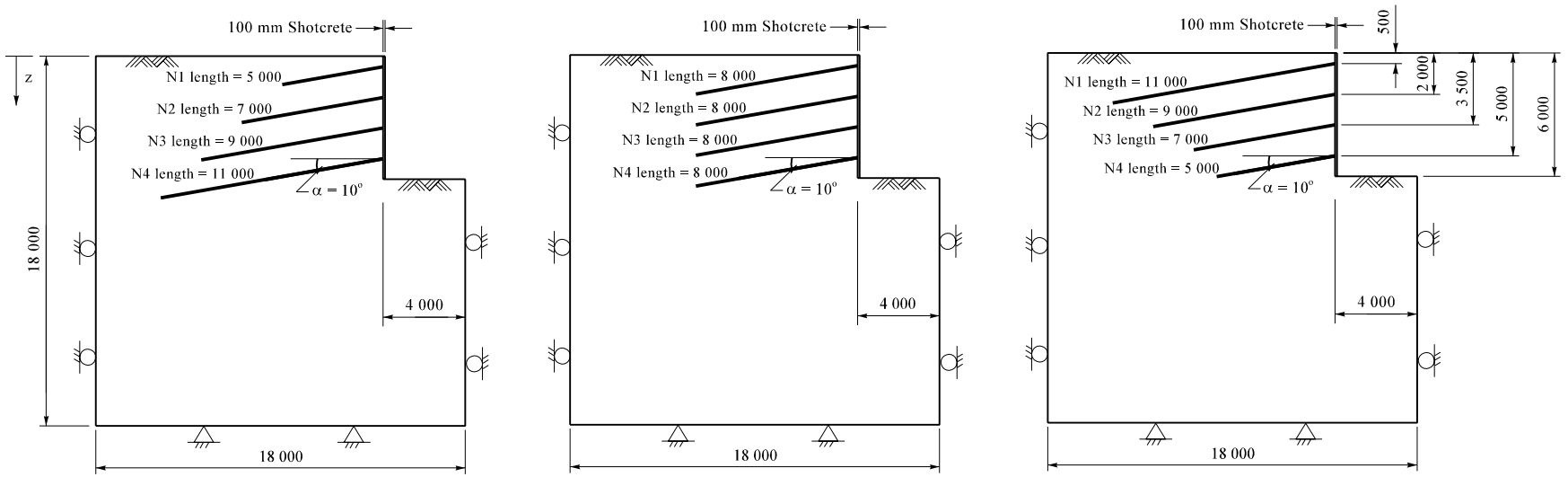

Pattern (1) Pattern (2) Pattern (3)

Soil Nails Properties:

Grout hole diameter = 100 mm
Bar diameter = 40 mm
Vertical spacing = 1 500 mm
Horizontal spacing = 1 500 mm
fy = 460 N/mm^2

Soil Parameters:

c' = 5 kPa
ϕ' = 39°
γ = 19 kN/m^3
E_{soil} = 10 MPa
ν_{soil} = 0.25

Figure 22 - Nail Length Patterns (1), (2) and (3)

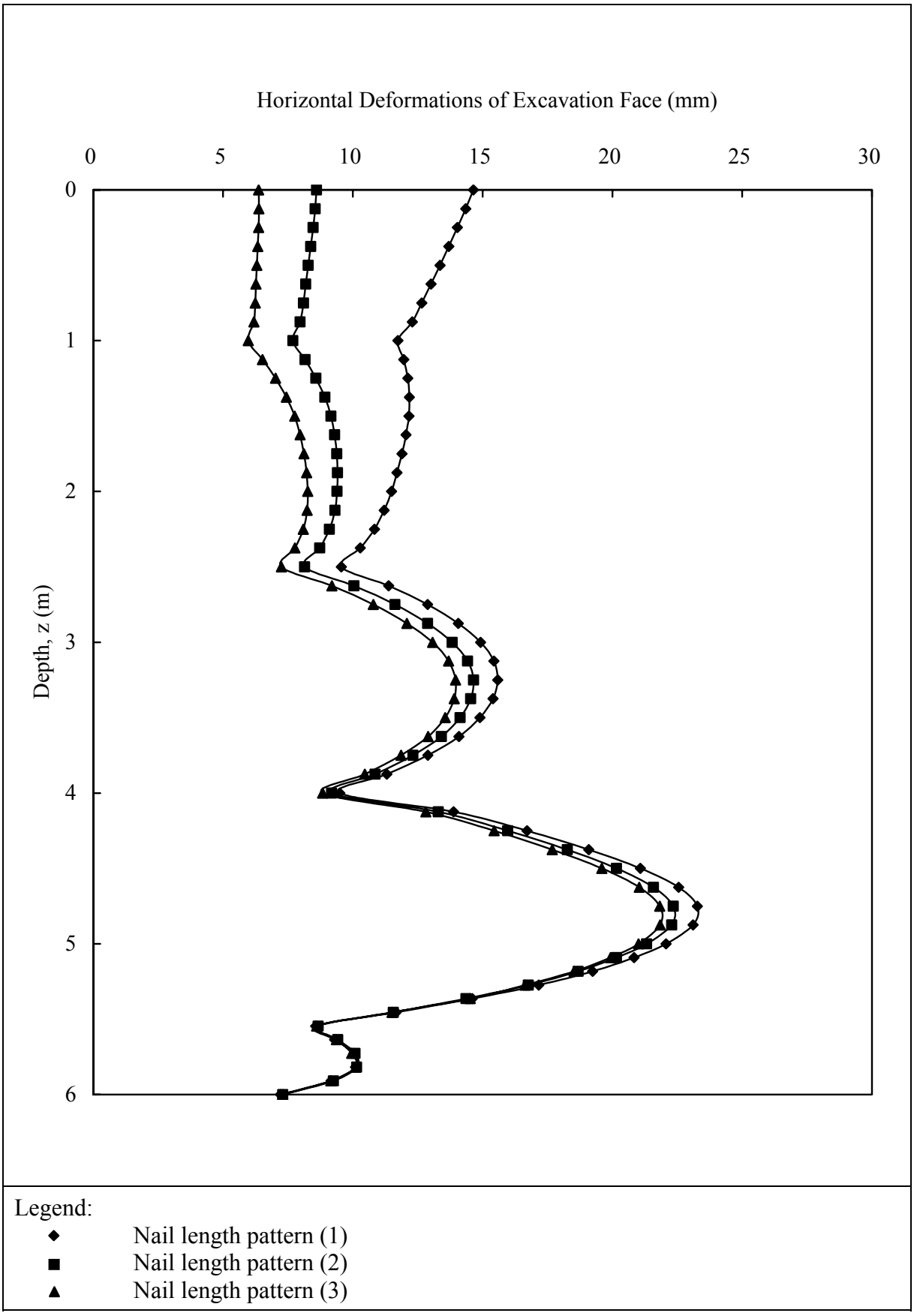

Figure 23 - Horizontal Deformation Profiles of Excavation Face for Different Nail Length Patterns

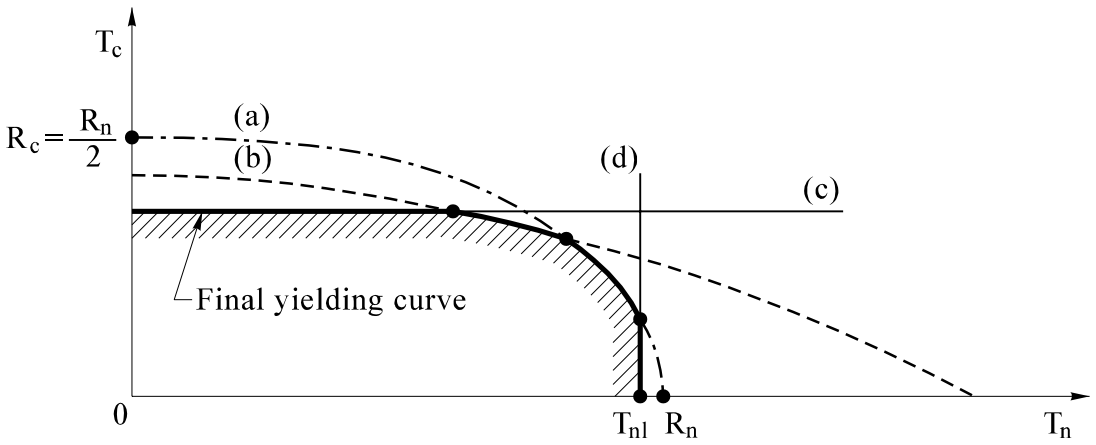

Criteria for Strength of Soil Reinforcement

$R_n = 2R_c$

$$\frac{T_n^2}{R_c^2} + \frac{T_c^2}{R_n^2} \leq 1$$

Legend:

(a)	Reinforcement strength (Ellipse)	T_n	Axial tensile force
(b)	Normal earth pressure with bending plastification (Parabola)	R_n	Tensile capacity
		T_c	Shear force
(c)	Normal earth pressure without bending plastification (Straight line)	R_c	Shear capacity
(d)	Soil-reinforcement friction		

Figure 24 - Multicriteria and Final Yielding Curve (after Schlosser, 1982)

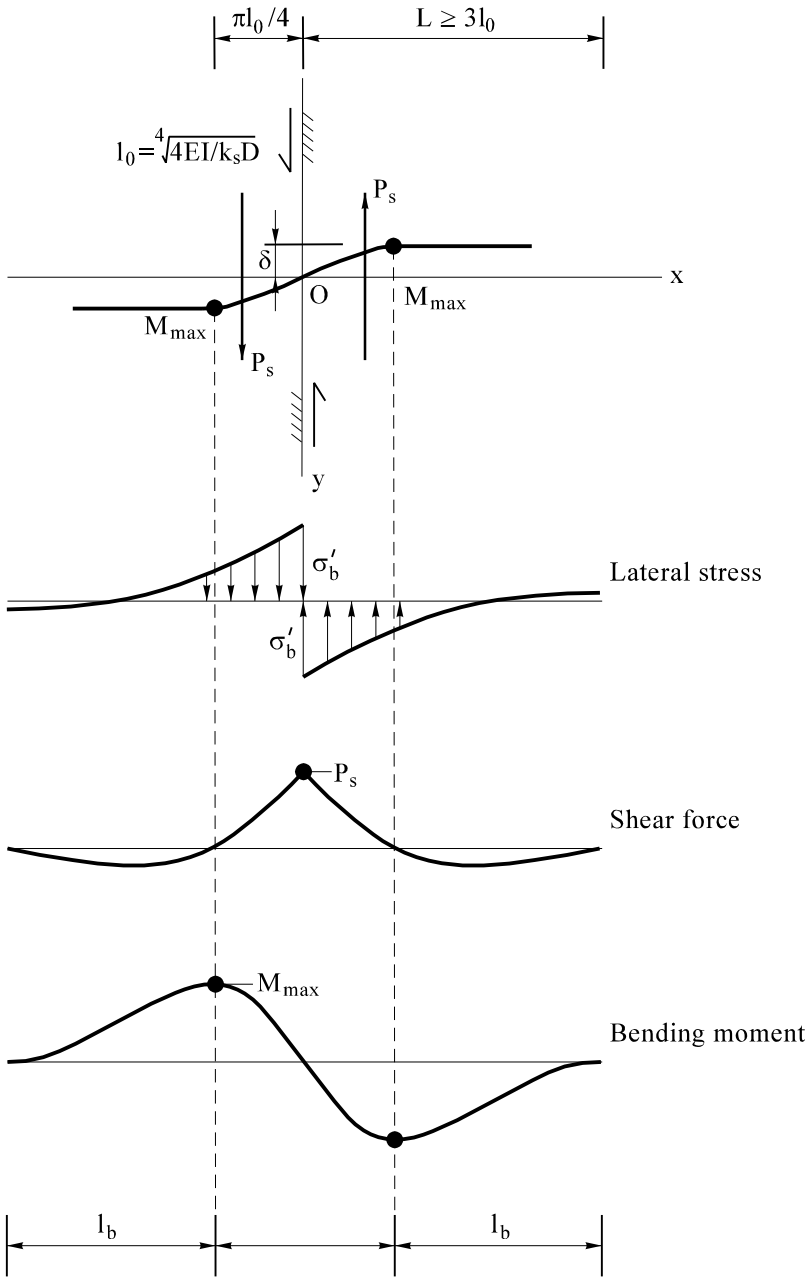

Legend:

k_s	Coefficient of subgrade reaction	l_o	Transfer length of nail
δ	Lateral displacement of nail	E	Modulus of Elasticity of nail
I	Nail moment of inertia	D	Nail diameter
M_{max}	Maximum bending moment in nail	P_s	Shear force in nail

l_b Minimum required length beyond point of maximum bending moment

l_s Distance between points of maximum moment on either side of shear plane

δ_b' Maximum soil bearing pressure

Figure 25 - Nails Subjected to Bending Moment and Shear Force (after Schlosser, 1982)

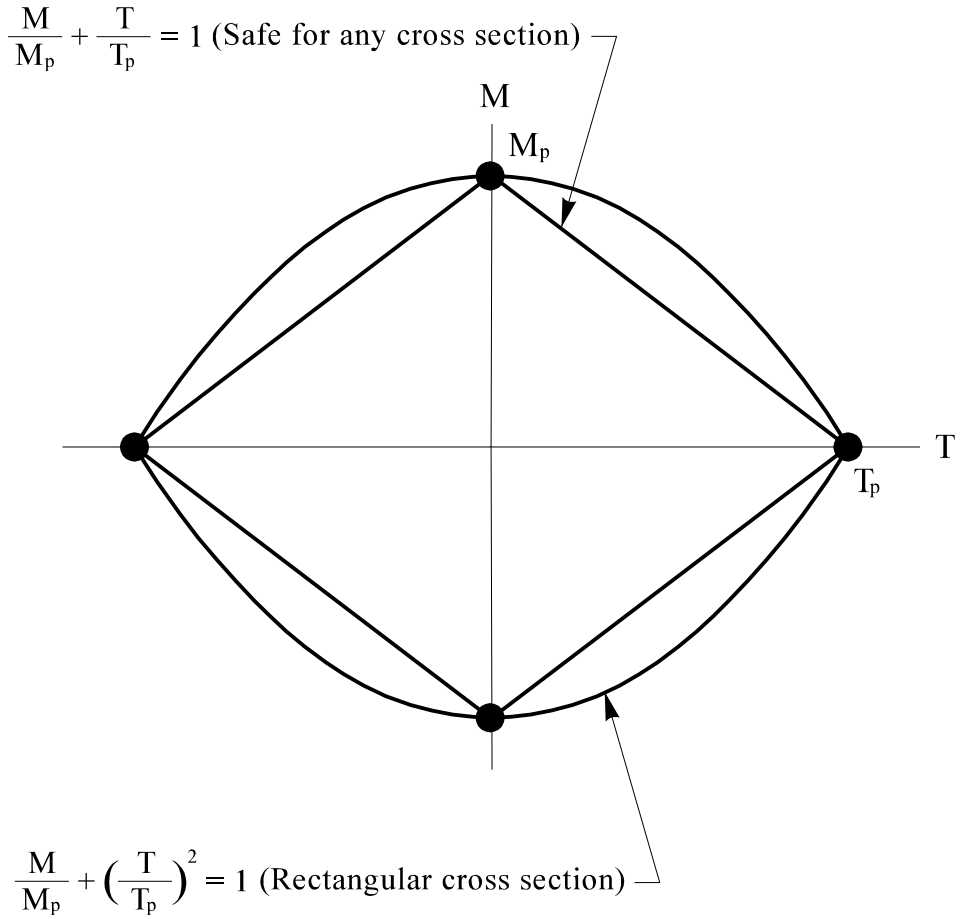

Legend:

T	Axial force per nail	M	Bending moment per nail
T_p	Axial force capacity per nail assuming M = 0	M_p	Bending moment capacity per nail assuming T = 0

Figure 26 - Relationship between M_p and T_p (after Calladine, 2000)

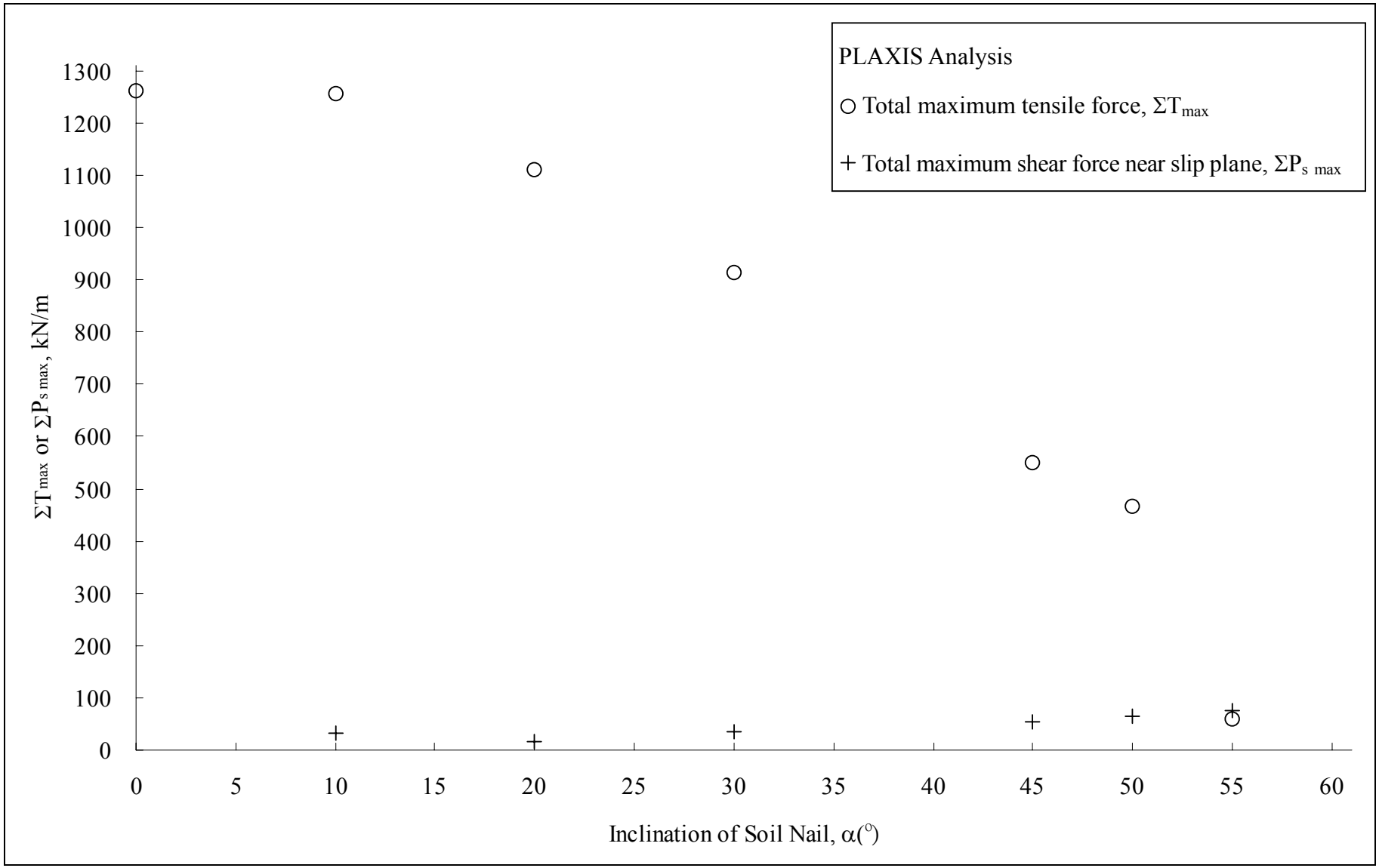

Figure 27 - Variation of Total Maximum Tensile Force (ΣT_{max}) and Total Maximum Shear Force ($\Sigma P_{s\ max}$) with Nail Inclination (α)

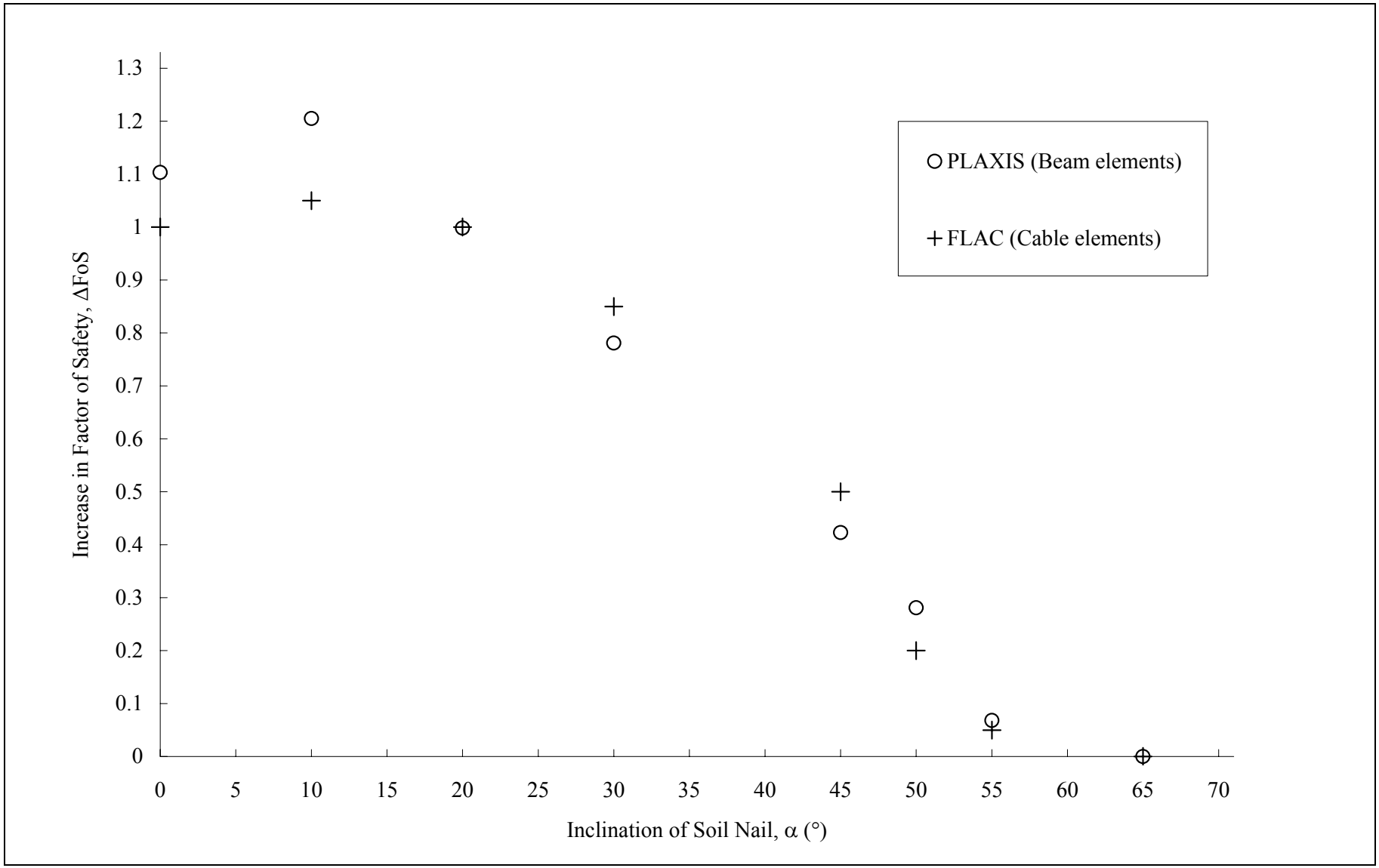

Figure 28 - Variation of ΔFoS with Nail Inclination (FLAC Analysis and PLAXIS Analysis)

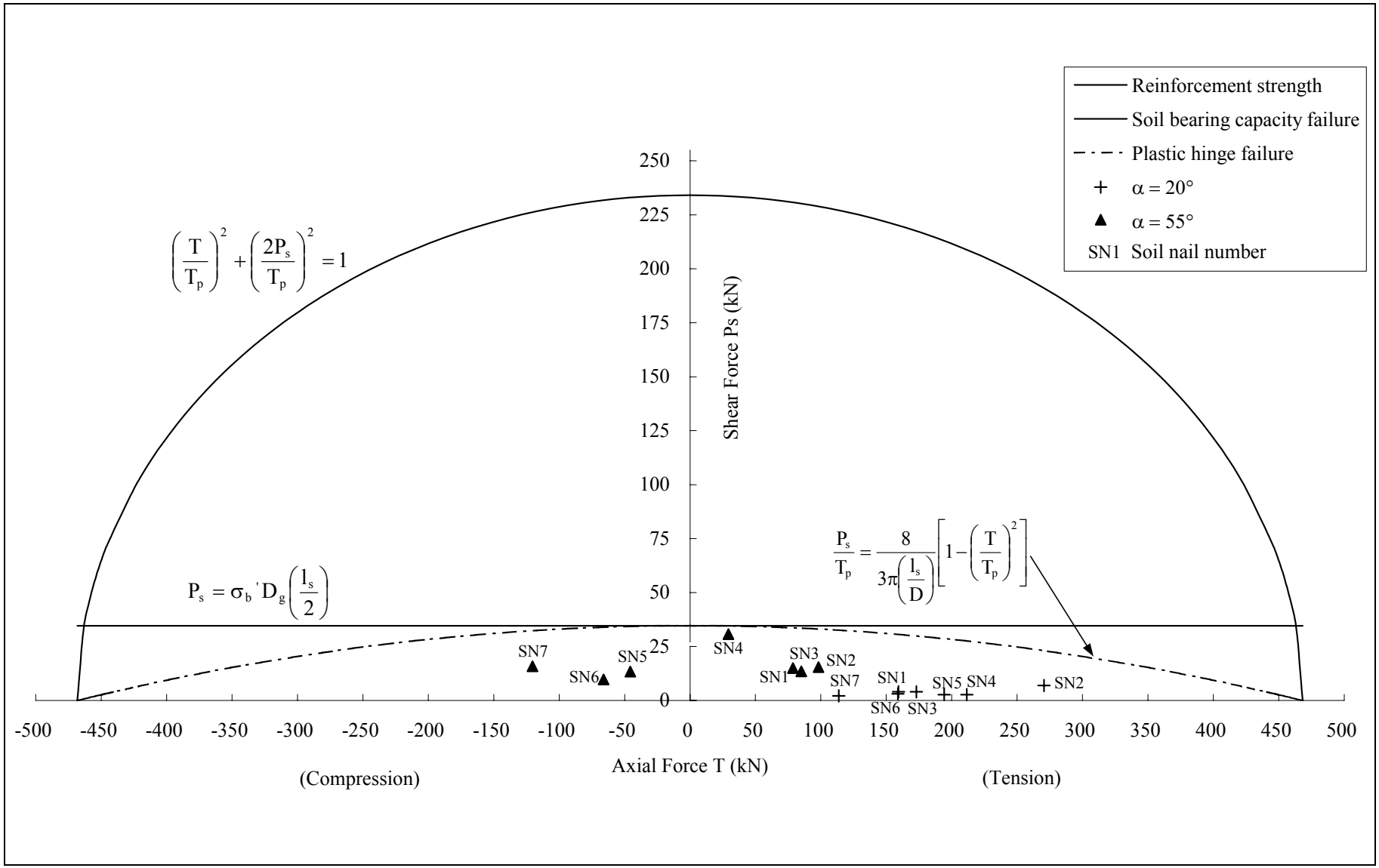

Figure 29 - Failure Envelopes and Combined Loading in Reinforcement Bar

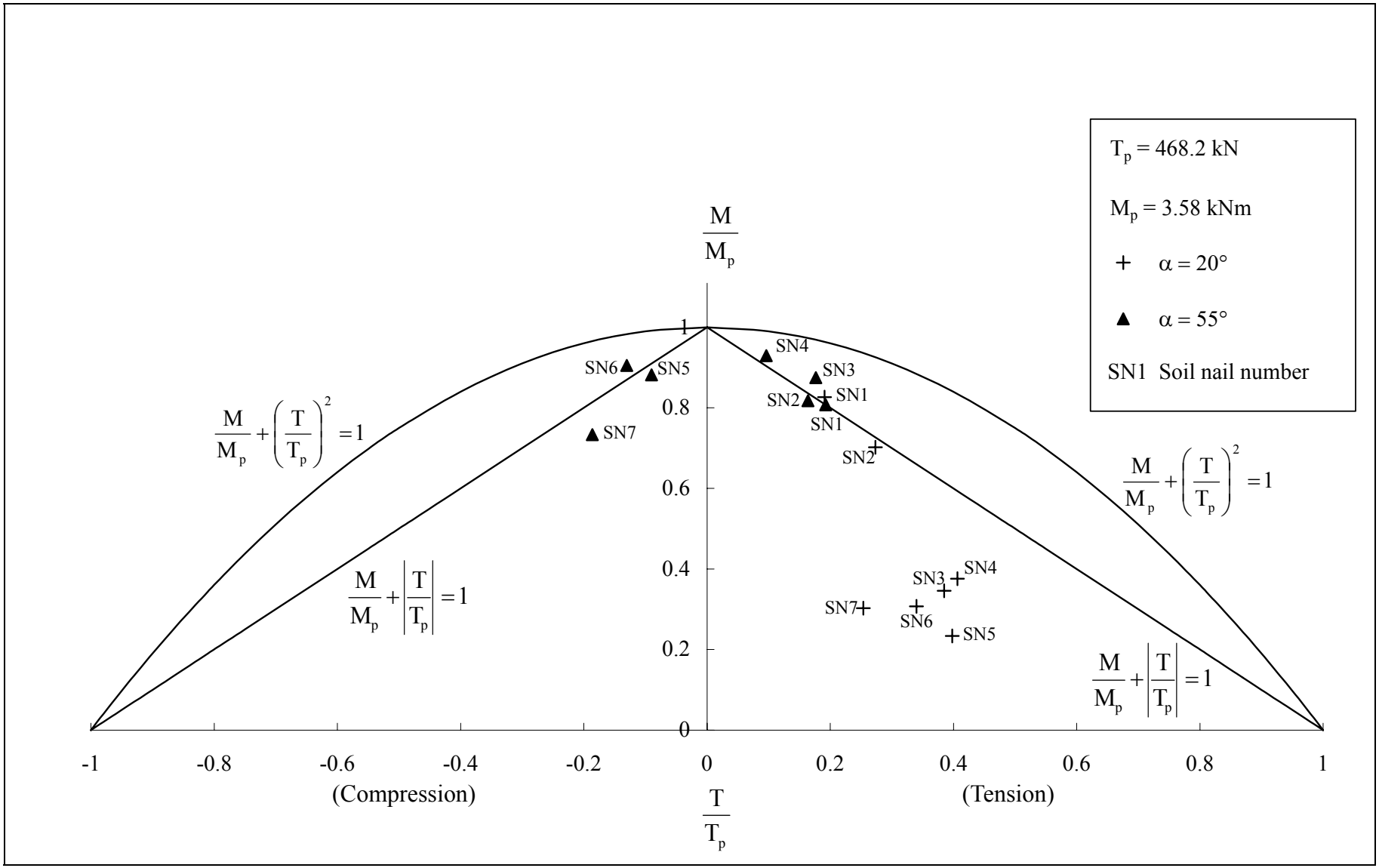

Figure 30 - Normalized Moment $\frac{M}{M_p}$ Vs Normalized Axial Force $\frac{T}{T_p}$

Table of Contents
Table of Contents
Table of Contents

APPENDIX A

PREVIOUS LABORATORY STUDIES ON EFFECT OF NAIL INCLINATION

A.1 PREVIOUS LABORATORY TESTS ON EFFECT OF NAIL INCLINATION

A.1.1 Jewell (1980) and Jewell & Wroth (1987)

Jewell (1980) investigated the fundamental behaviour of reinforced soil by carrying out a series of direct shear box tests on sand samples reinforced with bars and grid reinforcements. One of the significant findings of his work was that the shearing strength of the reinforced soil is dependent on the orientations of the reinforcements. Jewell's investigation shows that reinforcement significantly modifies the state of stress and strain in soil, and that by varying the orientation of the reinforcement, the reinforcement can either increase or decrease the shear strength of the soil. Figure A1 compares the pattern of strain in soil between the unreinforced and reinforced tests. The presence of the reinforcement causes a significant reorientation of the principal axes of strain increment of the soil (see Figure A1(b)). The soil strains close to the reinforcement are small because the reinforcement inhibits the formation of the failure plane. When the reinforcement is orientated in the same direction of the tensile strain increment of soil, tensile forces are induced in the reinforcement through the friction between the soil and the reinforcement. Likewise, compressive forces are induced in the reinforcement if the reinforcement is placed close to the compressive strain increment of the soil.

Figure A2 shows the orientations of the reinforcement in which compressive or tensile strain increments are experienced. The shear strength of the soil starts to increase when the reinforcement is placed in the direction of tensile strain increment, and it reaches a maximum when the orientation of the reinforcement is close to the direction of the principal tensile strain increment. When the reinforcing elements are oriented in a direction of a compressive strain increment, there is a decrease in shear strength of the reinforced soil. This shows that in order to optimise strength improvement of soil, the reinforcement should be placed in the directions of principal tensile strain in the soil. When the reinforcement deviates from its optimum orientation, strength improvements decrease.

Jewell & Wroth (1987) demonstrated that the tensile reinforcement force improved the shearing strength of the soil in two ways:

(i) reducing the driving shear force on the soil; and

(ii) increasing the normal stress on the failure plane of the soil and consequently increasing the frictional resistance of the soil.

For the case shown in Figure A3, the benefit of the reinforcement is to increase the shearing resistance τ by an amount:

$$\tau = \frac{p_R}{A_S}(\cos\theta \tan\phi + \sin\theta) \quad \text{.....(A1)}$$

where P_R is the reinforcement tensile force, A_s is the area on the central plane in the direct shear apparatus, θ is the orientation of the reinforcement and ϕ is the friction angle of the soil. This equation indicates that the effect of the reinforcement on the soil shearing strength depends directly on the mobilised reinforcement force P_R.

A.1.2 Marchal (1986)

Marchal (1986) reported a laboratory study on the behaviour of soil reinforced with nail. The apparatus used was a circular shear box, 600 mm in diameter and 500 mm in height. Two types of reinforcement were used: (i) rigid steel bar having a width of 50 mm and a thickness of 8.8 mm; and (ii) flexible aluminium alloy flat bars with a thickness of 2 mm and width varying between 10 and 20 mm. The nails were instrumented with strain gauges for measuring the stresses and bending moments. They were placed at various orientations in the study. Figure A4 shows the arrangement of the test.

Marchal (1986) observed that the shear resistance for the reinforced soil showed the presence of a peak followed by a decrease to constant value at large shear strains. Ratio of the measured shearing resistance mobilized in the reinforced soil (τ') to that of the unreinforced soil (τ) is plotted in Figure A5 for different reinforcement orientations. Figure A6 shows the variations in the relationship between the axial reinforcement force and the shear force (P/P_s) developed in the reinforcement as a function of nail inclination (θ) and shear displacement of the soil (Δl). Same for both rigid and flexible reinforcements, tensile or compressive forces were first mobilised when the reinforcements were gradually subjected to shear force. After certain shear displacements of the soil, 20 mm for rigid reinforcement and 60 to 70 mm for flexible reinforcement, the curves of the P/P_s ratios moved towards a constant minimum value.

The study result shows that the orientation of the reinforcement plays a significant role in the improvement of overall shear strength of the soil. A negative orientation can lead to the development of compressive force in the reinforcement and consequently losses of shear strength of the soil (see Figure A5). The study also indicates the existence of an optimum reinforcement orientation in terms of strengthening of the soil. This is consistent with the findings of Jewell (1980).

A.1.3 Hayashi et al (1988)

Hayashi et al (1988) presented results of simple shear tests carried out on sand samples reinforced with bronze bars or polymer grids. Strain gauges were installed in the reinforcement for measuring changes in stresses in the reinforcements during testing. The orientation of the reinforcement was varied between 20^o and -20^o. Figure A7 shows the changes in shear strength of the soil in relation to the reinforcement orientation. The test result confirms the importance of the orientation of reinforcement in improving the shear strength of the soil.

A.1.4 Palmeira and Milligan (1989)

Palmeira and Milligan (1989) reported results of experimental direct shear tests on sand samples reinforced by different types of grid and sheet reinforcement. A large direct shear apparatus (1 m^3) was used for the experiments. The orientations of the principal strains in unreinforced and reinforced samples at peak stress ratio (ratio of shear stress to normal stress) are presented in Figure A8. Figure A8(a) shows that the principal tensile strain was inclined to the vertical direction by approximately 30 degrees in the case of

unreinforced sand samples. Figure A8(b) indicates that the presence of the inclined reinforcement affected the general distribution of the principal strains of the soil at peak stress ratio. A greater portion of the soil sample was strained than in the unreinforced case, although the orientation of the principal tensile strain in the central region and away from the reinforcement was still predominantly parallel to the reinforcement plane. According to Palmeira and Milligan (1989), the presence of a reinforcement layer aligned in the direction of principal tensile strains caused a remarkable increase in the shear strength of a reinforced sample in comparison with an unreinforced one under the same operational conditions. Reinforcements placed in the direction of principal tensile strain inhibited shear strain development more due to the contribution from the horizontal component of the reinforcement force. They indicated that for the range of values tested, reinforcement bending stiffness was not an important parameter. However, no test data were presented.

LIST OF FIGURES

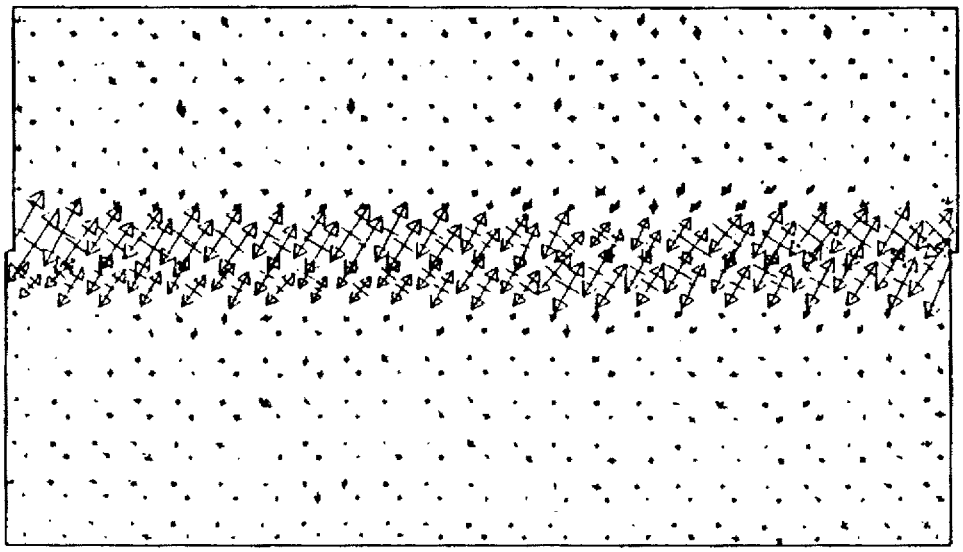

(a) Principal Strains in Unreinforced Sand after Peak

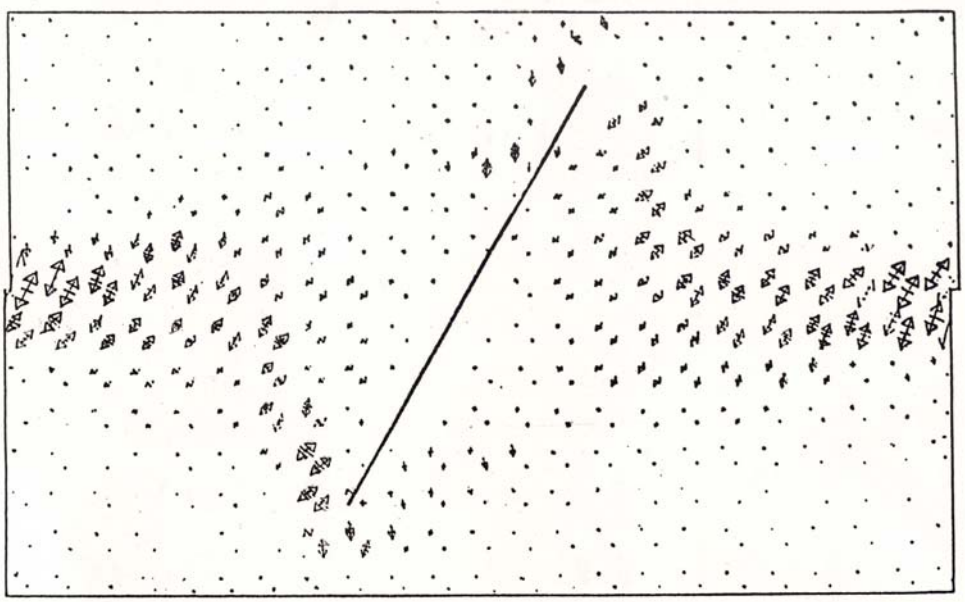

(b) Principal Strains in Sand Reinforced by a Grid at an Orientation θ = +30°

Legend:
Principal strains
— Compressive
↔ Tensile
↕ = 5% strain

Figure A1 - Incremental Strains at Peak Shearing Resistance in (a) Unreinforced Sand (b) Reinforced Sand (after Jewell, 1980)

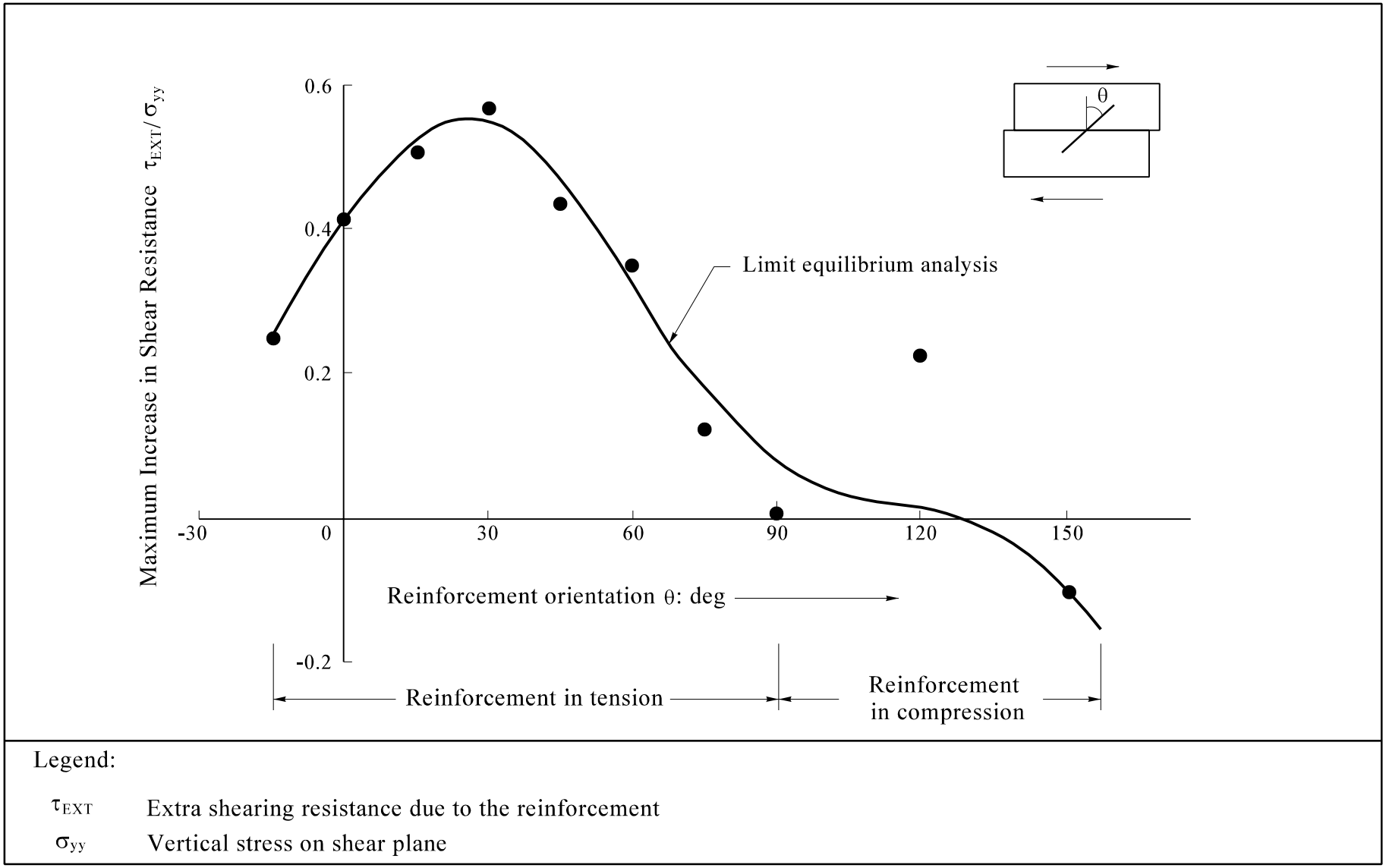

Legend:

τ_{EXT} Extra shearing resistance due to the reinforcement

σ_{yy} Vertical stress on shear plane

Figure A2 - Maximum Increase in Shear Resistance Measured for Reinforcement Placed at Different Orientations (after Jewell 1980)

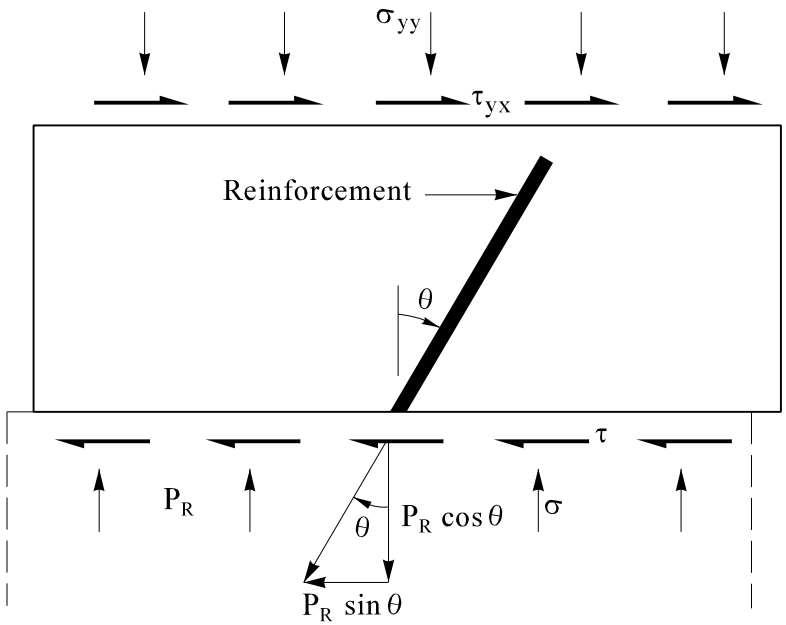

$$\tau = \left(\frac{P_R}{A_s}\right)(\cos\theta \tan\phi + \sin\theta)$$

Legend:

τ	Increase of shearing strength of soil
A_s	Area of soil shearing plane
P_R	Reinforcement tensile force

Figure A3 - Increase of Shearing Strength of Soil due to Tensile Reinforcement Force (after Jewell & Wroth, 1987)

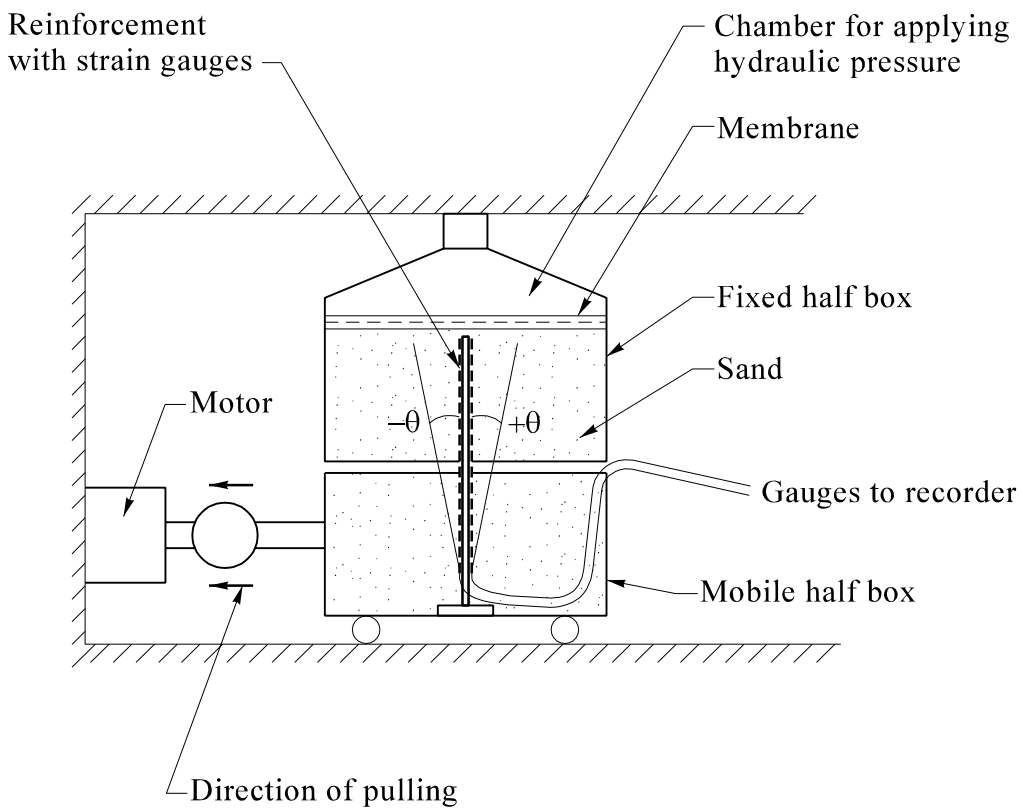

Figure A4 - Soil Laboratory Test Apparatus (after Marchal, 1986)

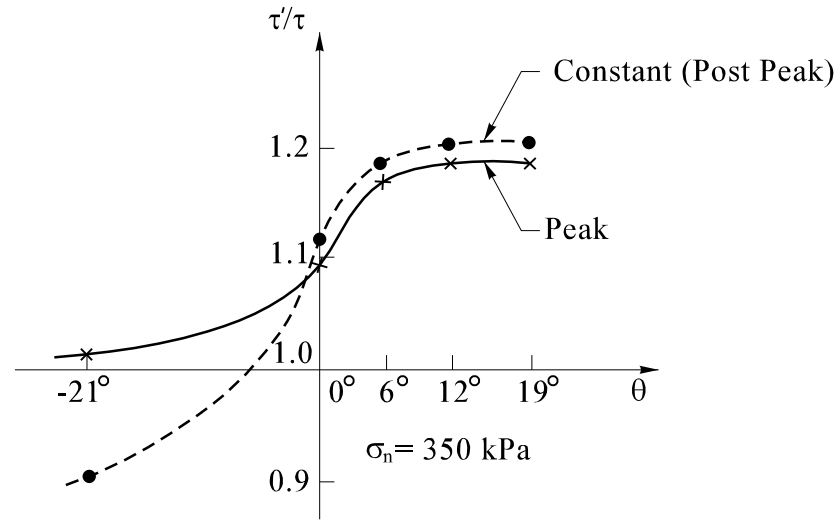

(a) Rigid Reinforcement

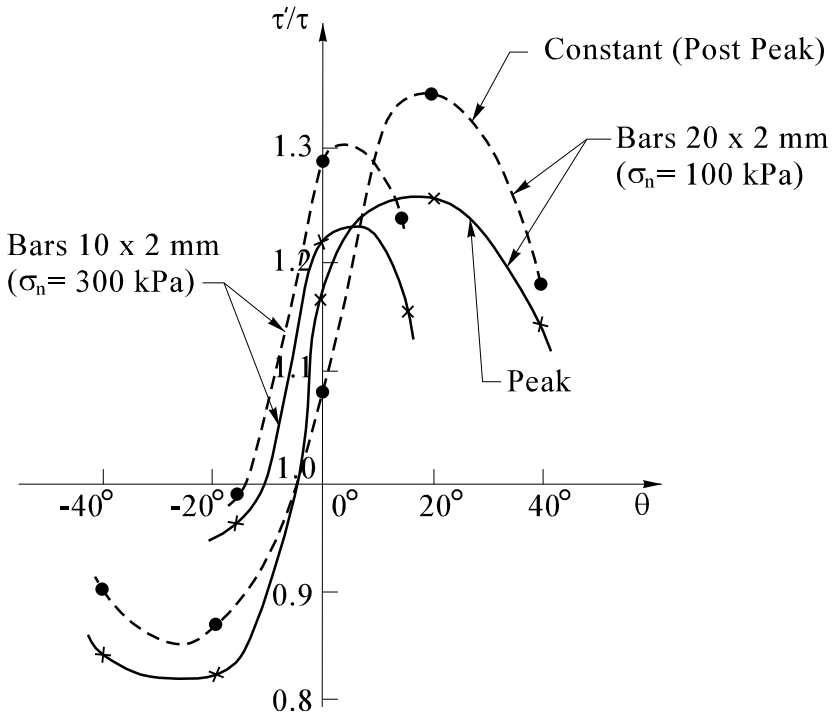

(b) Flexible Reinforcement

Legend:

τ	Shear strength of unreinforced soil
τ'	Shear strength of reinforced soil
σ_n	Normal stress on shear plane

Figure A5 - Development of the Ratio of Shear Strength of Nailed to Soil Alone as a Function of Nail Orientation (after Marchal, 1986)

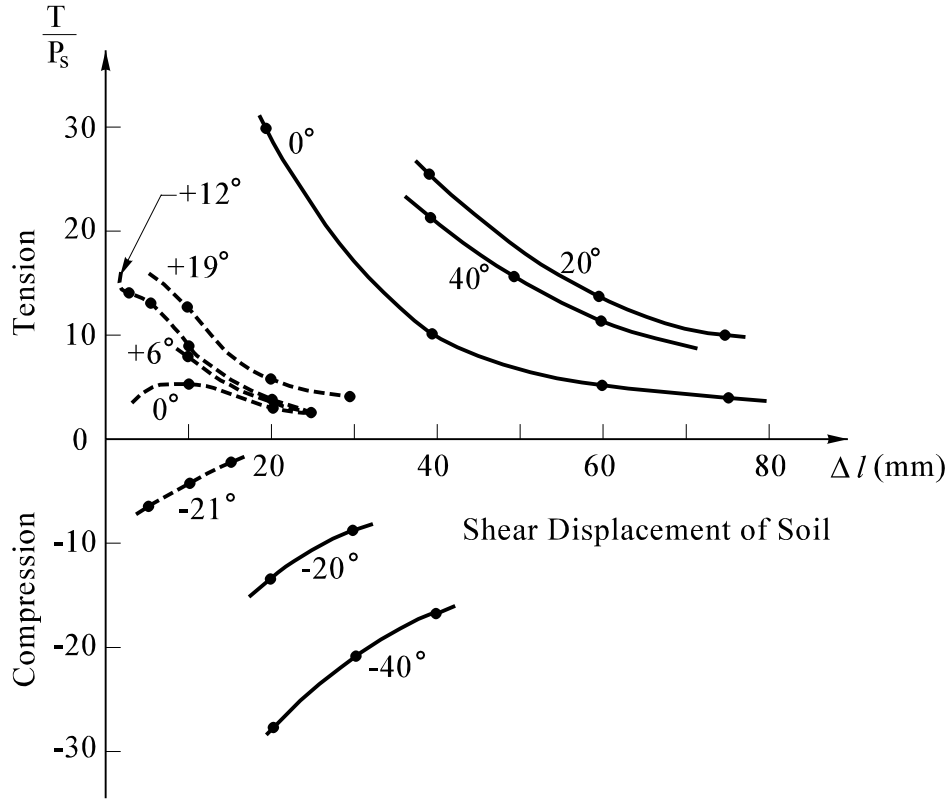

Legend:

●——●	Flexible (20 x 2 mm steel)	T	Nail axial force
●- - -●	Rigid (50 x 8.8 mm steel)	P_S	Nail shear force

Figure A6 - Development of the Relationship T/P_S as a Function of Shear Displacement Δl and Nail Orientation, θ (after Marchal, 1986)

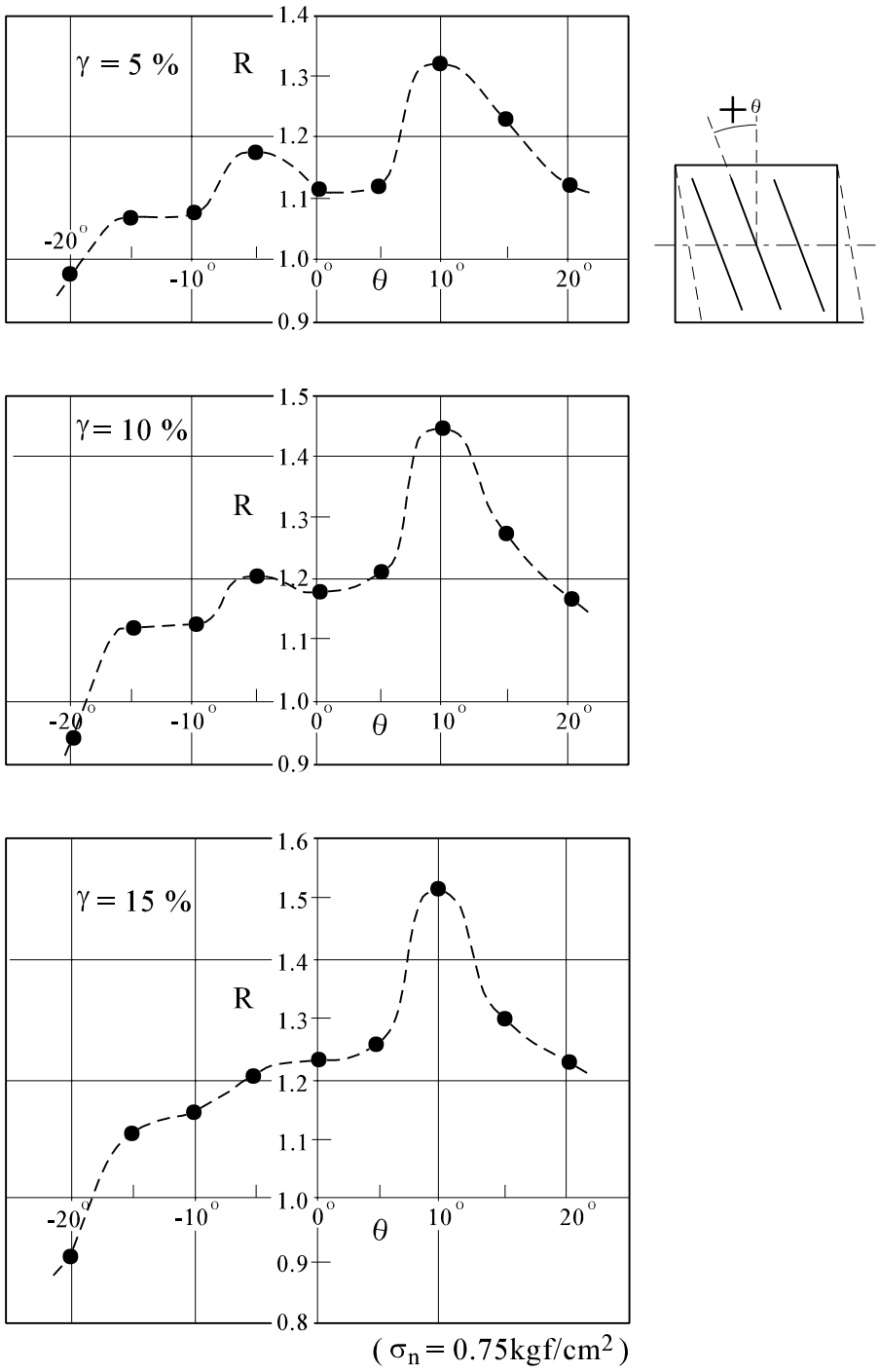

Legend:

γ Shear strain of soil

$$R = \frac{\text{Shear resistance of reinforced soil}}{\text{Shear resistance of unreinforced soil}}$$

Figure A7 - Ratio of Shearing Resistance of Reinforced Soil to Shearing Resistance of Unreinforced Soil for Reinforcement (Bronze Bar) at Different Orientations (after Hayashi et al, 1988)

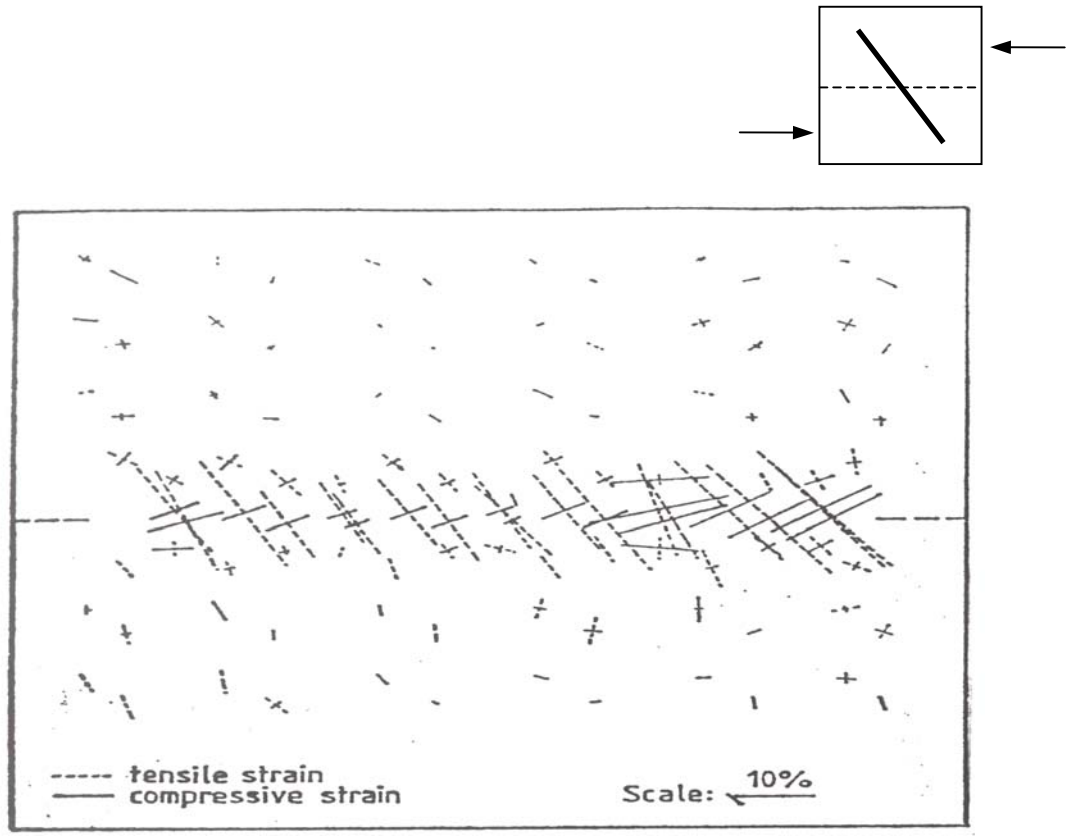

(a) Unreinforced

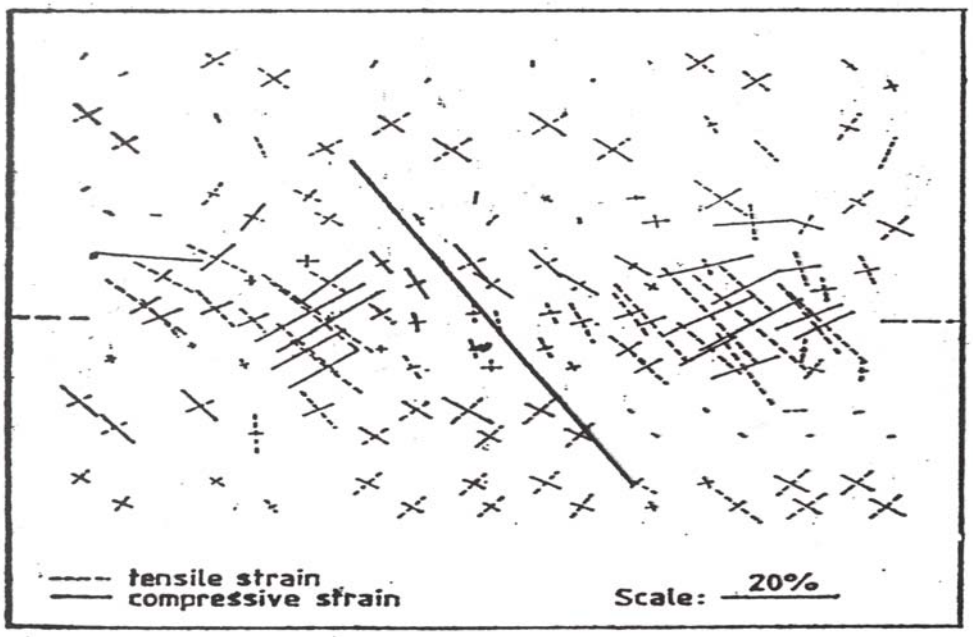

(b) Reinforced with Grid 4

Figure A8 - Principal Strain Orientation at Peak Stress Ratio (after Palmeira and Milligan, 1989)

Table of Contents
Table of Contents
Table of Contents

APPENDIX B

RESULTS OF FLAC ANALYSIS FOR NAILED SLOPES - AXIAL NAIL FORCE DISTRIBUTIONS AND SHEAR STRAINS OF SOIL FOR VARIOUS NAIL INCLINATIONS

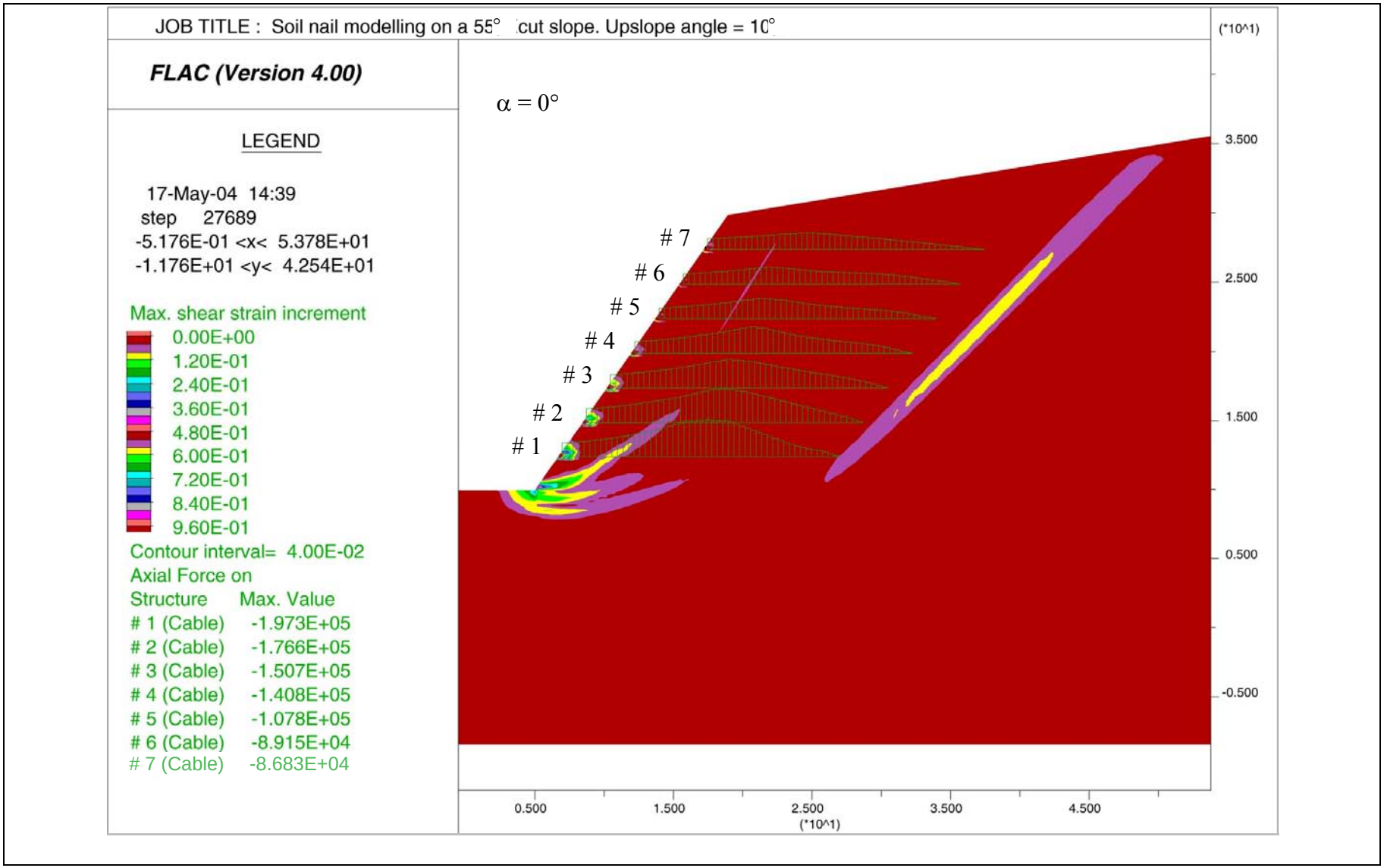

Figure B1 - Axial Nail Force Distribution and Shear Strains of Soil, α = 0°

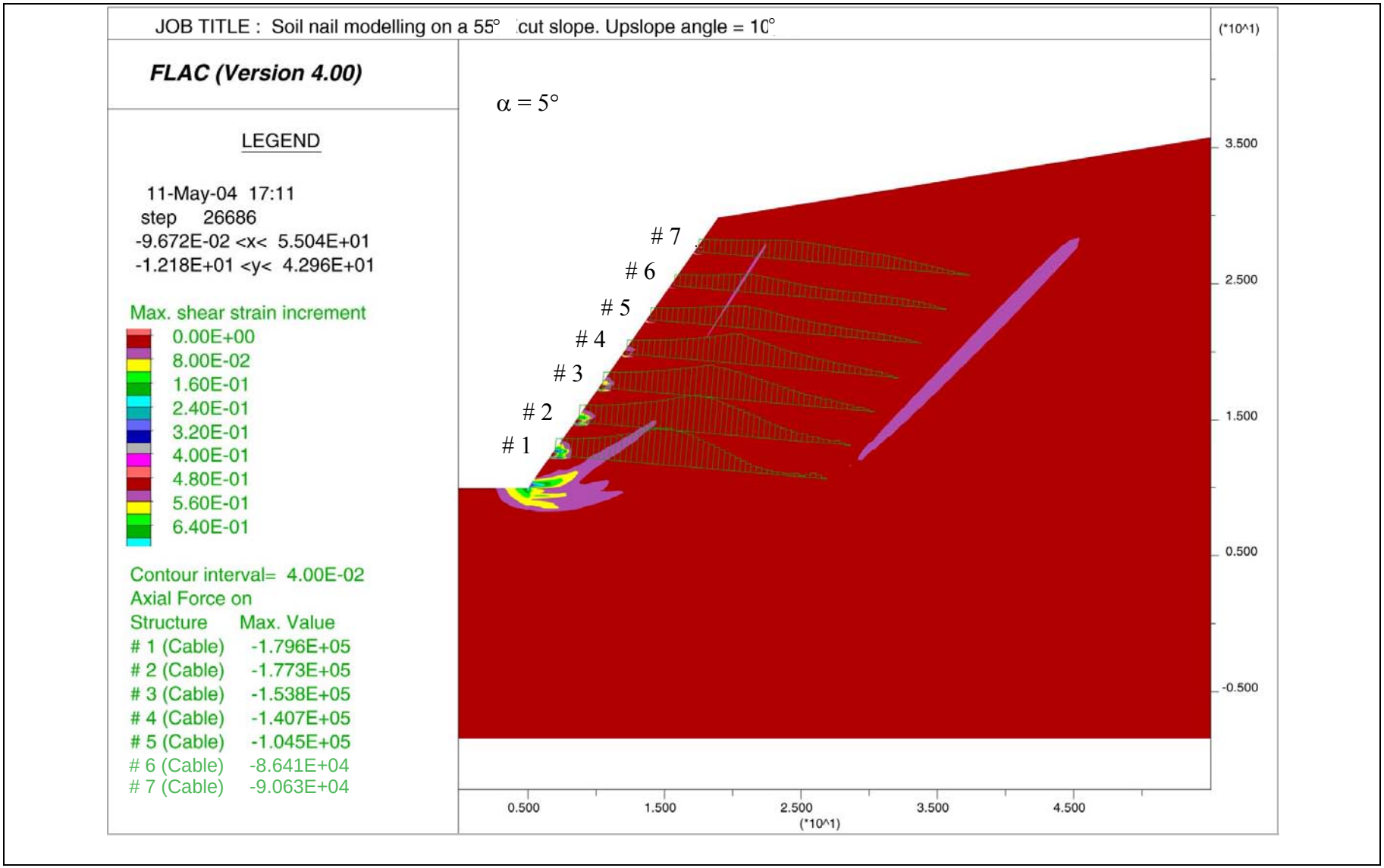

Figure B2 - Axial Nail Force Distribution and Shear Strains of Soil, α = 5°

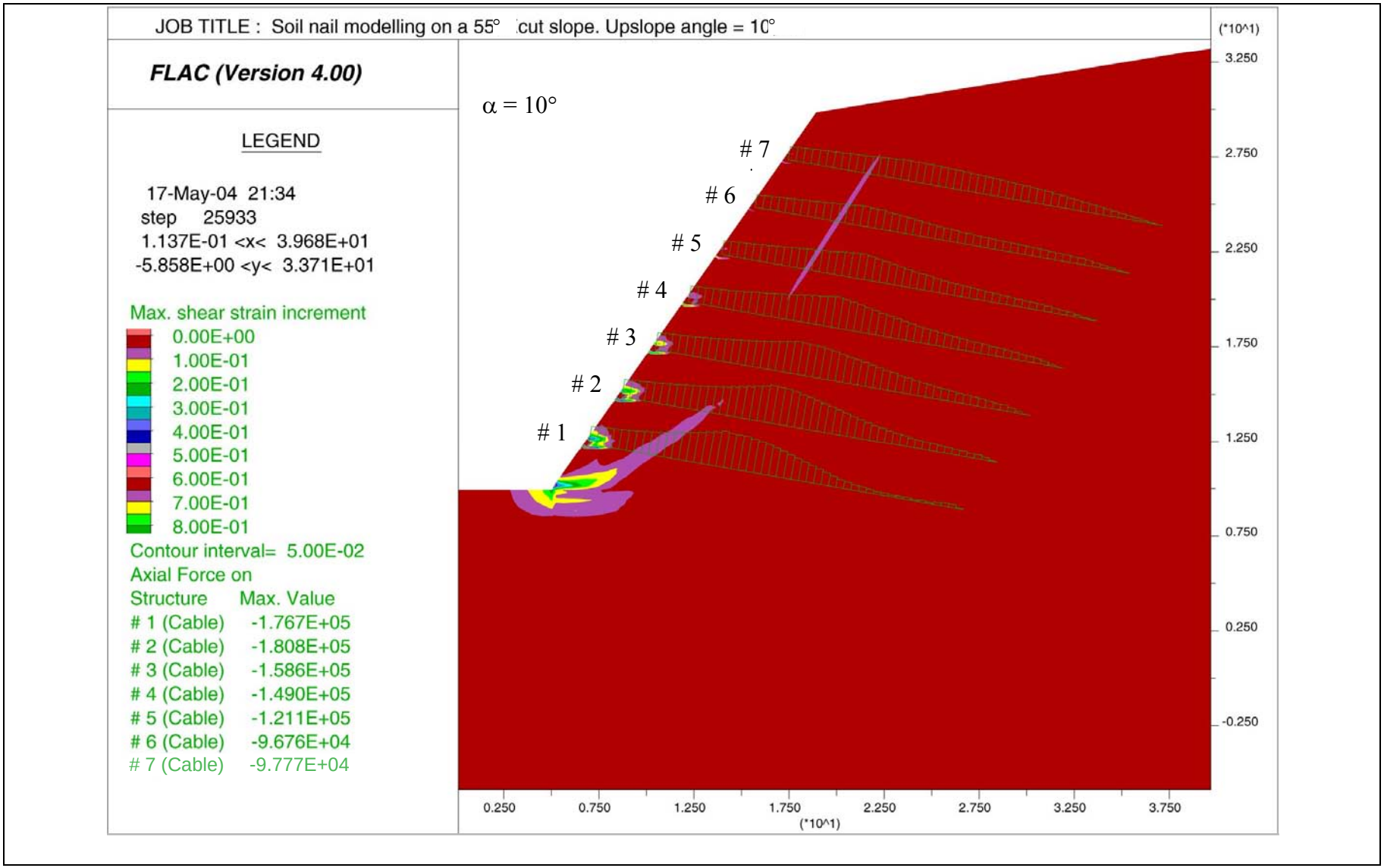

Figure B3 - Axial Nail Force Distribution and Shear Strains of Soil, α = 10°

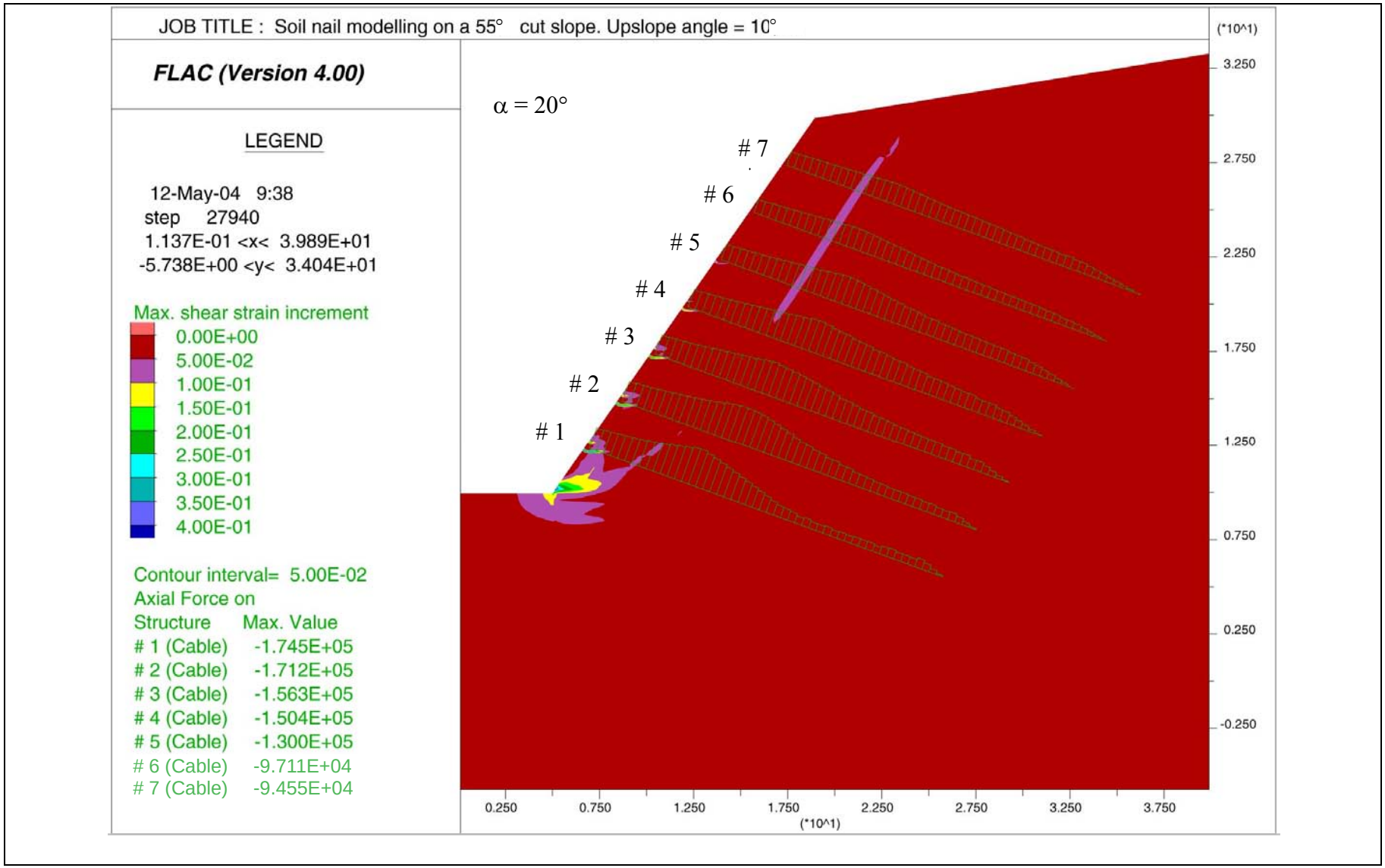

Figure B4 - Axial Nail Force Distribution and Shear Strains of Soil, α = 20°

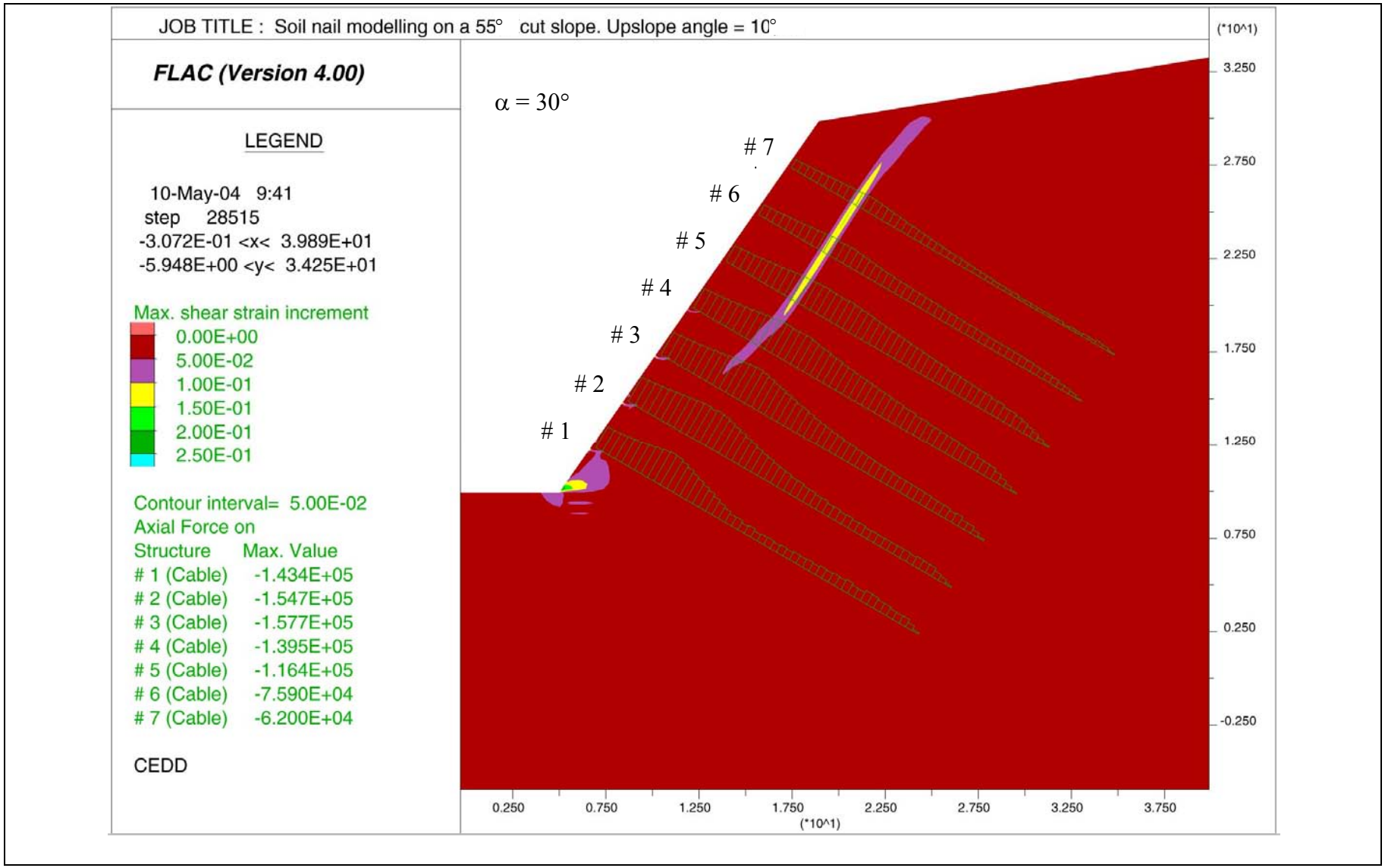

Figure B5 - Axial Nail Force Distribution and Shear Strains of Soil, α = 30°

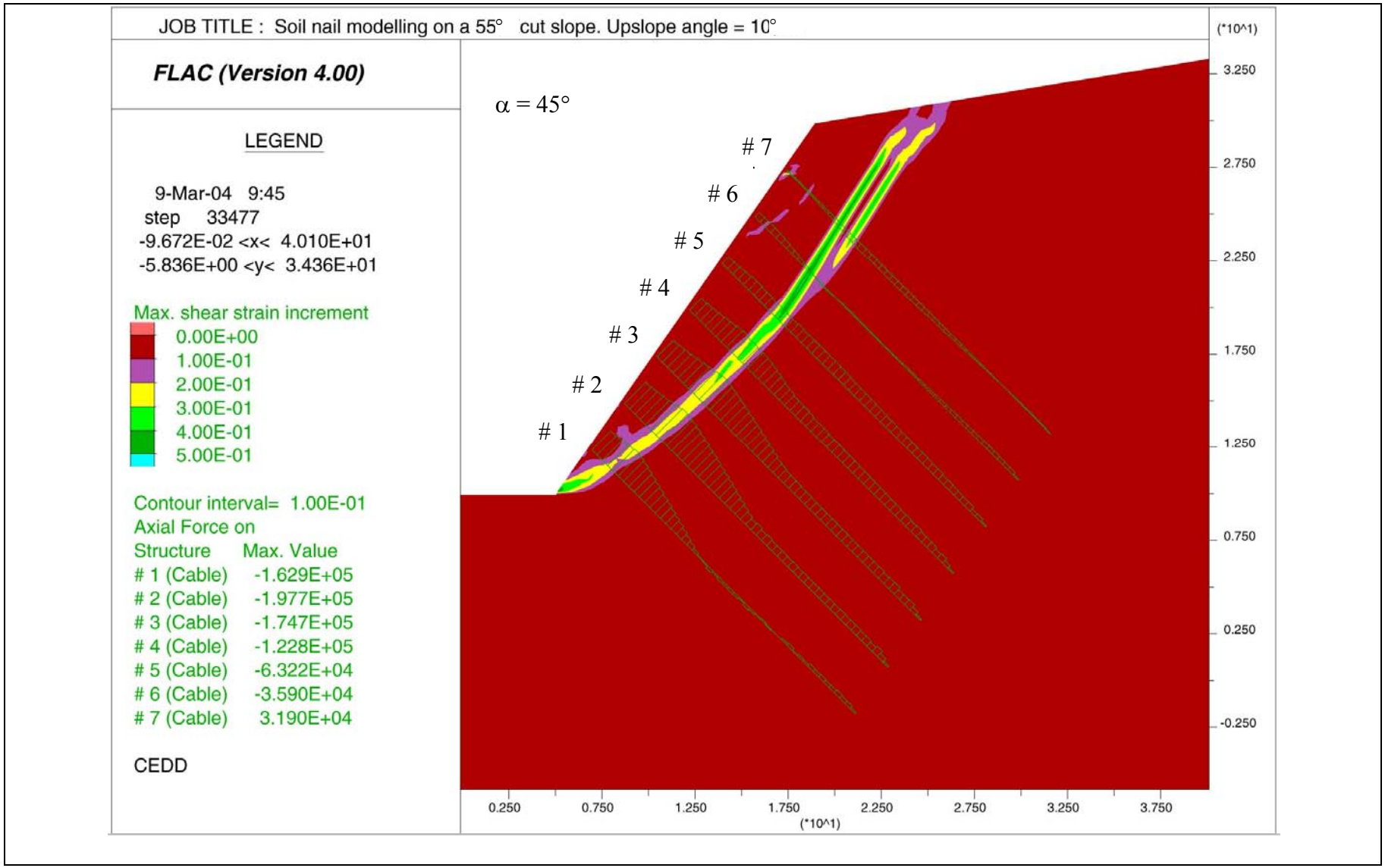

Figure B6 - Axial Nail Force Distribution and Shear Strains of Soil, α = 45°

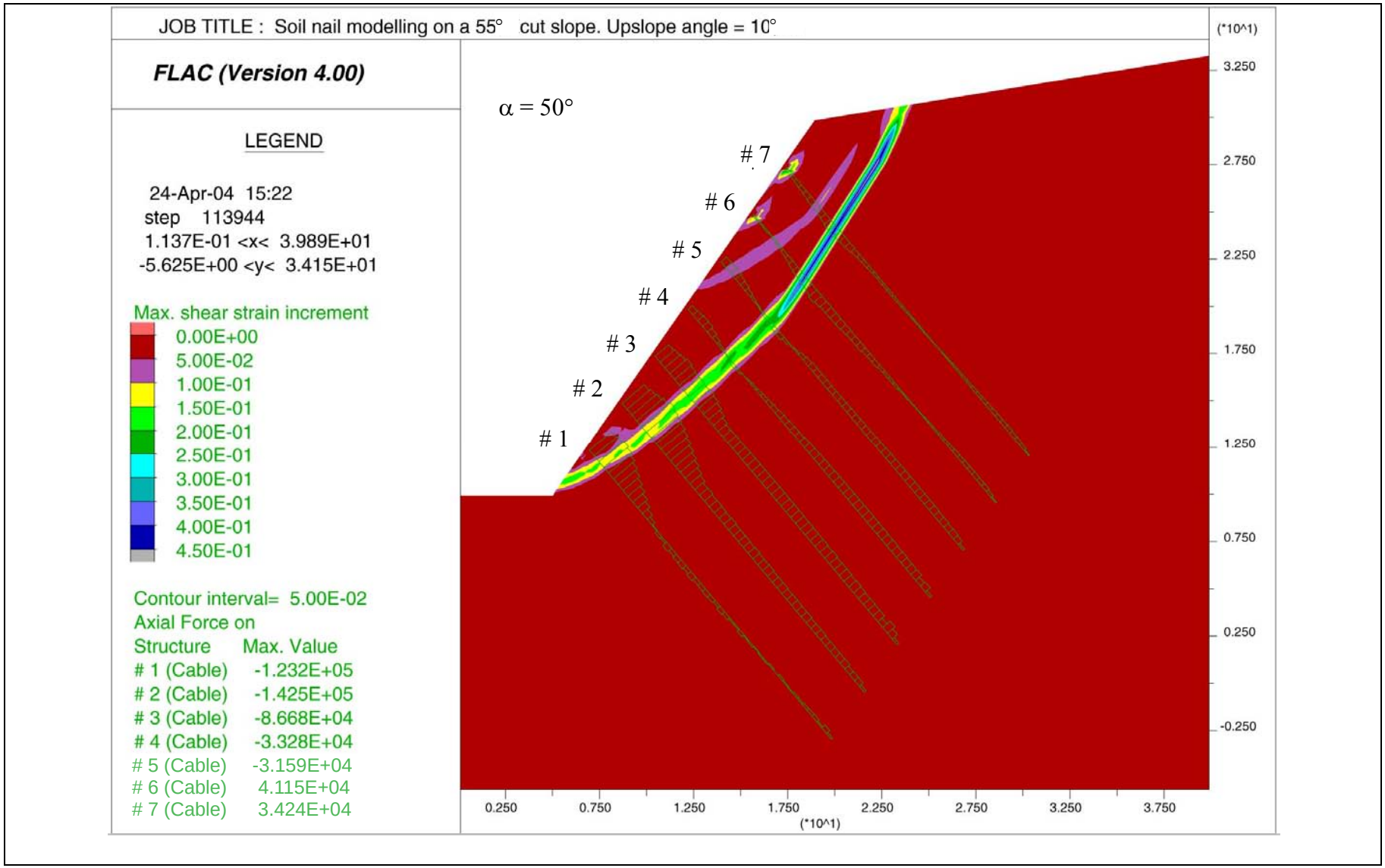

Figure B7 - Axial Nail Force Distribution and Shear Strains of Soil, α = 50°

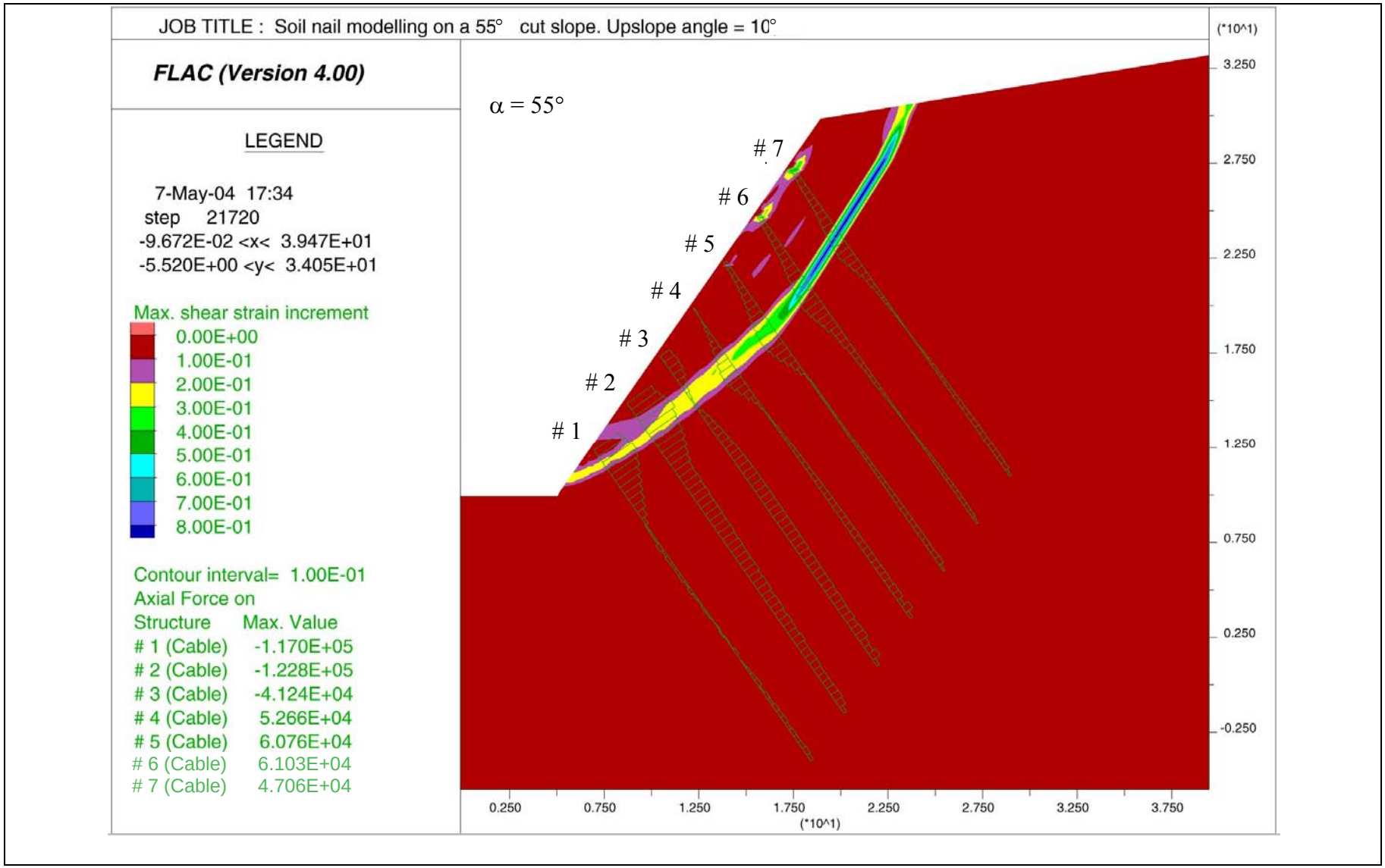

Figure B8 - Axial Nail Force Distribution and Shear Strains of Soil, α = 55°

Table of Contents
Table of Contents
Table of Contents

APPENDIX C

RESULTS OF FLAC ANALYSIS FOR NAILED EXCAVATIONS - AXIAL NAIL FORCE DISTRIBUTIONS AND SHEAR STRAINS OF SOIL FOR VARIOUS NAIL INCLINATIONS

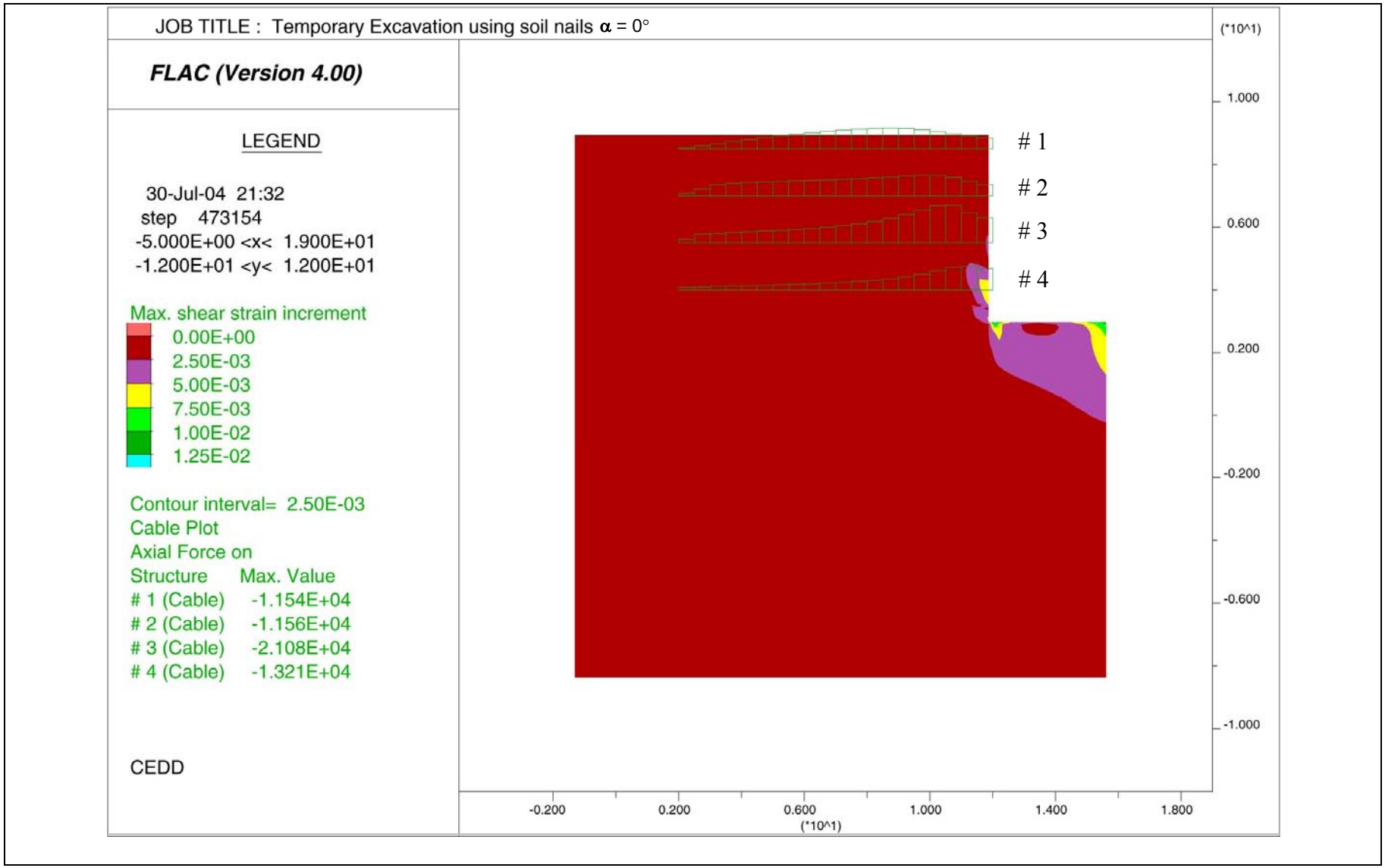

Figure C1 - Axial Nail Force Distribution and Shear Strains of Soil, α = 0°

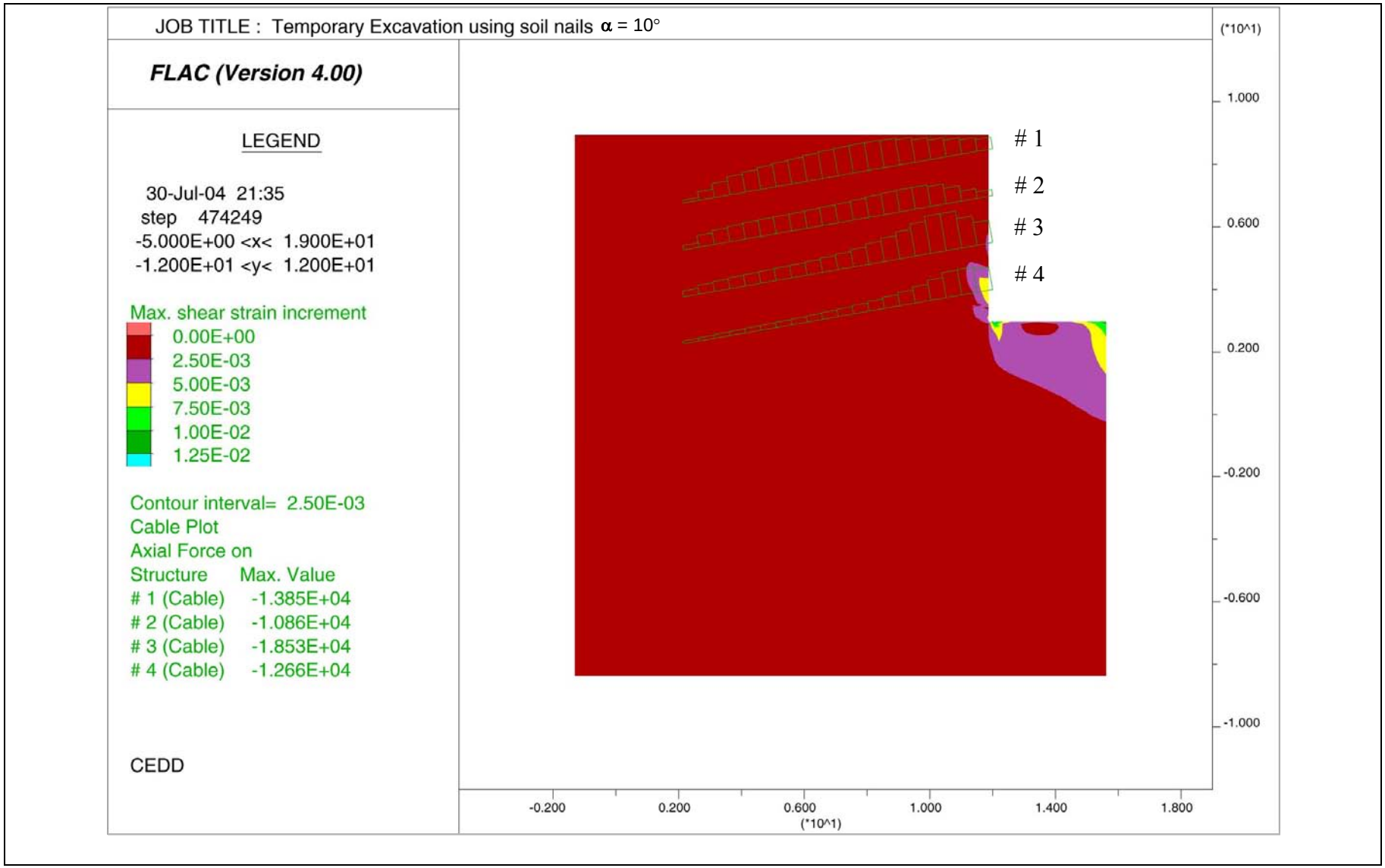

Figure C2 - Axial Nail Force Distribution and Shear Strains of Soil, α = 10°

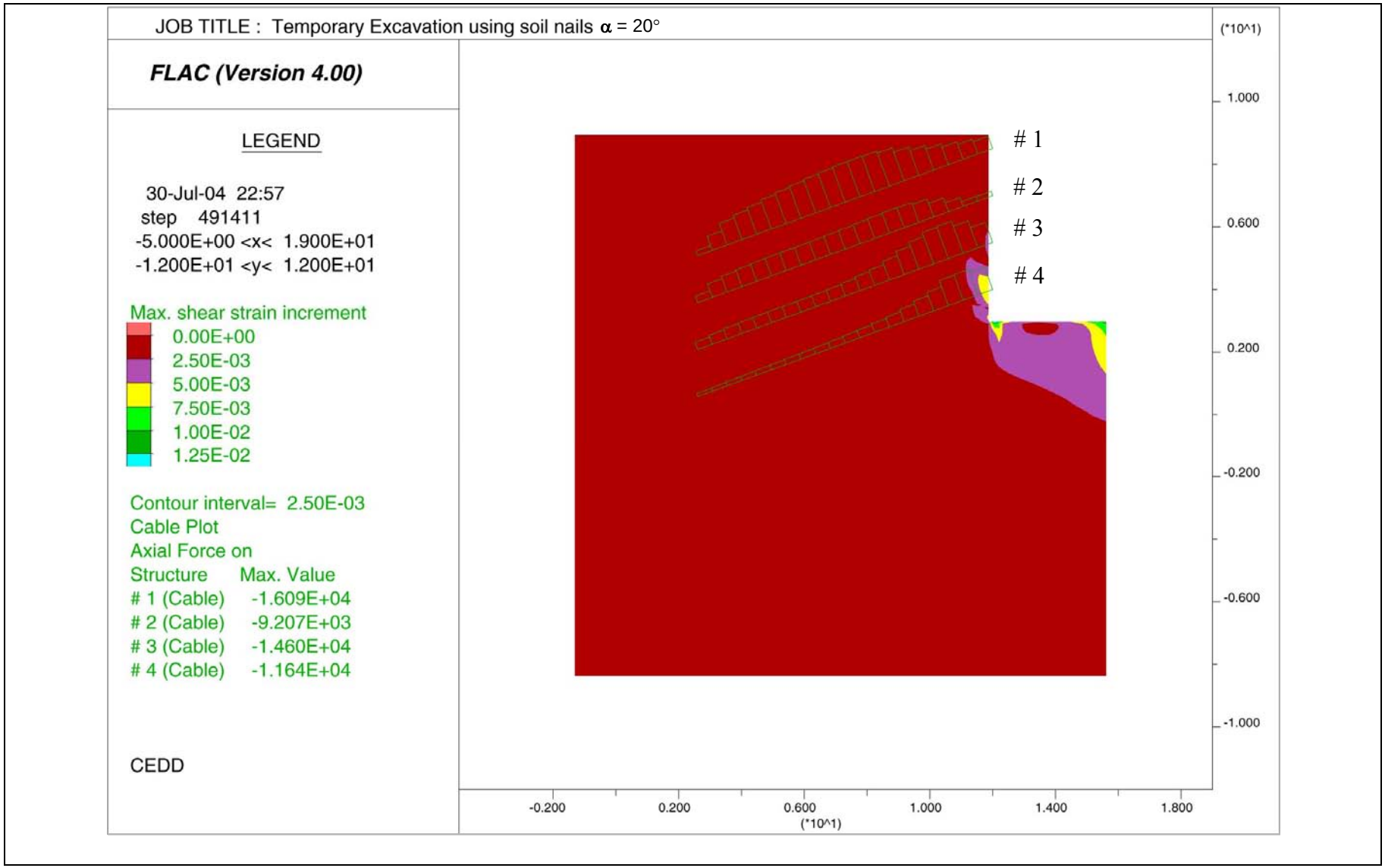

Figure C3 - Axial Nail Force Distribution and Shear Strains of Soil, α = 20°

Table of Contents
Table of Contents
Table of Contents
Table of Contents
Table of Contents

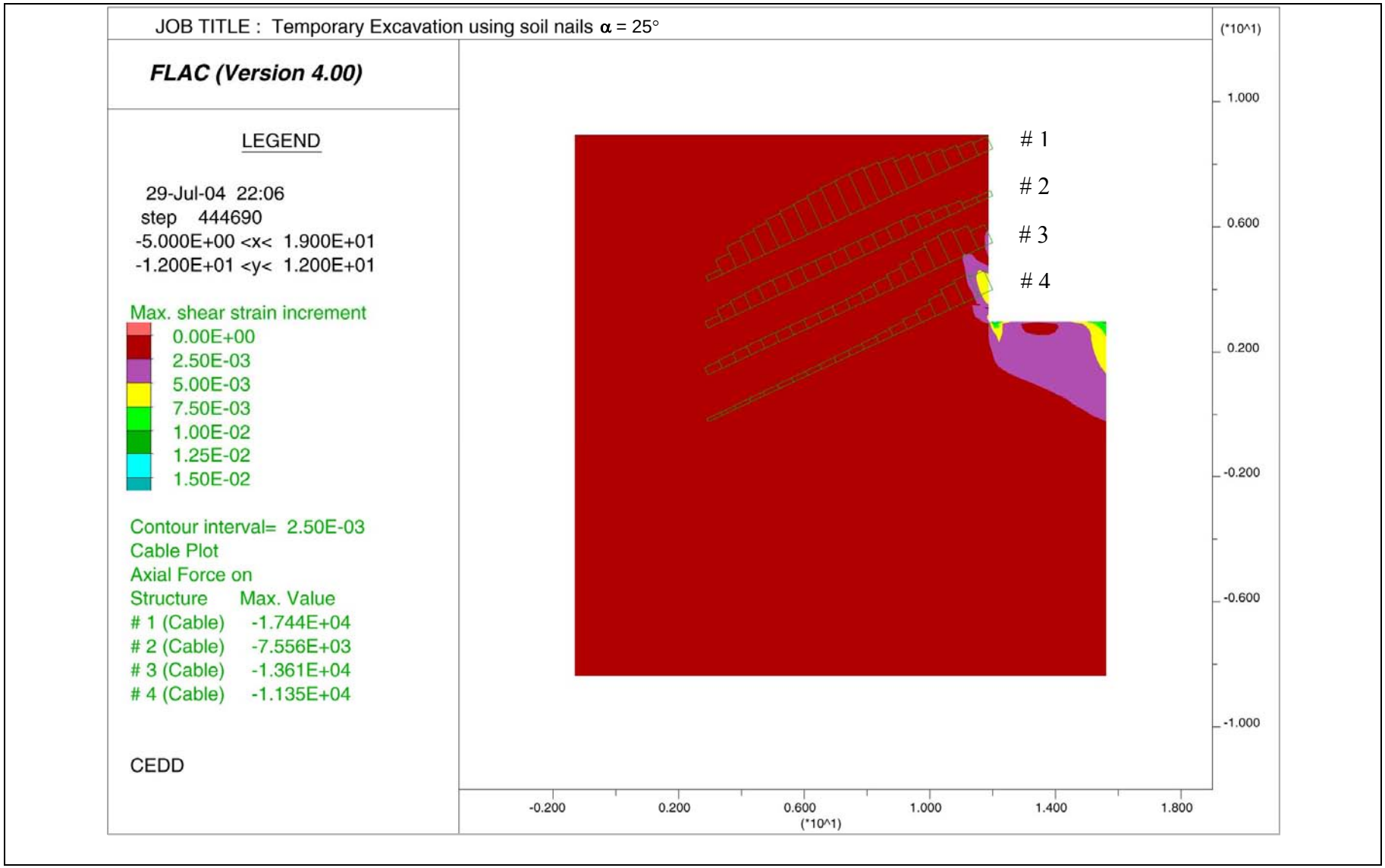

Figure C4 - Axial Nail Force Distribution and Shear Strains of Soil, α = 25°

Table of Contents
Table of Contents
Table of Contents
Table of Contents
Table of Contents

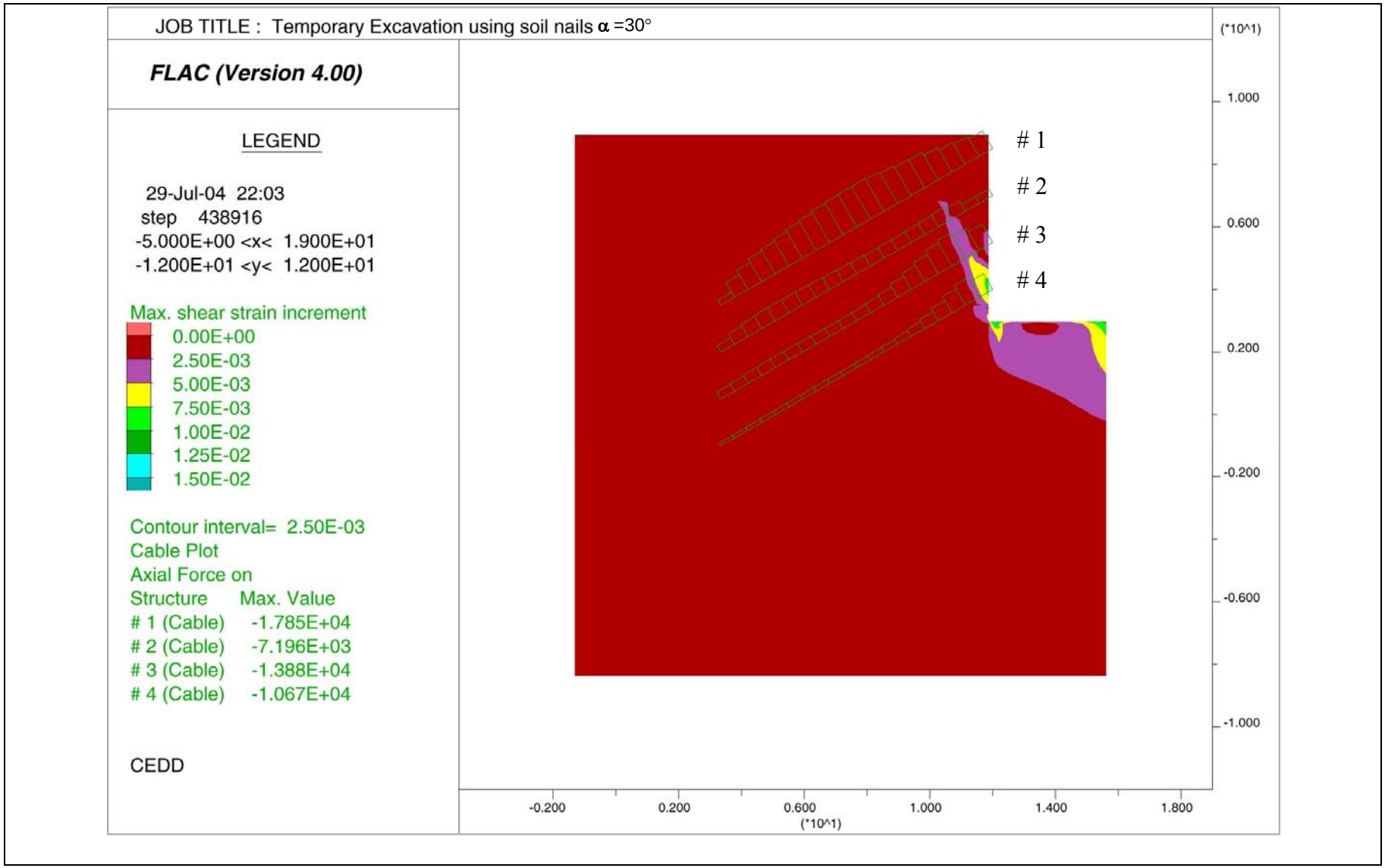

Figure C5 - Axial Nail Force Distribution and Shear Strains of Soil, α = 30°

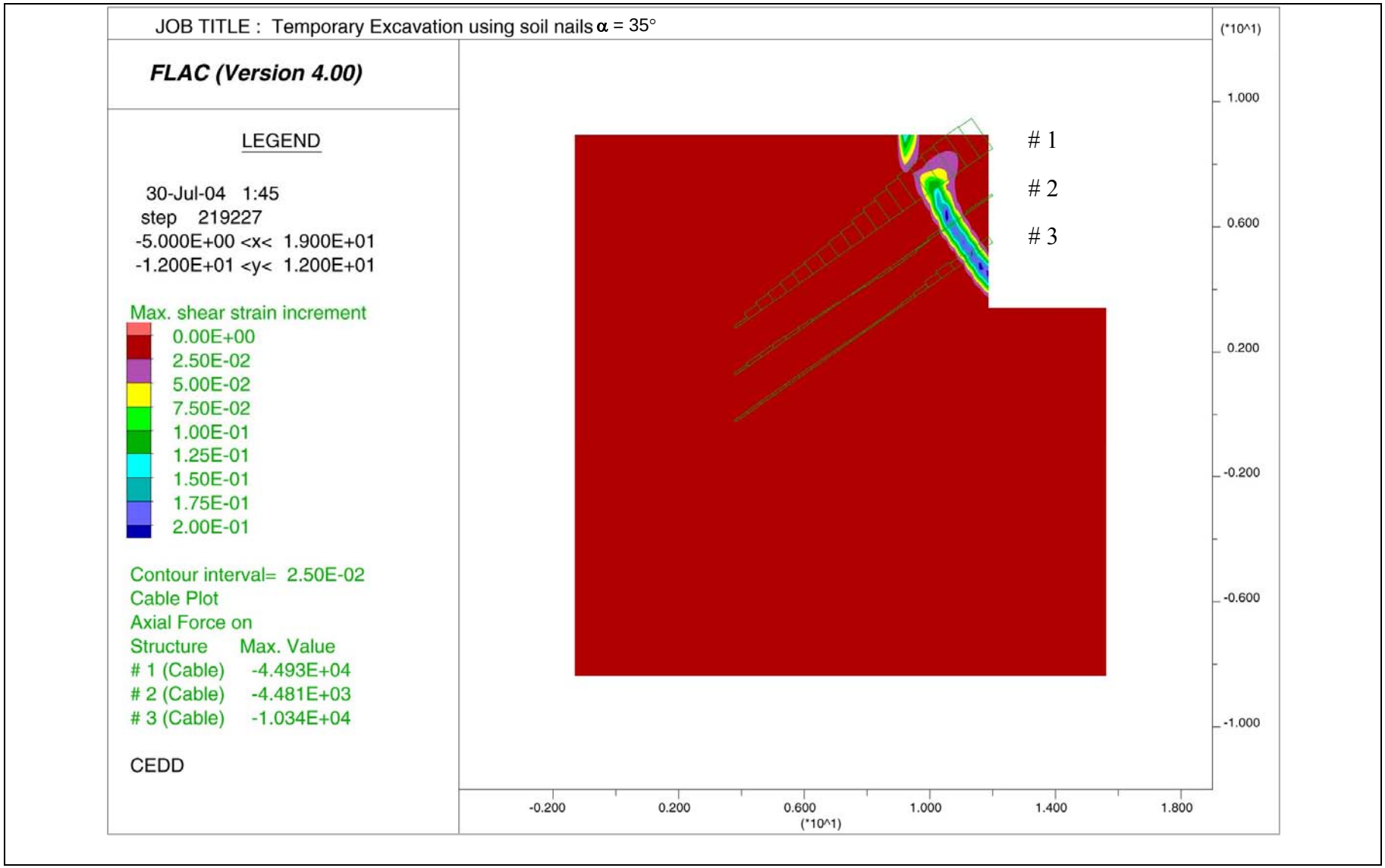

Figure C6 - Axial Nail Force Distribution and Shear Strains of Soil, α = 35°

Table of Contents
Table of Contents
Table of Contents

APPENDIX D

PREVIOUS STUDIES ON EFFECT OF BENDING STIFFNESS OF SOIL NAILS

D.1 PREVIOUS STUDIES RELATING TO EFFECT OF BENDING STIFFNESS OF SOIL NAIL

In the direct shear tests by Marchal (1986) as described in Appendix A, shear forces developed in the reinforcements were measured. The variations in the relationship between the axial tensile/compressive force and the shear force (T/P_s) developed in the reinforcement are shown in Figure A6 of Appendix A. Same for both rigid and flexible reinforcements, tensile or compressive forces were first mobilised when the reinforcements were gradually subjected to shear force. After relatively large shear displacements of the soil, 20 mm for rigid reinforcement and 60 to 70 mm for flexible reinforcement, the T/P_s approached a constant minimum value. Marchal (1986) observed that the shear displacements necessary to reach the peak shear of the reinforced soil were larger that those of unreinforced soil.

Gigan and Delmas (1987) presented a comparative study of various soil nail design computer programs. Some of the programs can incorporate the shear and bending contribution of nails. The study results showed that including the contribution of reinforcement shear stress in the calculation resulted in a maximum increase in factor of safety of about 10%.

Bridle and Davies (1997) reported results of a series of instrumented large scale shear box tests. The experiments revealed that the pull-out strength of the reinforcement was taken up prior to any significant development of shear load. Following mobilization of pull-out strength, shear loads increased with shear deformation. Typical test result for a reinforcement at right angle to the shear plane is shown in Figure D1. This is the optimum reinforcement orientation for mobilizing shear force in the reinforcement. Axial reinforcement forces developed due to the shear deformation of the reinforcement. Other results of the shear box tests indicated that there was an increase in maximum axial nail force with rotation from the normal to the shear plane up to a rotation of approximately 30^o. This is in agreement of the findings of Jewell (1980) and Pedley (1990).

Davies and Masurier (1997) presented results of large scale shear box tests. The shear box measured 3 m x 1.5 m x 1.5. Steel and aluminium nails of 2.8 m long and 25 mm diameter were tested. They observed that tensile forces in the nails developed immediately shear load was applied to the sample. The tensile forces increased rapidly to a peak after approximately 30 mm shear displacement and then remained constant with increasing shear displacement (Figure D2). The tensile force was mainly controlled by the pull-out capacity of the nail. Shear force in the nail did not start to develop until up to 20 mm shear displacement had occurred, the shear force then increased steadily. The maximum possible shear force was limited by the plastic moment at the nail.

Tan et al (2000) used a series of simplified failure modes to describe the behaviour of the soil-nail lateral action. They include: (i) failure due to soil yielding, (ii) failure due to nail yielding, and (iii) failure due to soil and nail reaching yield simultaneously. These failure modes are dependent on the relative stiffness and strengths of soil and nail as well as the relative lateral displacement. The extent to which the nail is deformed determines the shear force and the axial load developed in the nail. Expressions for calculating soil-nail lateral resistance were derived for the failure modes.

Smith and Su (1997) reported results of 3-dimensional finite element analysis of a soil nailed wall. The results indicate that little bending and shear resistance is developed in the

nails during construction and under service load. Shear stresses and bending moments were mobilised when the wall was under large surcharge load and close to collapse.

Pluemelle et al (1990) presented test results of an instrumented soil nailed wall (7 m in height) which was taken to failure by progressively saturating the nailed soil mass. Failure zone developed in the nailed wall is shown in Figure D3. It was reported that "the tensile force is the first mechanism mobilised, and it is developed progressively during excavation…Close to failure and under large deformations, the bending stiffness is mobilised, giving an additional safety factor". Shear forces and bending moments in the nails were not measured.

D.2 LABORATORY AND THEORETICAL STUDIES BY PEDLEY (1990) AND JEWELL AND PEDLEY (1990 & 1992)

Pedley (1990) conducted a comprehensive experimental and theoretical study to examine the performance of soil reinforcement in respect of reinforcement orientation, bending and shear. In the study, a series of direct shear tests were carried out in a large-scale direct shear apparatus (1 m x 1 m x 1 m). Three different types of circular cross sections were tested. They included solid steel bars (16 to 25.4 mm in diameter), metal tubes (15.88 to 25.4 mm in external diameter and 13.19 to 22.36 in internal diameter) and grouted bar (50.8 mm in diameter with steel bar diameters 6.71 to 16 mm). Strain gauges were fixed to the reinforcement to measure the axial and bending strains during shear.

In the direct shear tests, the effect of reinforcement in shear and bending was studied by varying the reinforcement cross-section, reinforcement orientation and the relative soil-reinforcement stiffness and strength. The problem can be simplified to that shown in Figure D4. The bending moment (M), shear force (P_s) and lateral stress (σ'_l) of the reinforcement were determined from the direct shear tests. Figure D5 shows the distributions of: (a) the reinforcement bending moment (M) normalised by the plastic moment capacity (M_p); (b) the reinforcement shear force (P_s) normalised by the full plastic axial capacity (T_p); and (c) the lateral stress on the reinforcement (σ'_l) normalised by the limiting soil bearing stress (σ'_b). These distributions were the stress conditions of the reinforcement at a shear displacement of soil of 60 mm. The test results show that even when the measured bending moments were close to the fully plastic moment ($M/M_p = 1$) in all the tests, the maximum shear force (P_s) in the reinforcement was less than 6% of the plastic axial capacity (P_p). Figure D6 displays the shapes of the some grouted and ungrouted nails after the tests. Some nails had been deformed to an S shape. Pedley observed that the soil had fully strain-softened before mobilisation of the limiting shear capacity of the reinforcement. The laboratory results were confirmed by theoretical analysis discussed below.

Pedley (1990) derived elastic and plastic models for determining the maximum shear force mobilised in the reinforcement bar. These models were also reported in Jewell and Pedley (1990 & 1992). The elastic analysis simply defines the stress condition before the reinforcement reaches plasticity, it does not represent the failure condition. As such, only the plastic analysis is discussed here. The plastic analysis will always give a larger reinforcement shear force than the elastic analysis.

The relationship between axial force T and bending moment M of a soil reinforcement

is shown in Figure 26. The limiting plastic envelope for a bar of rectangular cross-section is given by (Calladine, 2000):

$$\frac{M}{M_p}+\left(\frac{T}{T_P}\right)^2=1 \quad \text{.....(D1)}$$

Equation D1 is slightly conservative for circular bar. Since no simple relationship can be derived for circular bar, this equation has been adopted by Jewell and Pedley (1990).

The relation between maximum shear force P_s and the maximum moment M_{max} depends on the magnitude and distribution of the lateral loading on the reinforcement bar. For plastic analysis for a soil nail under the lateral loading shown in Figure D7, the equations for this distribution of lateral loading are:

$$(P_s)=\frac{4M_{max}}{l_s} \quad \text{.....(D2)}$$

and

$$\left(\frac{l_s}{D}\right)=\sqrt{\frac{4\sigma_y}{3\sigma_b'}} \quad \text{.....(D3)}$$

where l_s is the distance between the points of maximum moment on either side of the potential shear surface, (see Figure D7), D is the diameter of reinforcement bar, σ_y is the yield stress of the bar and and σ' is the limiting bearing stress between soil and reinforcement.

The limiting bearing pressure (σ_b') between the soil and the reinforcement required to achieve the plastic equilibrium is:

$$(\sigma_b')_{max}=\frac{8M_{max}}{l_s^2 D} \quad \text{.....(D4)}$$

The theoretical plastic limiting maximum shear force P_s that can be generated in an ungrouted round bar that also supports axial force, P, is:

$$\frac{P_s}{T_p}=\frac{8}{3\pi\ (l_s/D)}\left\{1-\left[\frac{T}{T_p}\right]^2\right\} \quad \text{.....(D5)}$$

Details of explanations and derivation of Equations (D1) to (D5) can be found in Pedley (1990).

An important point to note is that the reinforcement shear force P_s is limited by the shear width (l_s/D) which is related to the bearing capacity of soil (σ'_b). If no axial nail force is developed (i.e. $T/T_p = 0$), the maximum possible shear force is approximately:

$$\frac{P_s}{T_p} = \frac{0.85}{(l_s / D)} \quad \text{.....(D6)}$$

According to Pedley et al (1990b), the bearing capacity of soil limits the lateral loading that can be exerted on the reinforcement and as such the shear width for typical soil nailing is of the order (l_s/D) = 10 to 20. From equation (D6), the limiting shear force is then of the order (P_s/T_p) < 10%.

The limiting shear force and the axial force for an ungrouted reinforcement bar can be determined using equations (D3) and (D5). Jewell and Pedley (1992) presented envelopes of limiting combinations of shear force P_s and axial force T for ungrouted nail bar of 25 mm diameter with typical soil parameters. The equilibrium for a soil nail at depths of approximately 5 m, 10 m, and 20 m in a steep-sided excavation was considered. The envelopes are shown in Figure D8.

As discussed by Jewell and Pedley (1992), for grouted bar, there is very little benefit to the reinforcement bending stiffness from the grout. As such, a grouted reinforcement bar has the same overall bending stiffness as the bar alone (no benefit from the grout) but the effective diameter of the soil nails equals the diameter of the hole D_g. The larger diameter of the grouted bar D_g reduces the ratio (l_s/D) and equation (D3) is modified as follows:

$$\frac{l_s}{D} = \sqrt{\frac{4\sigma_y}{3\sigma'_b}\frac{D}{D_g}} \quad \text{.....(D7)}$$

The limiting envelopes of allowable load for the range of cases examined above can be recalculated to allow for the effect of grout. For a typical grouted hole diameter Dg = 100 mm, with all the other parameters unchanged, the results of the recalculation are summarised in Figure D9. It can be observed from both Figures D8 and D9 that the magnitude of the limiting shear force in the reinforcement can only be a small proportion of the axial force capacity. This is the case even when the reinforcement is oriented so as to mobilize the maximum shear force.

D.3 Overall Improved Shearing Resistance of Soil

The implication from the test and analytical results reported by Pedley (1990) and Jewell and Pedley (1992) is that reinforcement bending stiffness allows only a small additional shear force to be mobilised compared with the axial force capacity of the reinforcement.

According to Pedley (1990), the overall influence of reinforcement shear and axial force on soil shearing strength can be analysed by considering reinforcement crossing a potential shear surface at some orientation, angle θ, see Figure D10. The net change in shear strength of the soil (ΔS) due to the reinforcement axial force (T/T_p) and the reinforcement shear force (P_s/T_p) is:

$$\left[\frac{\Delta S}{T_P}\right] = \left[\frac{T}{T_P}\right](\cos\theta \tan\phi' + \sin\theta) + \left[\frac{P_S}{T_P}\right](\cos\theta - \sin\theta \tan\phi') \quad \text{.....(D8)}$$

It can be noted that the reinforcement shear force has a much smaller influence on soil shear strength improvement than the reinforcement axial force for two reasons: (i) a component of the reinforcement shear force reduces the normal stress in the soil and thereby decreases the soil strength; and (ii) the limiting reinforcement shear force is only a small percentage of the axial capacity of the reinforcement T_p. This shows that reinforcement used in shear and bending is much less efficient than that used in axial tension.

Pedley (1990) has back-analysed an instrumented 6 m high nailed wall that was loaded to failure. He found that the highest contribution of reinforcement shear force to soil strength improvement was less than 3% to that due to reinforcement axial force. This is in agreement with the theoretical study result that only very small amount of shear force can be mobilised in nail.

LIST OF FIGURES

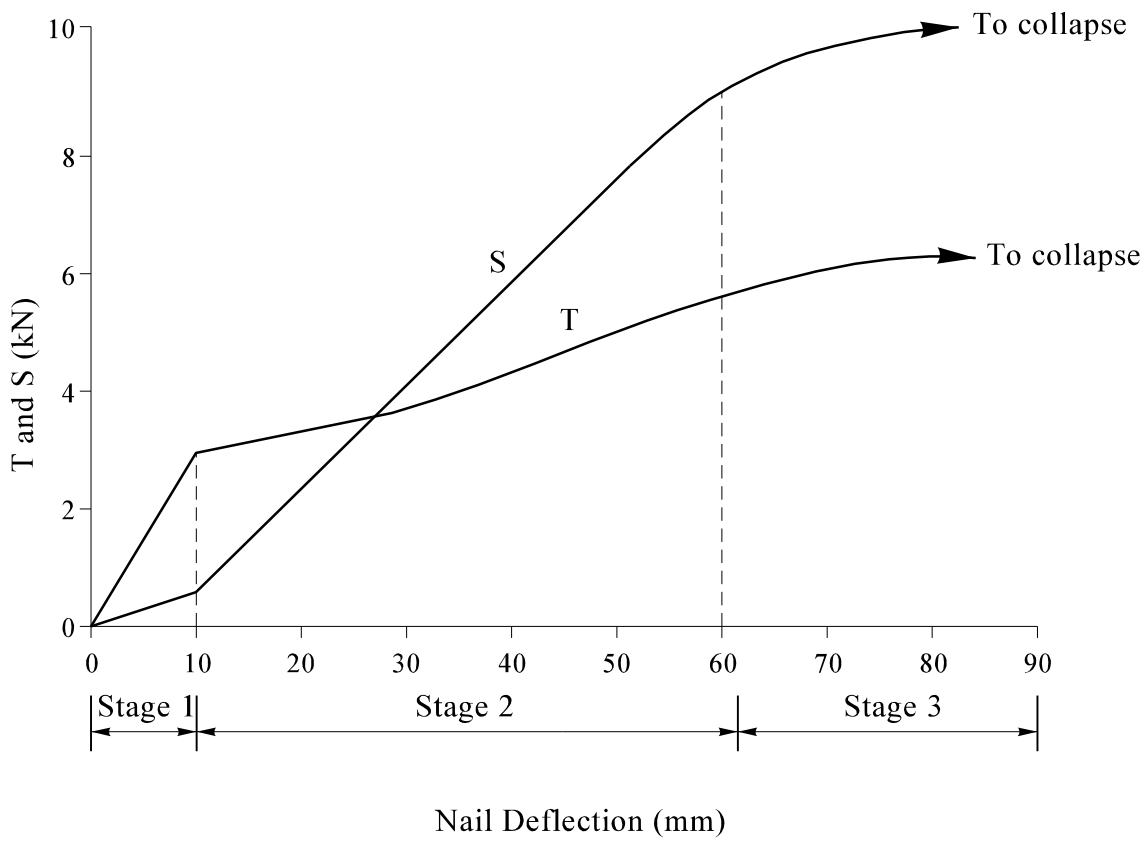

Stage 1: A rapid linear development in tensile load T in the nail with displacement. The shear force S in the nail rises relatively slowly.

Stage 2: The gradient of the tensile force curve changes markedly and there is an increase in the rate of development of shear force in the nail.

Stage 3: The nail undergoes permanent deformation. There is small increase in tensile load in deflection.

Legend:

S	Shear force in soil nail
T	Tensile force in soil nail

Note: Nail orientation - normal to slip surface.

Figure D1 - Development of Tensile and Shear Forces During Deflection of a Soil Nail (after Bridle & Davies, 1997)

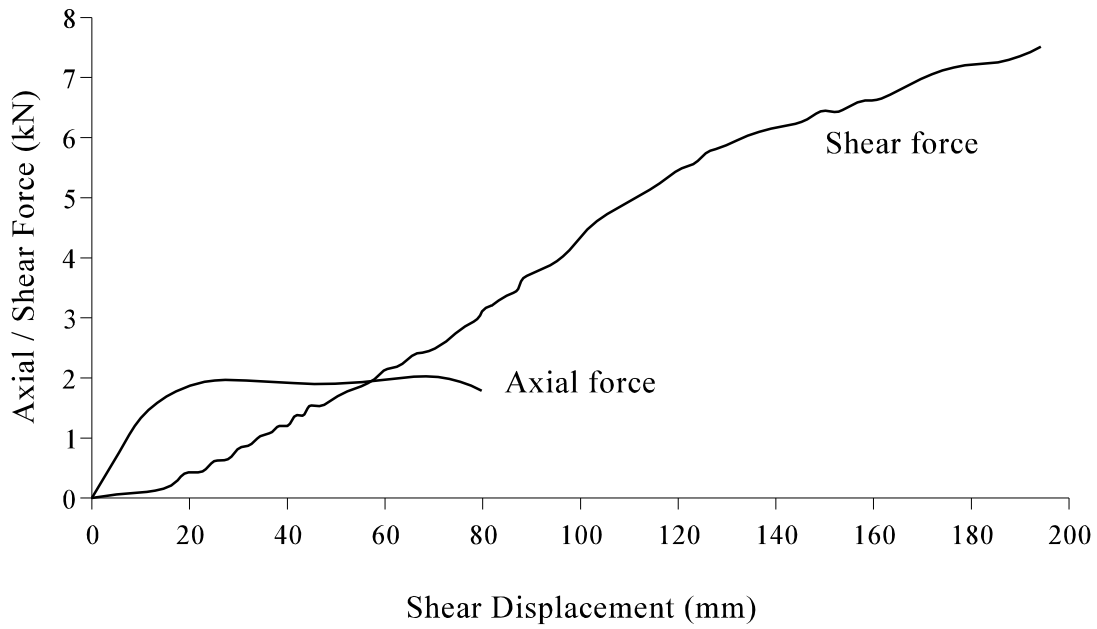

Note: Test at 200 kPa confining pressure.

Figure D2 - Development of Shear Forces and Tensile Forces in Soil Nail (after Davies and Le Masurier, 1997)

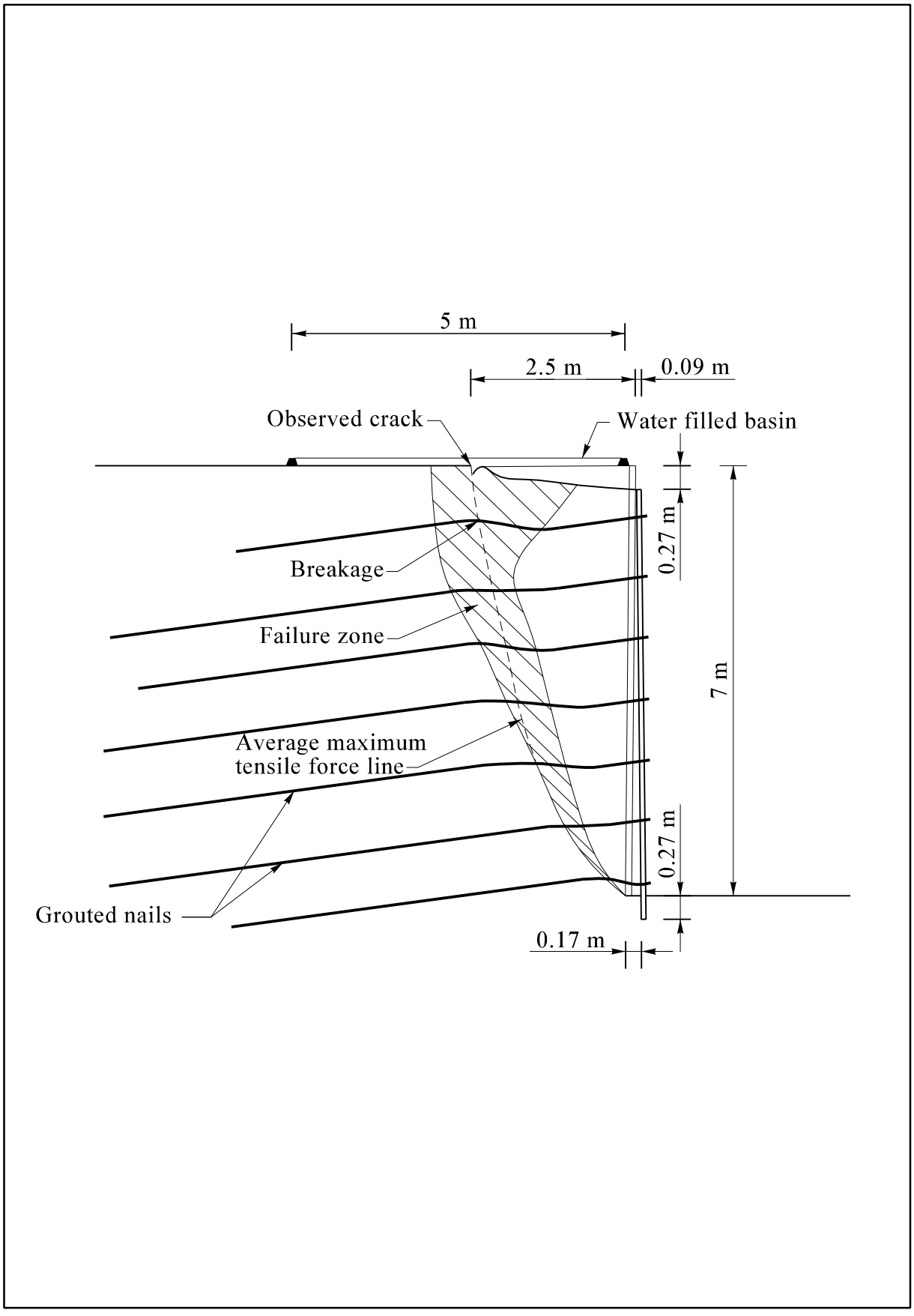

Figure D3 - Failure Zone Developed in Soil Nailed Wall (after Plumelle et al, 1990)

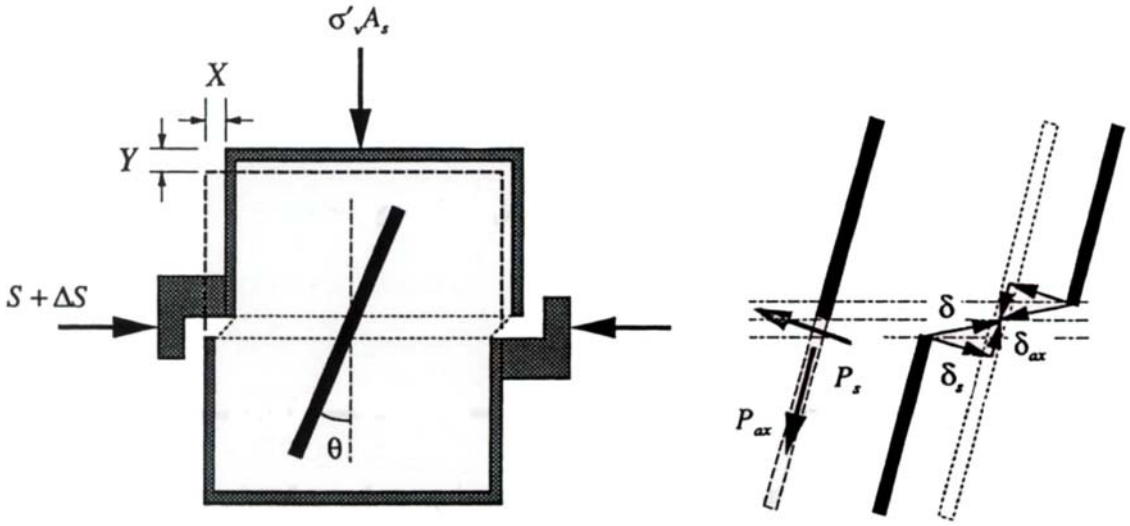

Legend:

S	Gross shear resistance of unreinforcement soil
Δs	Additional shearing resistance due to nail
θ	Reinforcement orientation
P_{ax}	Reinforcement axial force
P_s	Reinforcement shear force
δ	Reinforcement resultant displacement
δ_{ax}	Reinforcement axial displacement
δ_s	Reinforcement shear displacement

Figure D4 - Reinforcement Crossing a Potential Rupture Surface (after Pedley, 1990)

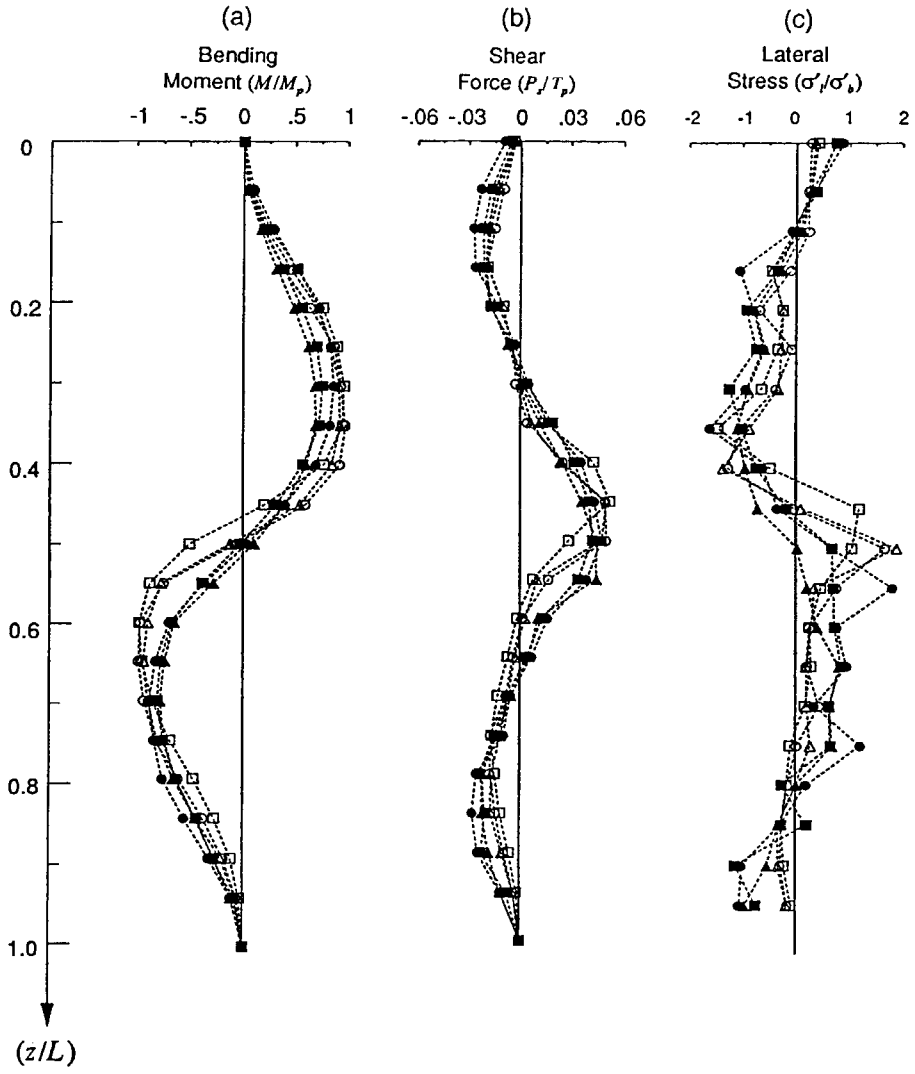

	Bar diameter (mm)	Nail orientation θ°		Bar diameter (mm)	Nail orientation θ°
○	15.88	0°	●	25.4	0°
□	15.88	15°	■	25.4	15°
△	15.88	25°	▲	25.4	25°

Legend:

M	Bending moment of nail
M_P	Fully plastic bending moment of nail
P_s	Nail shear force
T_P	Fully plastic axial force in nail
σ'_l	Lateral stress on nail
σ'_b	Limiting bearing stress

Figure D5 - Profiles of (a) Bending Moment (M/M_p), (b) Shear Force (P_s/P_p) and (c) Lateral Stress (σ'_l/σ'_b) at a Shear Displacement of 60 mm (after Pedley, 1990)

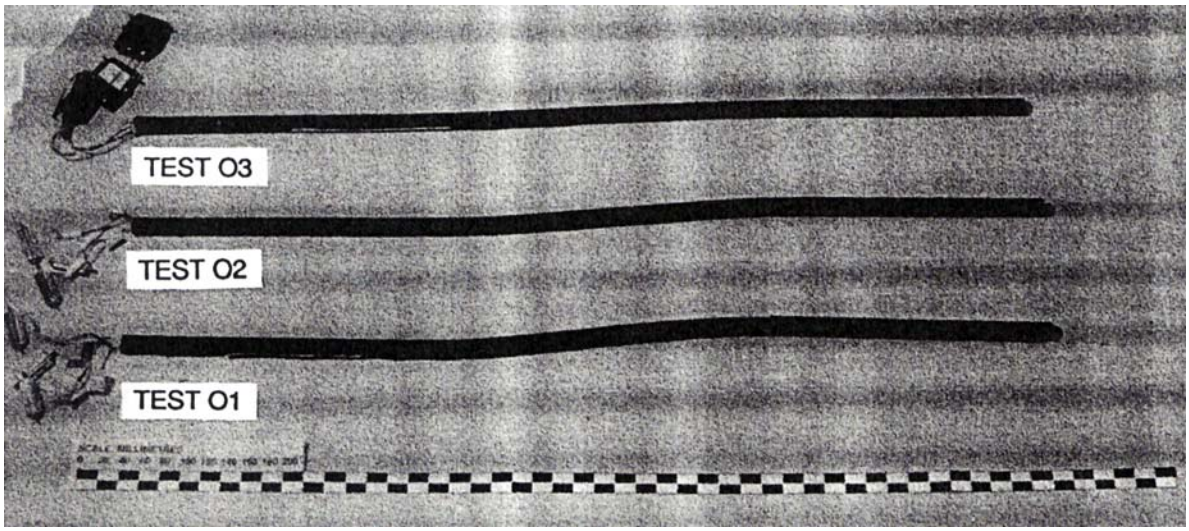

Test	θ
01	0°
02	15°
03	25°

(a) Post Test Deformation of D = 16 mm Reinforcement Tested at Different Orientations θ to the Vertical

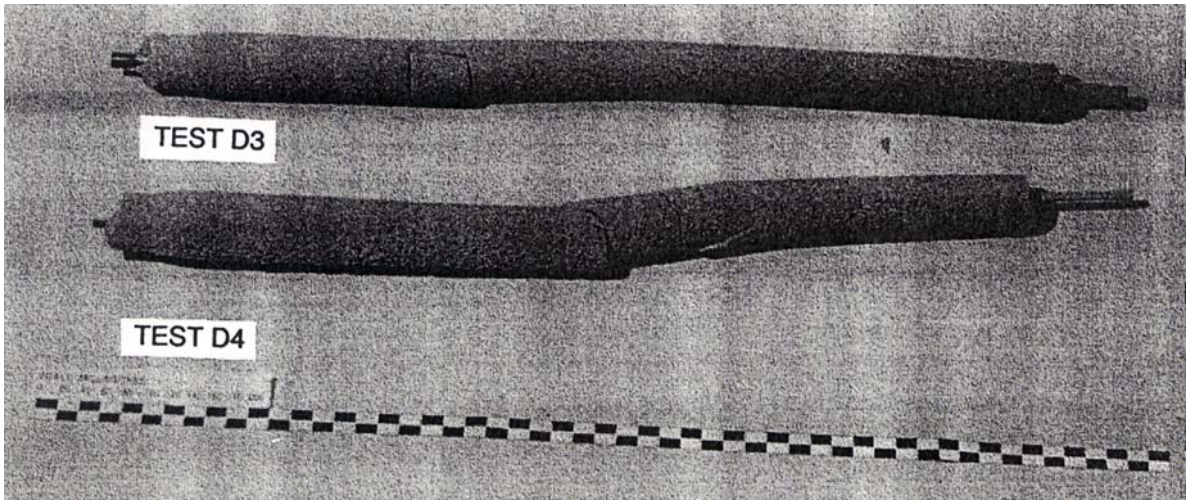

(b) Post Test Deformation of Grouted Reinforcement of External Diameter D_g = 51 mm and Internal Diameter D = 6.5 mm and D = 16 mm.

Figure D6 - Post Test Deformation of Reinforcement (after Pedley, 1990)

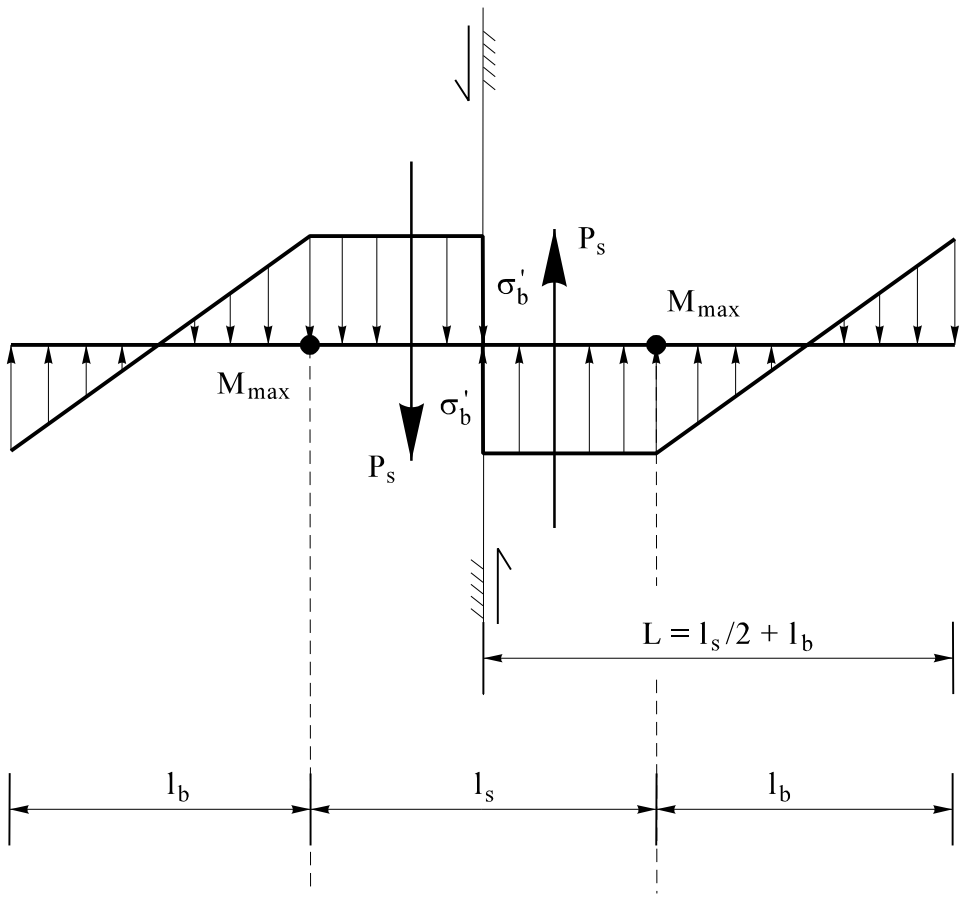

Legend:

P_s	Shear force
M_{max}	Maximum bending moment in nail
l_b	Minimum required length beyond point of maximum bending moment
l_s	Distance between points of maximum moment on either side of shear plane
σ_b'	Limiting bearing stress between soil and reinforcement

Figure D7 - Plastic Analysis of Soil-nail Interaction (after Jewell and Pedley 1992)

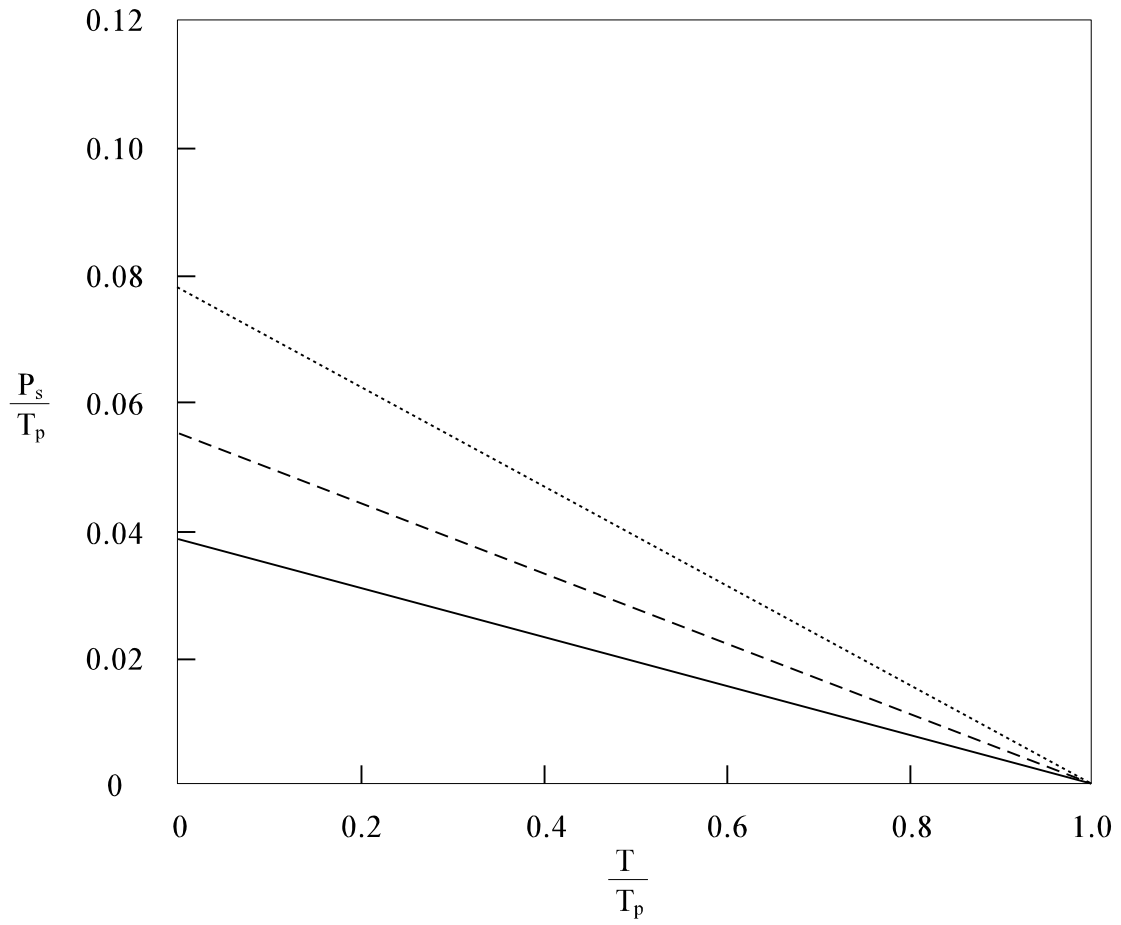

Soil Nail Parameters
Steel bar diameter = 25 mm
Modulus of subgrade reaction = 50 x 10^3 kN/m^3
$\phi' = 35^o$

Legend:

T	Axial nail force	P_s	Shear nail force
T_p	Fully plastic axial force in nail	σ_v	Vertical stress in soil
———	σ_v = 100 kN/m^2	– – – – –	σ_v = 200 kN/m^2
.....	σ_v = 400 kN/m^2		

Figure D8 - Limiting Combinations of Shear Force and Axial Force of Ungrouted Reinforcement for Plastic Analysis (after Jewell and Pedley, 1992)

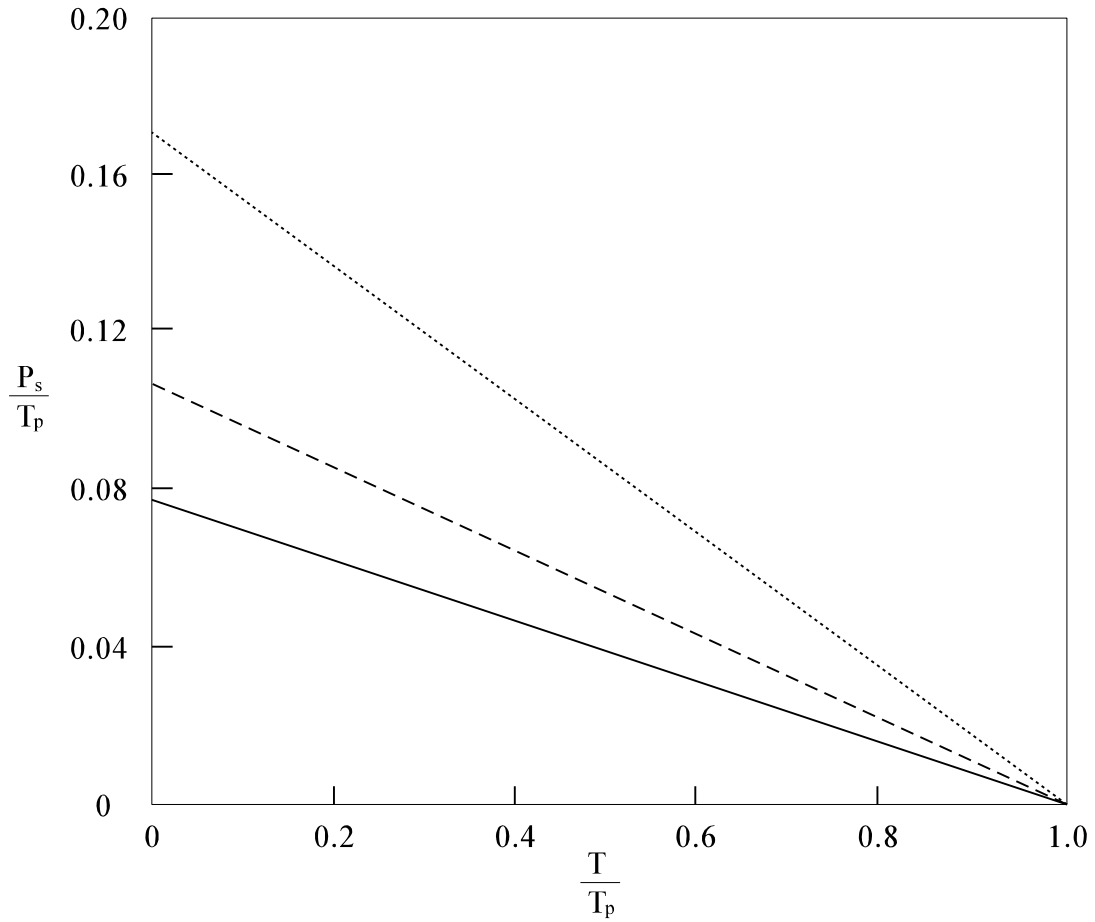

Soil Nail Parameters
Steel bar diameter = 25 mm
Grouted nail diameter = 100 mm
Modulus of subgrade reaction = 50 x 10^3 kN/m^3
$\phi' = 35^o$

Legend:

T	Axial nail force	P_s	Shear nail force
T_p	Fully plastic axial force in nail	σ_v	Vertical stress in soil
———	σ_v = 100 kN/m^2	– – – – –	σ_v = 200 kN/m^2
.....	σ_v = 400 kN/m^2		

Figure D9 - Limiting Combinations of Shear Force and Axial Force of Grouted Reinforcement for Plastic Analysis (after Jewell and Pedley, 1992)

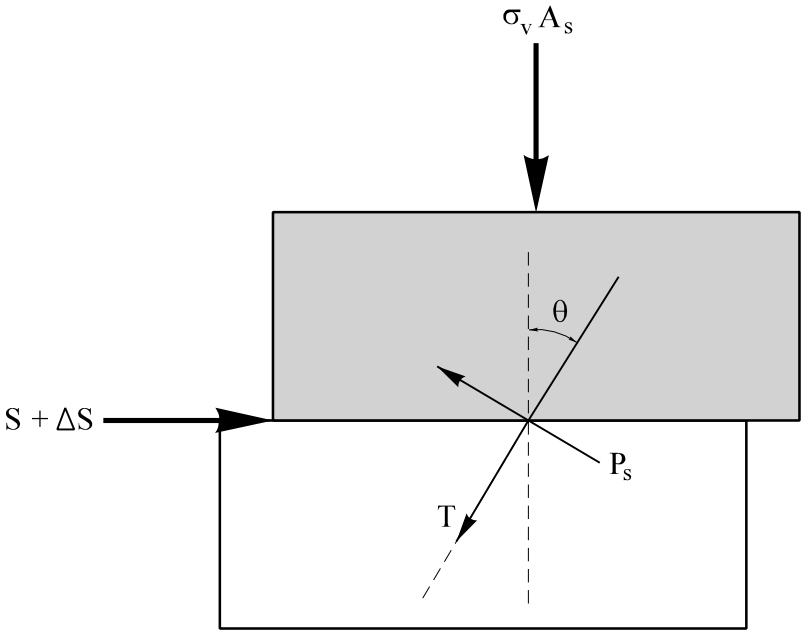

$$\left(\frac{\Delta S}{T_p}\right) = \left(\frac{T}{T_p}\right)(\cos\theta\tan\phi' + \sin\theta) + \left(\frac{P_s}{T_p}\right)(\cos\theta - \sin\theta\tan\phi')$$

Legend:

T	Axial nail force	P_s	Shear nail force
T_p	Fully plastic axial force in nail	σ_v	Vertical stress in soil
ΔS	Additional shearing resistance due to nail	A_s	Area of soil sample
S	Gross shearing resistance of unreinforced soil		

Figure D10 - Improvement in Shearing Resistance of Soil Reinforced with Nails (after Pedley, 1990)

Table of Contents
Table of Contents
Table of Contents

APPENDIX E

RESULTS OF PLAXIS ANALYSIS FOR NAILED SLOPES

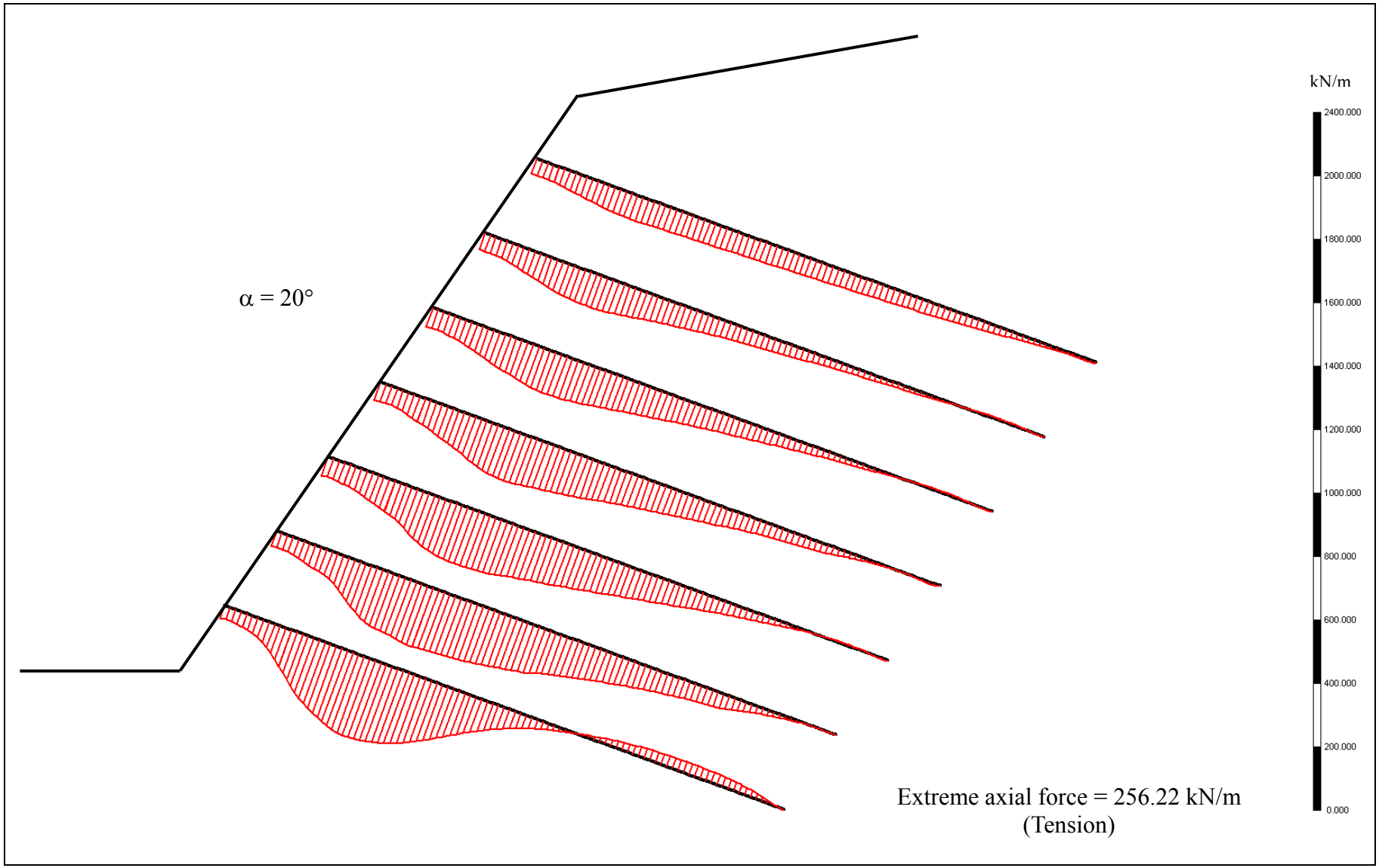

Figure E1 - Axial Nail Force Distribution, α = 20°

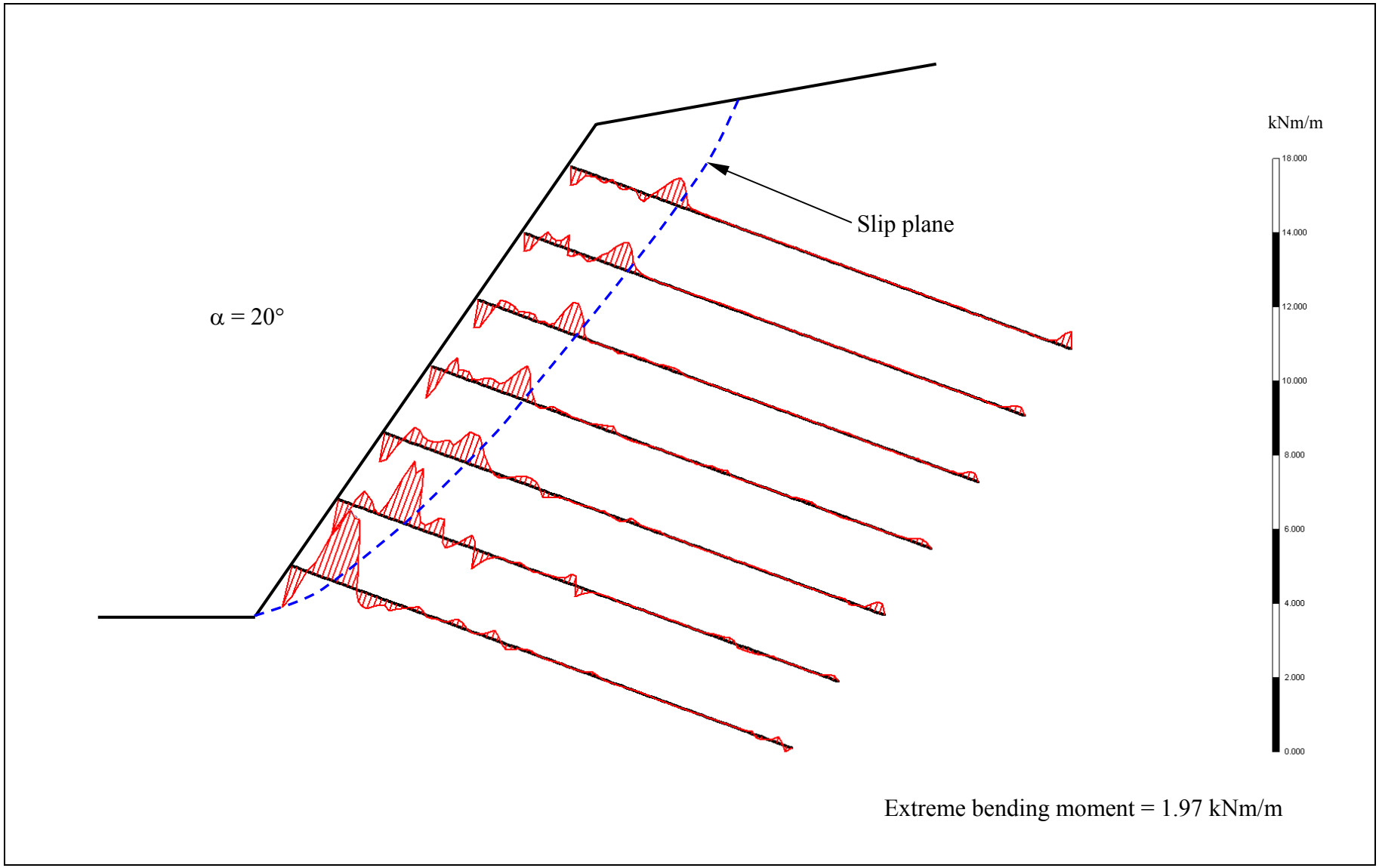

Figure E2 - Bending Moment Distribution in Nails, α = 20°

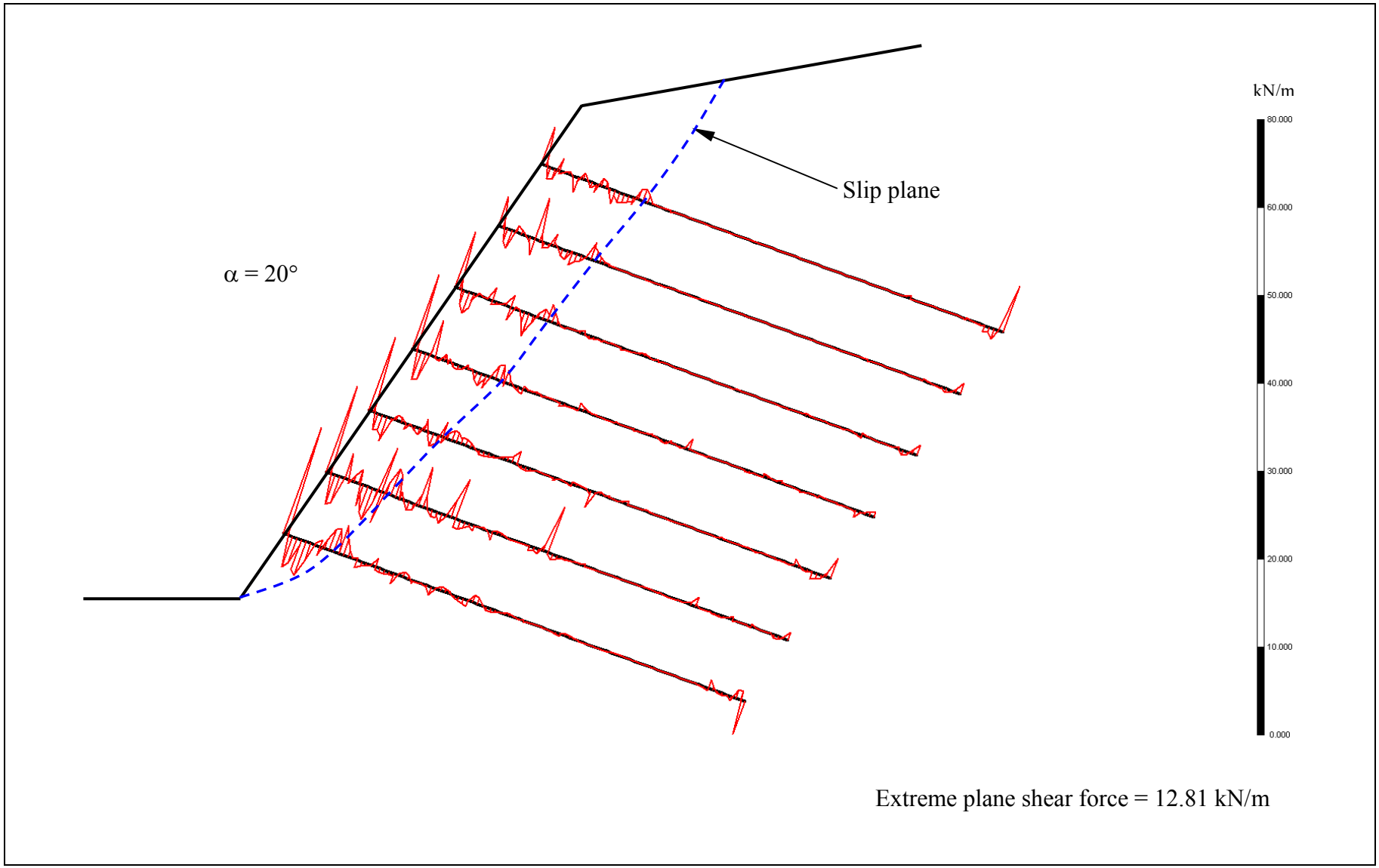

Figure E3 - Shear Force Distribution in Nails, α = 20°

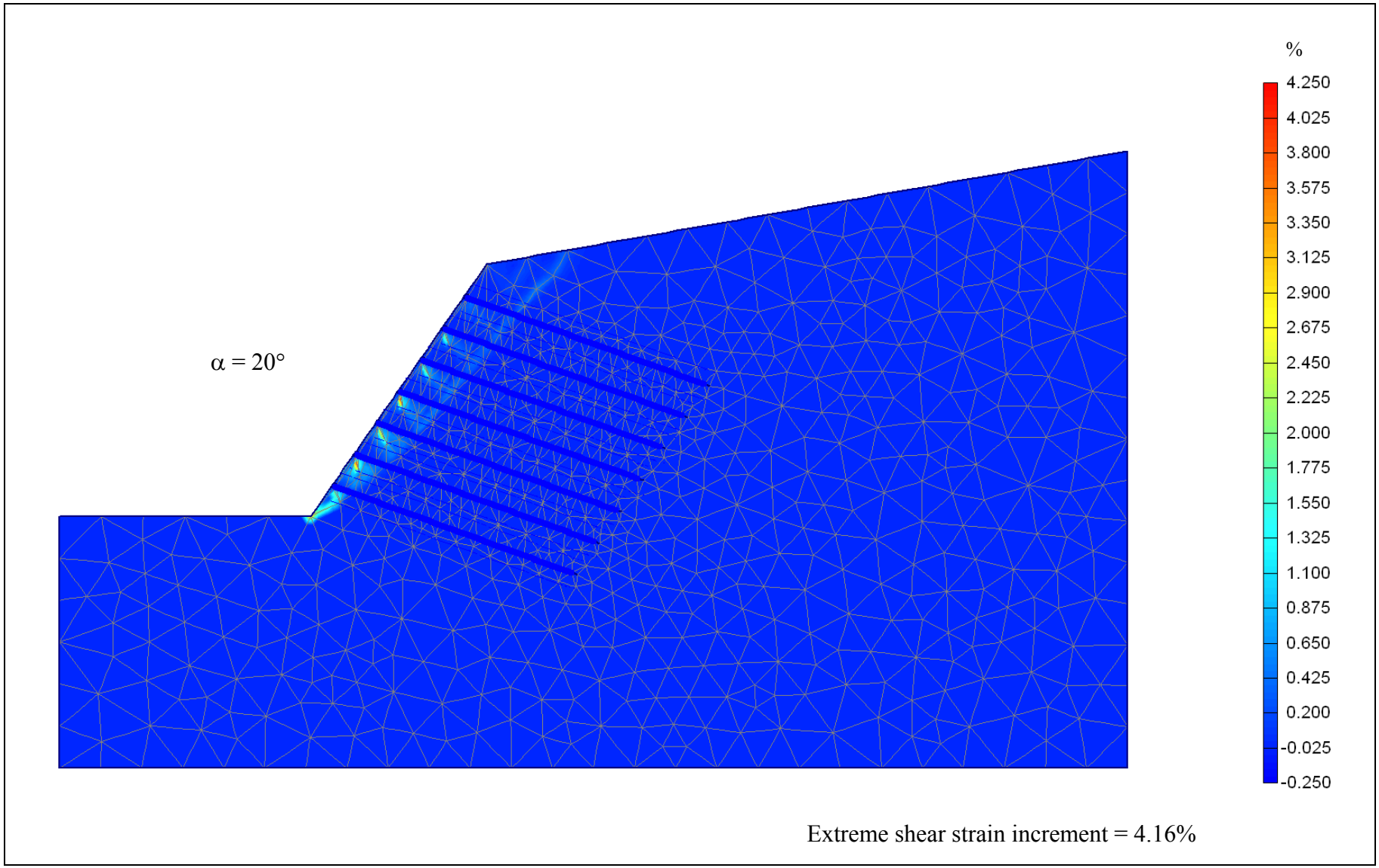

Figure E4 - Shear Strain Increment of Soil, α = 20°

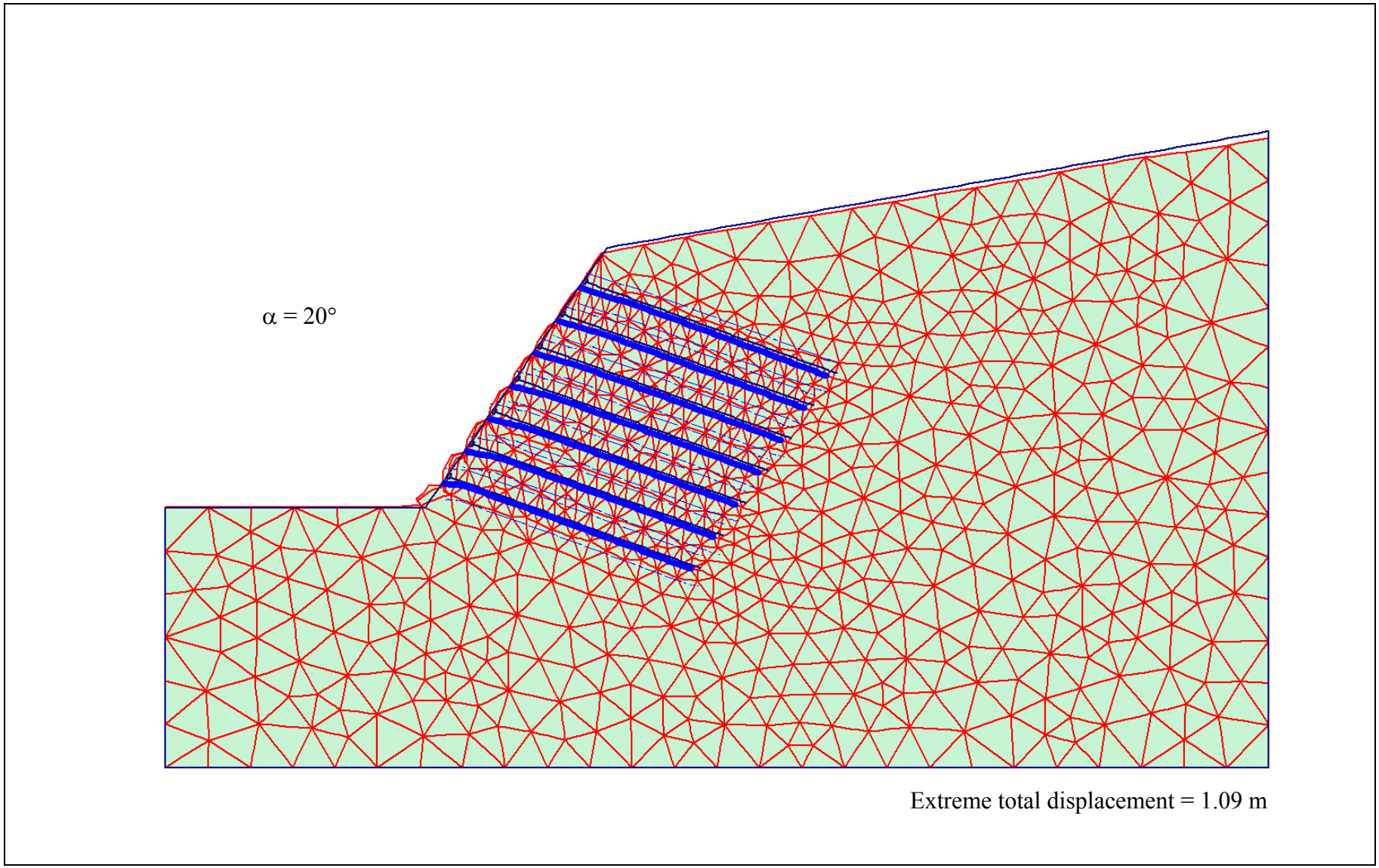

Figure E5 - Deformation of Soil Slope, α = 20°

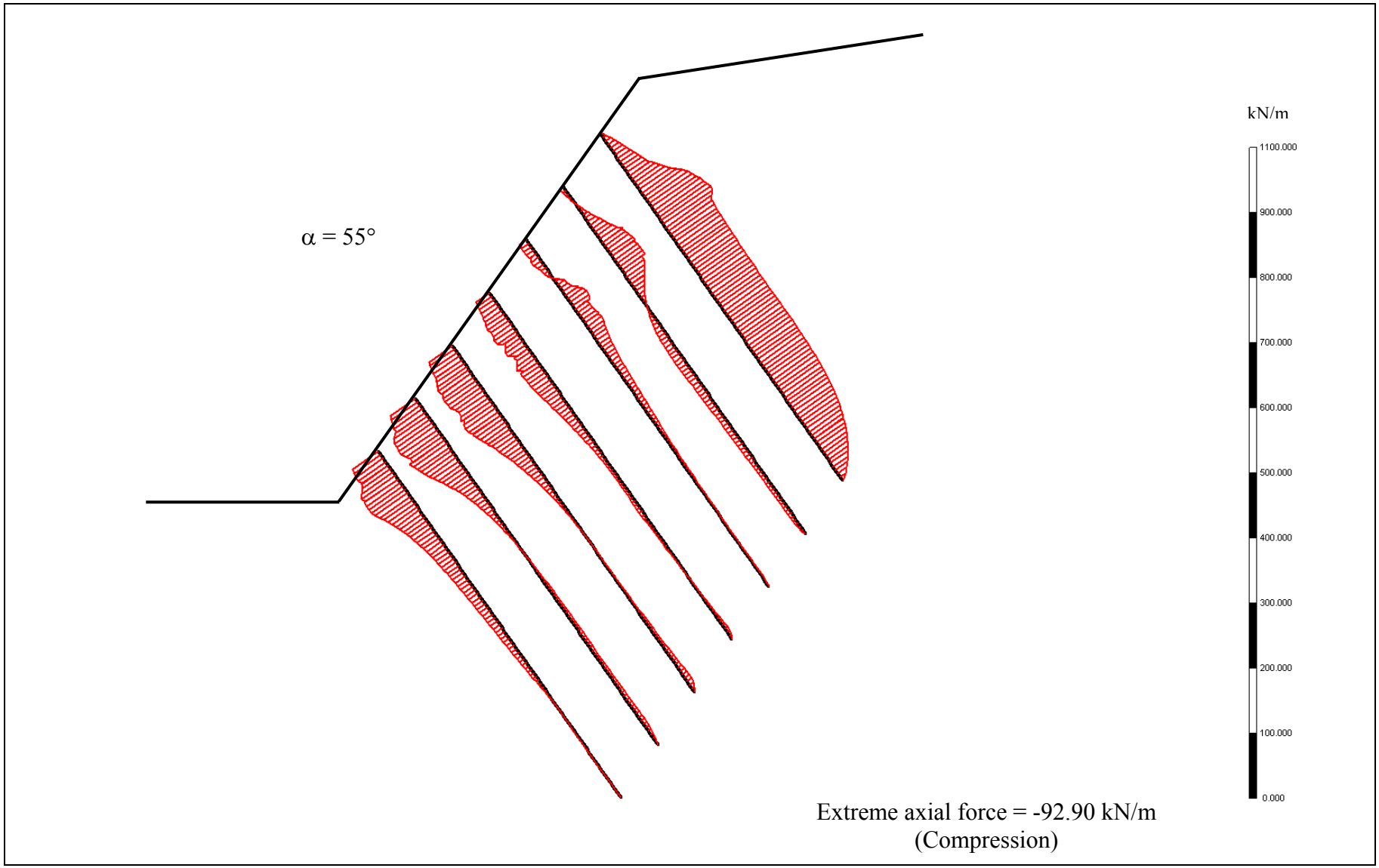

Figure E6 - Axial Nail force Distribution, α = 55°

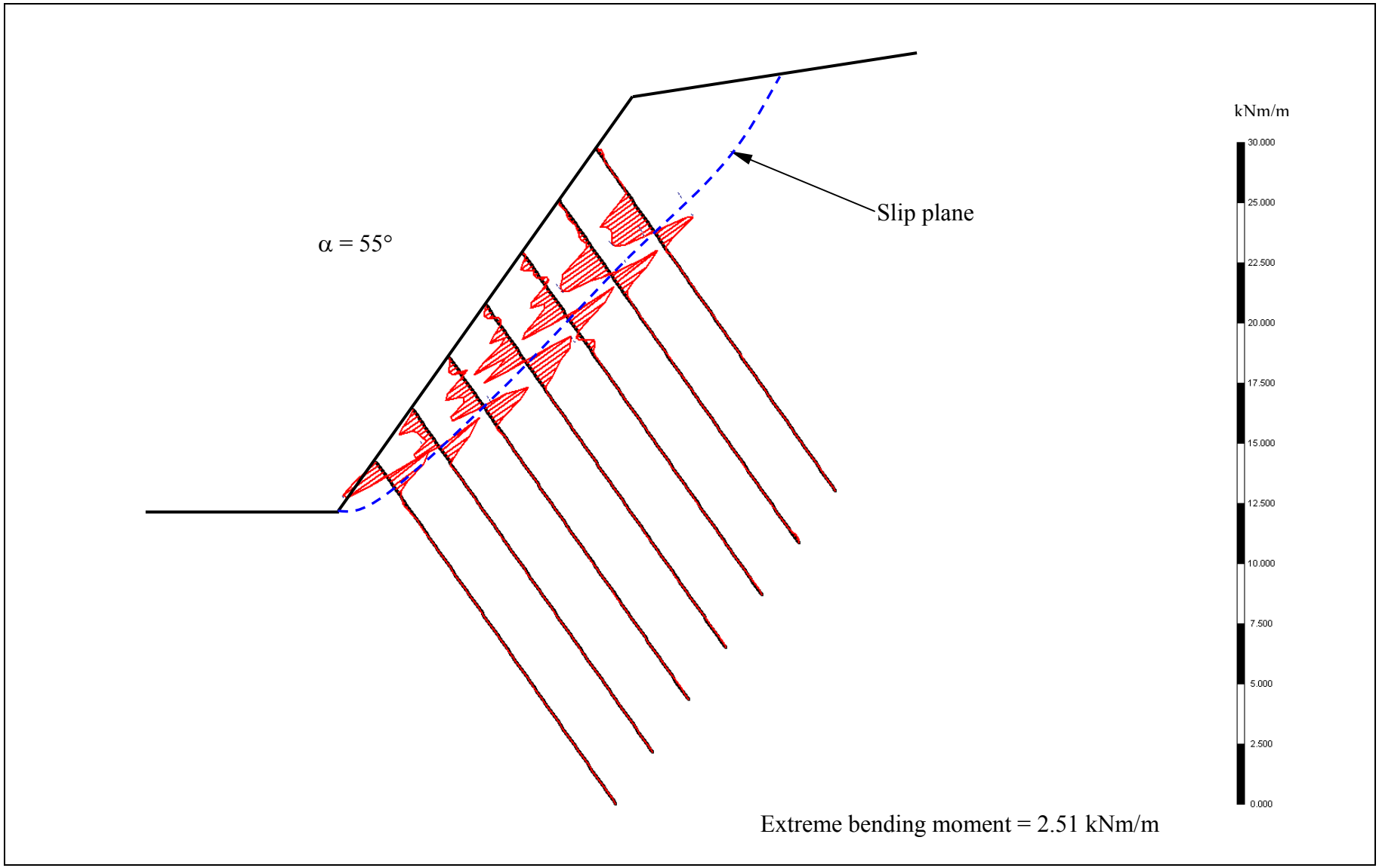

Figure E7 - Bending Moment Distribution in Nails, α = 55°

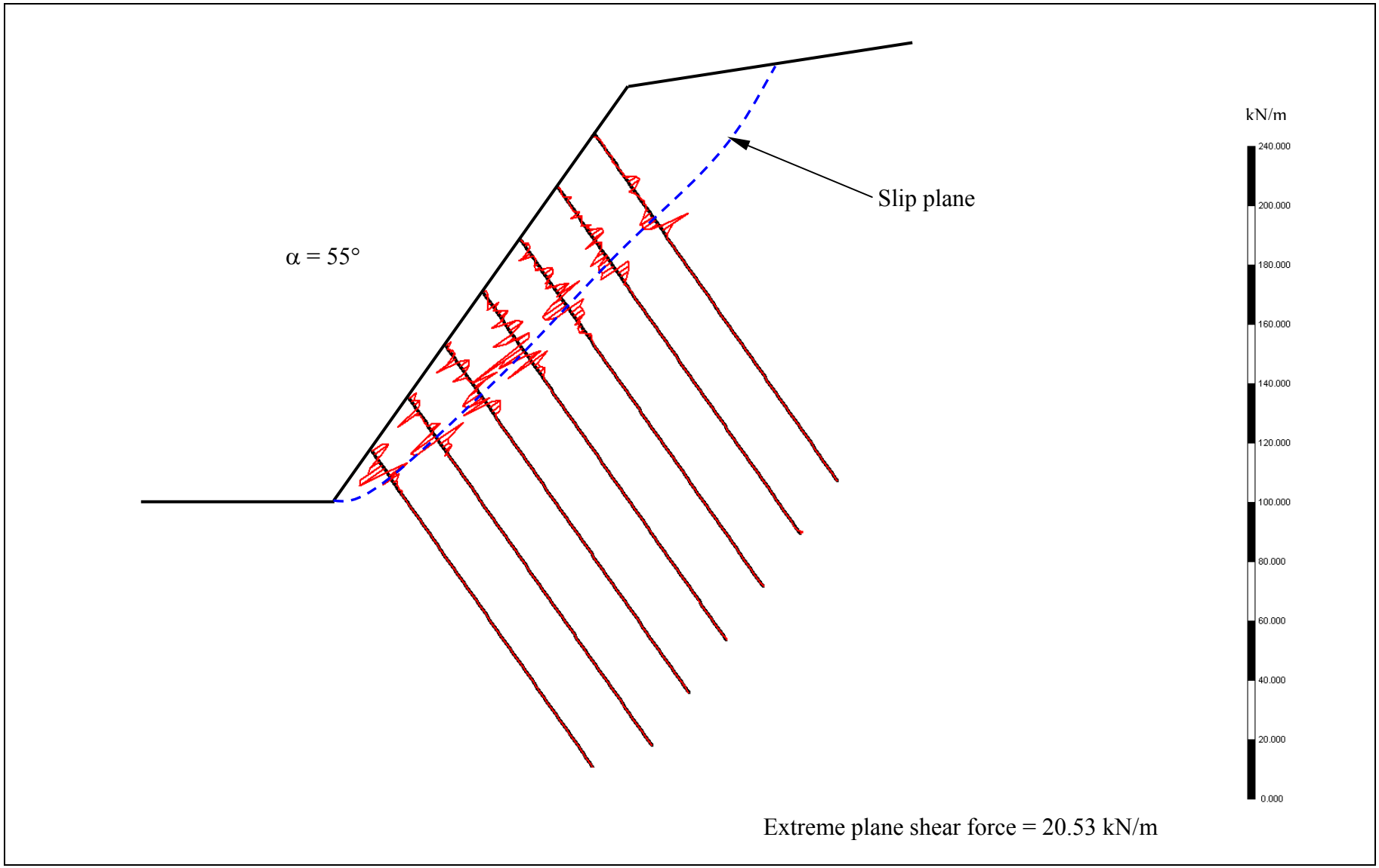

Figure E8 - Shear Force Distribution in Nails, α = 55°

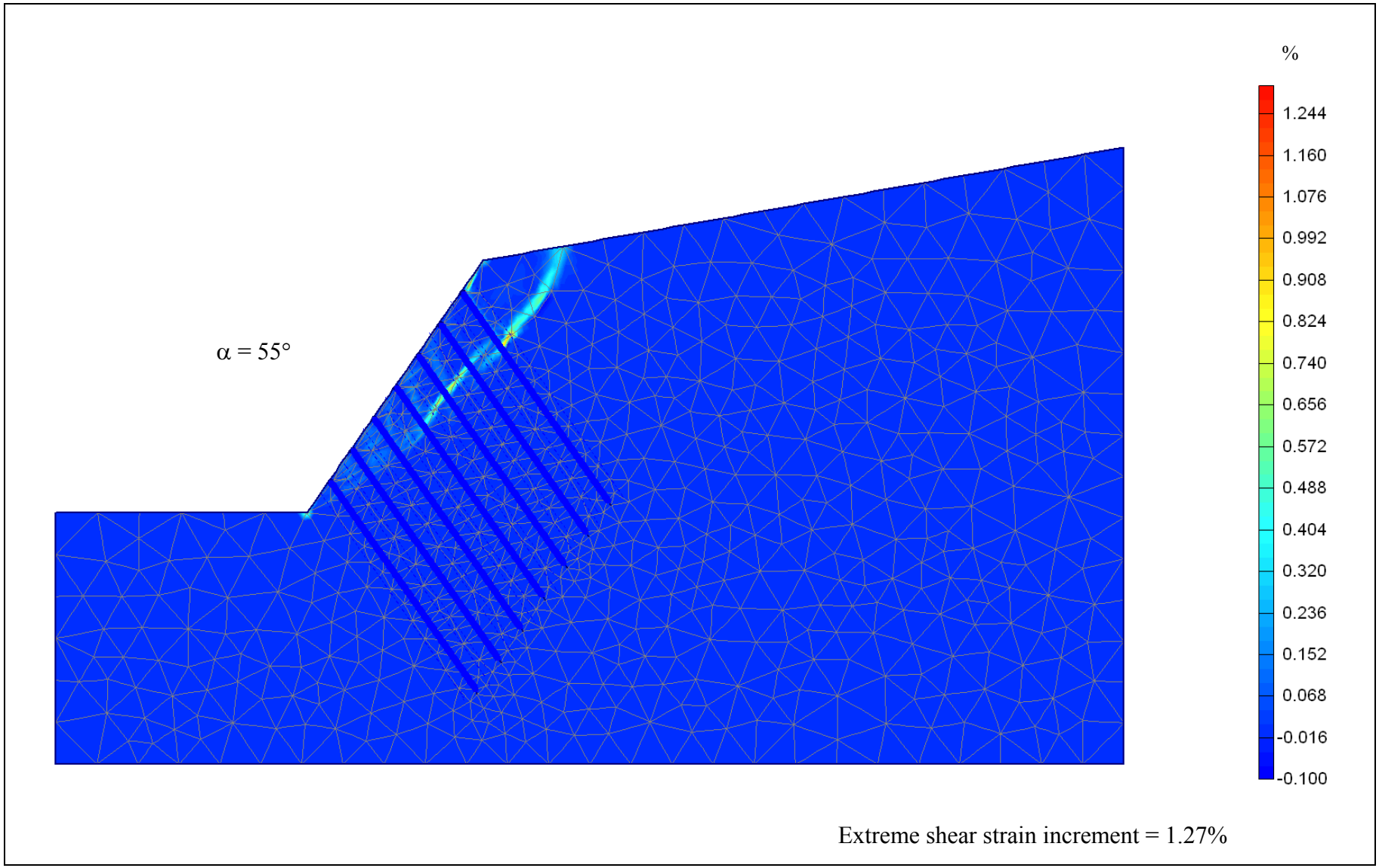

Figure E9 - Shear Strain Increment of Soil, α = 55°

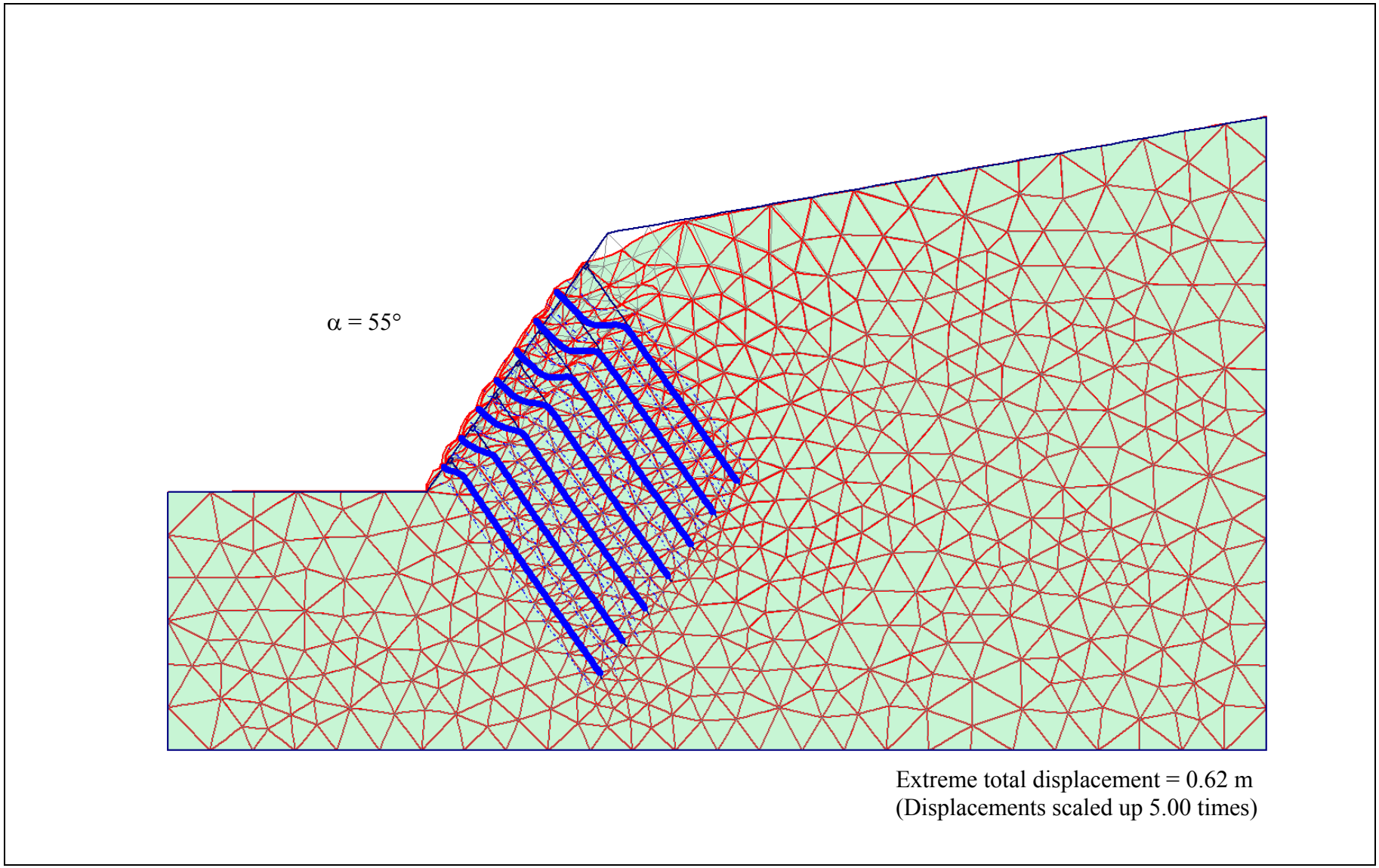

Figure E10 - Deformation of Soil Slope, α = 55°

GEO PUBLICATIONS AND ORDERING INFORMATION
土力工程處刊物及訂購資料

A selected list of major GEO publications is given in the next page. An up-to-date full list of GEO publications can be found at the CEDD Website http://www.cedd.gov.hk on the Internet under "Publications". Abstracts for the documents can also be found at the same website. Technical Guidance Notes are published on the CEDD Website from time to time to provide updates to GEO publications prior to their next revision.

部份土力工程處的主要刊物目錄刊載於下頁。而詳盡及最新的土力工程處刊物目錄，則登載於土木工程拓展署的互聯網網頁 http://www.cedd.gov.hk 的"刊物"版面之內。刊物的摘要及更新刊物內容的工程技術指引，亦可在這個網址找到。

Copies of GEO publications (except maps and other publications which are free of charge) can be purchased either by:

writing to
Publications Sales Section,
Information Services Department,
Room 402, 4th Floor, Murray Building,
Garden Road, Central, Hong Kong.
Fax: (852) 2598 7482

or
- Calling the Publications Sales Section of Information Services Department (ISD) at (852) 2537 1910
- Visiting the online Government Bookstore at http://bookstore.esdlife.com
- Downloading the order form from the ISD website at http://www.isd.gov.hk and submit the order online or by fax to (852) 2523 7195
- Placing order with ISD by e-mail at puborder@isd.gov.hk

讀者可採用以下方法購買土力工程處刊物(地質圖及免費刊物除外):

書面訂購
香港中環花園道
美利大廈4樓402室
政府新聞處
刊物銷售組
傳真: (852) 2598 7482

或
- 致電政府新聞處刊物銷售小組訂購 (電話：(852) 2537 1910)
- 進入網上「政府書店」選購，網址爲 http://bookstore.esdlife.com
- 透過政府新聞處的網站 (http://www.isd.gov.hk) 於網上遞交訂購表格，或將表格傳真至刊物銷售小組 (傳真：(852) 2523 7195)
- 以電郵方式訂購 (電郵地址：puborder@isd.gov.hk)

1:100 000, 1:20 000 and 1:5 000 maps can be purchased from:

Map Publications Centre/HK,
Survey & Mapping Office, Lands Department,
23th Floor, North Point Government Offices,
333 Java Road, North Point, Hong Kong.
Tel: 2231 3187
Fax: (852) 2116 0774

讀者可於下列地點購買1:100 000，1:20 000及1:5 000地質圖：

香港北角渣華道333號
北角政府合署23樓
地政總署測繪處
電話: 2231 3187
傳真: (852) 2116 0774

Requests for copies of Geological Survey Sheet Reports, publications and maps which are free of charge should be sent to:

For Geological Survey Sheet Reports and maps which are free of charge:
Chief Geotechnical Engineer/Planning,
(Attn: Hong Kong Geological Survey Section)
Geotechnical Engineering Office,
Civil Engineering and Development Department,
Civil Engineering and Development Building,
101 Princess Margaret Road,
Homantin, Kowloon, Hong Kong.
Tel: (852) 2762 5380
Fax: (852) 2714 0247
E-mail: jsewell@cedd.gov.hk

For other publications which are free of charge:
Chief Geotechnical Engineer/Standards and Testing,
Geotechnical Engineering Office,
Civil Engineering and Development Department,
Civil Engineering and Development Building,
101 Princess Margaret Road,
Homantin, Kowloon, Hong Kong.
Tel: (852) 2762 5345
Fax: (852) 2714 0275
E-mail: ykhui@cedd.gov.hk

如欲索取地質調查報告、其他免費刊物及地質圖，請致函：

地質調查報告及地質圖:
香港九龍何文田公主道101號
土木工程拓展署大樓
土木工程拓展署
土力工程處
規劃部總土力工程師
(請交:香港地質調查組)
電話: (852) 2762 5380
傳真: (852) 2714 0247
電子郵件: jsewell@cedd.gov.hk

其他免費刊物:
香港九龍何文田公主道101號
土木工程拓展署大樓
土木工程拓展署
土力工程處
標準及測試部總土力工程師
電話: (852) 2762 5345
傳真: (852) 2714 0275
電子郵件: ykhui@cedd.gov.hk

Table of Contents
Table of Contents
Table of Contents

MAJOR GEOTECHNICAL ENGINEERING OFFICE PUBLICATIONS
土力工程處之主要刊物

Table of Contents

GEOTECHNICAL MANUALS

Geotechnical Manual for Slopes, 2nd Edition (1984), 300 p. (English Version), (Reprinted, 2000).

斜坡岩土工程手冊(1998)，308頁(1984年英文版的中文譯本)。

Highway Slope Manual (2000), 114 p.

GEOGUIDES

Geoguide 1	Guide to Retaining Wall Design, 2nd Edition (1993), 258 p. (Reprinted, 2000).
Geoguide 2	Guide to Site Investigation (1987), 359 p. (Reprinted, 2000).
Geoguide 3	Guide to Rock and Soil Descriptions (1988), 186 p. (Reprinted, 2000).
Geoguide 4	Guide to Cavern Engineering (1992), 148 p. (Reprinted, 1998).
Geoguide 5	Guide to Slope Maintenance, 3rd Edition (2003), 132 p. (English Version).
岩土指南第五冊	斜坡維修指南，第三版(2003)，120頁(中文版)。
Geoguide 6	Guide to Reinforced Fill Structure and Slope Design (2002), 236 p.

Table of Contents

GEOSPECS

Geospec 1	Model Specification for Prestressed Ground Anchors, 2nd Edition (1989), 164 p. (Reprinted, 1997).
Geospec 3	Model Specification for Soil Testing (2001), 340 p.

GEO PUBLICATIONS

GCO Publication No. 1/90	Review of Design Methods for Excavations (1990), 187 p. (Reprinted, 2002).
GEO Publication No. 1/93	Review of Granular and Geotextile Filters (1993), 141 p.
GEO Publication No. 1/2000	Technical Guidelines on Landscape Treatment and Bio-engineering for Man-made Slopes and Retaining Walls (2000), 146 p.
GEO Publication No. 1/2006	Foundation Design and Construction (2006), 376 p.

Table of Contents

GEOLOGICAL PUBLICATIONS

The Quaternary Geology of Hong Kong, by J.A. Fyfe, R. Shaw, S.D.G. Campbell, K.W. Lai & P.A. Kirk (2000), 210 p. plus 6 maps.

The Pre-Quaternary Geology of Hong Kong, by R.J. Sewell, S.D.G. Campbell, C.J.N. Fletcher, K.W. Lai & P.A. Kirk (2000), 181 p. plus 4 maps.

TECHNICAL GUIDANCE NOTES

TGN 1	Technical Guidance Documents

Table of Contents